AN ABSTRACT OF THE DISSERTATION OF

Lian Ma for the degree of Doctor of Philosophy in Pharmacy presented on June 13, 2013.

Title: Analysis of Nonlinear Pharmacokinetic Systems and The Nonlinear Disposition of Phenylbutazone in Equine (horses)

Abstract approved:

John Mark Christensen

The first part of the dissertation is to evaluate the use of proposed and established equations for area under the plasma concentration versus time (AUC) for molecules undergoing nonlinear Michaelis–Menten pharmacokinetic elimination. The effects of varying Michaelis-Menten parameters, rate of drug absorption, or bioavailability on the predictability of drug exposure (AUC) for single-dose data were performed by computer simulation for one- compartment model with first-order drug absorption and two- compartment model with i.v.-bolus administration. Results show that the use of our proposed equation for one-compartment 1^{st}-order absorption model is adequate in most cases of dose, k_a and clearance ratio. The use of the established equation for two-compartment i.v. model, however, was indentified to be limited under low doses and high clearance ratio (V_m/K_m).

The second part is to study the potential drug interaction between Phenylbutazone and Ranitidine in thoroughbred horses. Pharmacokinetic

study was conducted in a cross-over design in which the horses received co-administration of ranitidine or control treatment. The study started with single-dose oral administrations of 2.2, 4.4, and 8.8 mg/kg phenylbutazone, and then multiple-dose administrations 2.2, 4.4, and 8.8 mg/kg phenylbutazone with a 1-week washout period between trials. Neither plasma concentration profiles nor the observed pharmacokinetic parameters of phenylbutazone were significantly altered by ranitidine treatment. The results suggest that concurrent treatment with ranitidine and phenylbutazone does not result in elevations of plasma phenylbutazone concentrations. Ranitidine should be safe to be co-administered with phenylbutazone in thoroughbred horses.

The third part is about two pharmacokinetic studies investigating *O,O*-dimethylphosphate (DMP) and xanthohumol (XN) respectively, in Male Sprague-Dawley rats. Levels of urinary dialkylphosphates (DAPs) are currently used as a biomarker of human exposure to organophosphorus insecticides (OPs). It is known that OPs degrade on food commodities to DAPs at levels that approach or exceed those of the parent OP. However, little has been reported on the extent of DAP absorption, distribution, metabolism and excretion. Rats were administered DMP at 20 mg/kg via oral gavage and I.V. injection. DMP bioavailability was found to be 107 $\pm$ 39 % and the amount of the orally administered dose recovered in the urine was 30 $\pm$ 9.9 % by 48 hrs. The *in vitro* metabolic stability, high bioavailability and extent of DMP urinary excretion following oral exposure in a rat model suggests that measurement of DMP as a biomarker of insecticide exposure may lead to overestimation of human exposure. Xanthohumol (XN) is a dietary flavonoid found in hops showing health protective actions against cardiovascular disease and type 2 diabetes. This study provides basic pharmacokinetics (PK) parameters for XN and its major metabolites in rats. The maximum concentration (C_{max}) and area under the curve ($AUC_{0-\infty}$) of total XN (free and conjugated) were 2.9 ± 0.1 mg/L and 2.5 ± 0.3 h*mg/L in

the IV group, 0.019 ± 0.002 mg/L and 0.84 ± 0.17 h*mg/L in the oral low group, 0.043 ± 0.002 mg/L and 1.03 ± 0.12 h*mg/L in the oral medium group, and 0.15 ± 0.01 mg/L and 2.49 ± 0.10 h*mg/L in the oral high group. The bioavailability of XN is dose-dependent and approximately 0.33, 0.13 and 0.11 in rats, for the low, medium and high dose groups, respectively.

Analysis of Nonlinear Pharmacokinetic Systems and The Nonlinear Disposition of Phenylbutazone in Equine (horses)

By

Lian Ma

A DISSERTATION

submitted to

Oregon State University

In partial fulfillment of
the requirements for the
degree of

Doctor of Philosophy

Presented June 13, 2013
Commencement June 2014

Doctor of Philosophy dissertation of Lian Ma presented on June 13, 2013.

APPROVED:

Major Professor, representing Pharmacy

Dean of the College of Pharmacy

Dean of the Graduate School

I understand that my dissertation will become part of the permanent collection of Oregon State University libraries. My signature below authorizes release of my dissertation to any reader upon request.

Lian Ma, Author

ACKNOWLEDGMENTS

Many people helped in the completion of this thesis in many different ways. First and foremost, I would like to first express my appreciation and grateful thanks to my advisor, Dr. John Mark Christensen, for opening the door of pharmaceutics for me, supporting and guiding me through my research and study, and helping me to grow in this field.

I would also like to thank Dr. Rosita R. Proteau who provided excellent advice often on my research and shared with me her own experience and resources. Her intelligent guidance and generous support encouraged me in all respect.

Special thanks go to the members of my supervisory committee, Dr. Gary E. DeLander, Dr. Lisa Madsen, Dr. Jeffrey K. Stone and Dr. Yanming Di for their broad knowledge, technical support, as well as valuable discussion on my work.

Extended special thanks go to the research groups of Dr. Jan Fred Stevens and Dr. Kim Anderson (in the Department of Environmental and Molecular Toxicology) for letting me join their research projects. It has really been a wonderful experience to learn from them and work with them.

I would also like to take this opportunity to express my gratitude to Ms. Debra Peters and other administrative staffs in our department, for their great help and constant support throughout my Ph.D. study.

I am deeply grateful for my internship mentors at FDA, Dr. Ying Fan, Dr. Ping Ji and Dr. Yaning Wang for their patient guidance and warm help to make my internship experience impressive and rewarding.

Last but not least, I would like to give my appreciation to all my family, friends, lab mates, our department faculty, staff, graduate students and post-doc fellows for their support and friendship. Thanks from the bottom of my heart to my parents, for their unconditional understanding, support, patience and encouragement. I could never complete my work without their love.

CONTRIBUTION OF AUTHORS

Dr. Mutasim Al-Ghazawi and Dr. Triporn Wattananat contributed to the work in Chapter 1.

Dr. Shun-wen Chang, Dr. Linda L. Blythe and Dr. A. Morrie Craig contributed to the work in Chapter 2.

Dr. Rosita R. Proteau and Dr. Norman Forsberg (in the Department of Environmental and Molecular Toxicology) contributed to the study design, data collection and writing of Chapter 3.

Dr. Rosita R. Proteau, Dr. Jan F. Stevens (Linus Pauling Institute) and Dr. LeeCole Legette, Ralph L. Reed in Dr. Stevens' research group contributed to the study design, data collection and analysis, as well as writing of Chapter 4.

TABLE OF CONTENTS

Page

TABLE OF CONTENTS (CONTINUED)

LIST OF FIGURES

Figure | Page

LIST OF FIGURES (CONTINUED)

Figure Page

LIST OF FIGURES (CONTINUED)

Figure Page

LIST OF FIGURES (CONTINUED)

Figure Page

LIST OF TABLES

Table | Page

LIST OF ABBREVIATIONS

AUC	Area under the plasma concentration time curve
BW	Body weight
C_{max}	Maximum plasma concentration
$C_{ss,max}$	Steady state peak concentrations
$C_{ss,min}$	Steady state trough concentrations
CL	Systemic total body clearance
CL_D	Inter-compartment distribution clearance
FDA	Food and Drug Administration
GI	Gastrointestinal
i.v.	Intravenous
k_a	Absorption rate constant
$t_{1/2}$	Half-life of elimination
T_{max}	Time required to reach maximum plasma concentration
V_c	Central compartment volume
V_p	Peripheral compartment volume
V_d	Apparent volume of distribution
V_{ss}	Total steady state volume of distribution
LOD	Limit of detection

This document is dedicated to my parents and all the friends who supported me.

CHAPTER 1

SIMULATION FOR ACCURATE PREDICTION OF DRUG EXPOSURE (AUC) FOLLOWING NONLINEAR PHARMACOKINETIC ELIMINATION

Lian Ma, John Mark Christensen, Mutasim Al-Ghazawi, and Triporn Wattananat

ABSTRACT

Proposed and established equations were evaluated to predict area under the plasma concentration versus time (AUC) for pharmacokinetic systems with nonlinear elimination. The effects of varying Michaelis-Menten parameters, absorption rate of drug, or bioavailability on the predictability of *AUC* for single-dose data were performed by computer simulation of one- and two- compartment models.

Our proposed equation for one-compartment 1st-order absorption model yielded good approximation of *AUC* and can be applied to most scenarios of dose, k_a and inter-compartmental clearance ratios. The accuracy of the established equation for two-compartment i.v. model was identified to be limited under low doses and high clearance (V_m/K_m).

These equations and simulations provide insight into factors determining drug exposure for drugs following nonlinear elimination. It is a step forward in nonlinear pharmacokinetics which is highly unexplored.

NONLINEAR PHARMACOKINETICS

The pharmacological response of a drug is generally believed to be directly correlated to its concentration at the site of action, which in turn is dependent on a number of processes, including absorption, distribution, biotransformation and excretion. Some of these processes, such as drug metabolism, secretion and protein binding; involve enzymes or proteins with finite capacities for drug binding/interactions that are easily saturable.

Clinically, absorption and elimination of most drugs follow linear kinetics, and pharmacokinetic parameters describing absorption and elimination of a drug do not change over the therapeutic drug concentration of the dose range. However, dose-dependent pharmacokinetics (nonlinear pharmacokinetics) has been reported more frequently in preclinical studies (Wilkinson, Reynolds et al. 1980; Pancorbo, Benson et al. 1983; Straka, Lalonde et al. 1987; Browne, Szabo et al. 1993; Toffoli, Robieux et al. 1997), particularly in toxicity studies, where high doses are often employed. Various factors for these dose-dependent behaviors in ADME (Absorption, Distribution, Metabolism, and Elimination) processes and corresponding examples are summarized in Table 1-1.

Recognizing Nonlinear Pharmacokinetics

When the system is linear, the pharmacokinetic parameters such as dose-normalized exposure levels (AUC/dose, AUMC/dose, and C_{max}/dose), T_{max}, $t_{1/2}$, CL, V_{ss}, and MRT should remain constant regardless of the dose or concentration levels. The most noticeable characteristic of nonlinearity of drug disposition is the lack of superimposition of concentration vs. time profiles at different dose or concentration levels (Chow and Jusko 1987).

Superposition (also called “dose-proportionality”) of drug disposition under linear conditions implies that dose-normalized drug concentrations and $AUC_{0-\infty}$ at different doses are the same. On the other hand, nonlinearity can

be viewed as “lack of superposition” at different doses. Virtually, all pharmacokinetic systems can be nonlinear at high dose or concentration levels owing to the saturation of various enzymatic or carrier-mediated processes. Figure 1-1 and 1-2 illustrates the relationship between *AUC* / dose or normalized *AUC* to doses to show linear and nonlinear conditions (Jusko 1989).

In general, when nonlinear pharmacokinetics occurs, there is a more than dose-proportional increase in $AUC_{0-\infty}$ as the dose increases. Occasionally, however, an increase in $AUC_{0-\infty}$ with dose that is less than dose-proportional can be observed, which may be due to an increased systemic clearance associated with an increase in the unbound drug fraction at higher drug concentrations. In this case, a further increase in dose will eventually result in an over proportional increase in $AUC_{0-\infty}$ due to saturation of the clearance mechanisms. Another example of a less than dose-proportional increase in $AUC_{0-\infty}$ after oral administration is impairment of absorption due to limited solubility of a drug or saturation of active transporters in the intestinal membranes at higher doses.

A minimum of three different pharmacokinetic profiles from three dose levels are required to adequately determine nonlinearity. The dose-dependent changes of the following parameters are indicative of the presence of a nonlinear pharmacokinetic system or process. Potential causes for the lack of superposition of those parameters are also discussed.

1. $C(t)$/dose: Some type of dose-dependence exists, but further study is needed to determine the causes for nonlinearity.

2. $AUC_{0-\infty}$ /dose: Bioavailability or systemic clearance is nonlinear.

3. $AUMC_{0-\infty}$ /dose: Absorption rate, CL, or V_{ss} is nonlinear

Important differences in definitions and terminology of linear and nonlinear pharmacokinetic processes are summarized in Table 1-2.

Pharmacokinetic Implications of Michaelis-Menten Kinetics

The elimination of drug by a saturable enzymatic process is described by Michaelis-Menten kinetics. If *C* is the concentration of drug in the plasma, then:

$$V \cdot \frac{dC}{dt} = -\frac{V_m \cdot C}{K_m + C} \qquad (Eq.1)$$

Where *C* is concentration of the drug at time *t*, *dC*/*dt* is the rate of drug elimination from the sampling compartment at time *t*; *V* is apparent volume of distribution, V_m is the maximum elimination rate and K_M is the Michaelis constant that reflects the capacity of the enzyme system. It is important to note that K_M is not an elimination constant, but is actually a hybrid rate constant in enzyme kinetics, representing both the forward and backward reaction rates and equal to the drug concentration or amount of drug in the body at half V_m.

Under two different extreme conditions, Equation 1 can be simplified into either first- or zero-order kinetics as shown below.

First-Order Kinetics: When drug concentrations are substantially lower than K_m (usually $C(t) < 0.01 \times K_m$), the rate of change in the plasma drug concentration becomes a first-order function of the concentration:

$$\frac{dC(t)}{dt} = -\frac{V_m \cdot C(t)}{K_m} = -k \cdot C(t)$$

In this case, the rate of drug disappearance is directly proportional to the concentration, and, thus, the plasma concentration–time profile of the drug follows first-order kinetics with a rate constant of V_m/K_m.

Zero-Order Kinetics: When plasma drug concentrations are substantially higher than K_m (usually $C(t) > 100 \times K_m$), the value at which the enzymatic process can be saturated, the rate of change of the drug concentration becomes independent of the concentration itself:

$$\frac{dC(t)}{dt} = -V_m$$

Under these conditions, the rate of drug disappearance is constant (zero-order kinetics).

Area under the curve for Nonlinear Pharmacokinetics

The area under the plasma concentration versus time curve is derived from drug concentration and time giving a measure of the amount of drug absorbed into the circulatory system (drug exposure). It is also an important parameter for comparison between drug products in bioequivalence or bioavailability studies.

In linear pharmacokinetics, the *AUC* is linearly proportional to the dose administered for drugs eliminated by first-order kinetics. For drugs that are eliminated by capacity-limited processes or Michaelis-Menten kinetics, however, the *AUC* is not linearly proportional to the dose due to saturation of the clearance mechanism.

A list of four typical pharmacokinetic models following nonlinear elimination is shown in Table 1-3. For a drug having Michaelis-Menten elimination only from the central compartment after single i.v. bolus dosing, Wagner et al. (Wagner 1973; Wagner, Szpunar et al. 1985) have derived the following important equation for the one-compartment model (model i):

$$AUC = \frac{D}{V_m}\left(\frac{D}{2V} + K_m\right) \qquad (Eq.2)$$

Mathematical expressions of MRT, CL has also been derived and validated for this model (Wagner 1973; Chow and Jusko 1987). These equations have been validated and applied to bioavailability studies (Browne, Szabo et al. 1992; Browne, Szabo et al. 1993),

Similarly, for two-compartment i.v. bolus model (model iii), *AUC* has been derived as:

$$AUC = \frac{D}{V_m}\left(\frac{D}{2V_{ss}} + K_m\right), \qquad V_{ss} = V_c + V_p \qquad (Eq.3)$$

Where V_{ss} is the apparent volume of distribution at steady state, V_c and V_p represent the volume of distribution of central and peripheral compartment, respectively. How well this equation works and the boundary of it accuracy is unknown.

For the case of first order input and Michaelis-Menten elimination, no solution has been given. Mathematical expression cannot be derived directly from the differential equations, due to mathematical difficulty in the integration. The effect of input rate on systemic availability is reported following some numerical integration (Wagner, Szpunar et al. 1985). The effect of slow input in reducing systemic bioavailability when Michaelis-Menten elimination kinetics are operative is stressed and the implications of this in the field of sustained-release medication mentioned (Wagner, Szpunar et al. 1985).

In the current study, equations to predict *AUC* for drugs following one-compartment open model with 1st-order absorption have been proposed as following:

$$AUC = \frac{k_a FD}{V\left(k_a - \frac{V_m{}'}{K_m + FD/V}\right)}\left(\frac{K_m + FD/2V}{V_m{}'} - \frac{1}{k_a}\right) \qquad (Eq.4)$$

The objective of this study is to verify the derived *AUC* equation for a two-compartment i.v. model (Eq. 3) and the proposed *AUC* equation for the one-compartment model with 1st-order absorption (Eq. 4).

MATERIALS AND METHODS

Numerical integrations of the appropriate differential equations were performed using the Runge-Kutta method (See Appendix) to obtain plasma concentration-time data after single dosing of a hypothetical drug for the following models: (ii) One-Compartment Michaelis-Menten system with 1st-Order absorption, and (iii) Two-Compartment Michaelis-Menten system with i.v. bolus administration (Table 1-3).

A scheme showing the whole workflow of study is depicted in Figure 1-3. Simulations were carried out in MATLAB® (R2010b version) to generate data for the hypothetical drug after intravenous and oral administration given various values of input parameters Dose, V_m, K_m, k_a, V_c and F. The obtained concentration-time data were used to estimate *AUC* values by using the combination of the regular and logarithmic trapezoidal rules. These observed values were then compared with the theoretical values predicted by the equation given for the individual model. The difference between the observed and predicted values was expressed as a percent error, which was calculated at the absolute value of the percent deviation from the observed value of *AUC*:

$$Percent\ error\ \% = \frac{AUC_{predicted} - AUC_{observed}}{AUC_{observed}} \times 100\%$$

The percent error calculated for each simulation was compared to the cumulative truncation error calculated for the curve which was between 0.1 and 0.2 percent.

For one-compartment system (Model ii), simulations were performed using the following values: Dose = 0 - 2500 mg/kg, V_m = 0 - 100 mg/hr, V_m/K_m ratio = 0 – 10 mg/L, k_a = 0 - 10 hr^{-1}, V = 44.8 L and F = 1. The range of doses used in the case ensures that typical behavior would be observed at the limiting low-dose and middle-dose situations. Similarly, for two-compartment system (Model iii), simulations were performed by using the following values:

Dose = 0 - 2500 mg/kg, V_m = 0 - 60 mg/hr, V_m/K_m ratio = 0 - 10 mg/L, V_c = 20 L, CL_D (inter-compartment distribution clearance) = $k_{12} \times V_c = k_{21} \times V_p$ = 0 - 100 L/hr.

RESULTS

Concentration-time data and profiles were generated based on simulation by varying the models pharmacokinetic parameters. The overall truncation error calculated for the simulation was very small (around 0.1 - 0.2%). Since for most curves the percent error was similar to the cumulative truncation error accurate assessments of the simulations and predictions by the equations could be determined.

The difference between the observed and predicted *AUC* (percent error %) were plotted against model parameters, in order to visualize the percent error under all given conditions.

For one-compartment 1st-order model, the effects of dose and clearance ratio (V_m/K_m) on the percent error given a fixed k_a (0.5 - 5 hr^{-1}) and V_m (20 mg/hr) are shown in Figure 1-4. The effect of absorption rate constant (k_a) and V_m value on the percent error given a fixed dose (100 mg/kg, 1000 mg/kg) and clearance ratio (V_m/K_m = 1 L/hr) is shown in Figure 1-5.

For two-compartment i.v. bolus model, the effects of dose and clearance ratio (V_m/K_m) on the percent error given a fixed inter-compartment CL_D (25 L/hr) and V_m (20 mg/hr) are shown in Figure 1-6. The effects of CL_D and V_m value on the percent error given a fixed Dose (100 mg/kg, 1000 mg/kg) and clearance ratio (V_m/K_m = 1 L/hr) are shown in Figure 1-7.

Based on the scales of plots in Figure 1-4, our proposed equation for the one-compartment open model with first order absorption appears to work well in most cases with percent error < 1%. The only exception is observed when the absorption rate is low (k_a < 1 hr^{-1}) and clearance ratio is high (V_m/K_m > 10 L/hr). Further exploration with fixed dose and clearance show that the percent error increases at low k_a (< 1 hr^{-1}) and low V_m (<1 L/hr), but all values remain within the acceptable error range (< 0.5%) (Figure 1-5).

For two-compartment model, the established equation appears to underestimate the *AUC* values in most cases based on overall negative error values in Figure 1-6. The highest errors are greater than 1% in all cases, which is not acceptable as they exceed the cumulative truncation error by too large a margin. Especially with low dose (less than 100 mg/kg) and high clearance ratio (V_m/K_m > 8 L/hr), the percent error in *AUC* estimation becomes very significant. The percent error was also shown to be affected significantly by low V_m and low inter-compartment clearance (CL_D) (Figure 1-7). When CL_D was lower than 0.5 L/hr, the error rose to 10% and higher (~ 50%) with decreasing V_m.

DISCUSSION

Since the differential equations explaining model (ii) to (iv) cannot be integrated. Using the proposed equation is an alternative way to approximate *AUC* values of drugs following these nonlinear processes.

For a one-compartment with 1st-order absorption model, our proposed equation overall gives a very good prediction, except at low absorption rate and high clearance ratio, which might indicate flip-flop kinetics. This might suggest a limitation of this proposed equation for sustained-release formulations for drugs that follow nonlinear pharmacokinetics.

For two-compartment i.v. model, the use of the established equation appears to be only limited to conditions of low dose and high clearance ratio, with percent error lower than 1%. A possible explanation may be that when drug concentrations are substantially lower or higher than K_m, the plasma concentration–time profile of the drug transforms from nonlinear to linear (first-order/zero-order) kinetics.

Table 1-1. Factors causing dose-dependent pharmacokinetics

Cause	Drug
GI Absorption	
Saturable transport in gut wall	Riboflavin, gebapentin, L-dopa, baclofen
Intestinal metabolism	Salicylamide, propranolol
Drugs with low solubility in GI but relatively high dose	Chorothiazide, griseofulvin, danazol
Saturable gastric or GI decomposition	Penicillin G, omeprazole, saquinavir
Distribution	
Saturable plasma protein binding	Phenylbutazone, lidocaine, salicylic acid, ceftriaxone, diazoxide, phenytoin, warfarin
Cellular uptake	Methicillin (rabbit)
Tissue binding	Imiprimine (rat)
CSF transport	Benzylpenicillins
Saturable transport into or out of tissues	Methotrexate
Renal Elimination	
Active secretion	Mezlocillin, para-aminohippuric acid
Tubular reabsorption	Riboflavin, ascorbic acid, cephapirin
Change in urine pH	Salicylic acid, dextroamphetamine
Metabolism	
Saturable metabolism	Phenytoin, salicyclic acid, theophylline, valproic acid
Cofactor or enzyme limitation	Acetaminophen, alcohol
Enzyme induction	Carbamazepine
Altered hepatic blood flow	Propranolol, verapamil
Metabolite inhibition	Diazepam
Note: Capacity-limited metabolism is the most common and fundamentally important nonlinear mechanism in pharmacokinetics.	
Biliary Excretion	
Biliary secretion	Iodipamide, sulfobromophthalein sodium
Enterohepatic recycling	Cimetidine, isotretinoin

Table 1-2. A Summary of Definitions and Characteristics of Linear and Nonlinear Kinetics in a One-Compartment System

Kinetics	**Linear**	**Nonlinear**	
Definition	**First-order kinetics**	**Zero-order kinetics**	**Michaelis-Menton kinetics**
Elimination rate [d*C*(t)/dt]	$-k \cdot C(\mathrm{t})$	$-k_0$ (constant)	$-\frac{V_{\max} \cdot C(\mathrm{t})}{K_{\mathrm{m}} + C(\mathrm{t})}$
Systemic clearance	Constant	Inversely related with *C*(t)	Constant at low *C*(t) and inversely related to *C*(t) at high *C*(t)
Slope of plasma concentration-time profile after iv. Injection on a semilog scale	$-k/2.303$	No definitive description available	Changing from shallower slopes at high concentratoins during the initial phase to steeper slopes reaching $-V_{\mathrm{m}}/(2.303 \cdot K_{\mathrm{m}})$ at low concentrations during the terminal phase
Synonyms	Dose (concentration) independent kinetics	Dose (concentration) dependent, or capacity-limited kinetics	

Table 1-3. Four typical pharmacokinetic models following nonlinear elimination

Theoretical Models	Differential equations
(i) One-Compartment IV-Bolus administration	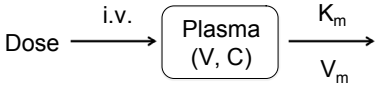 $\frac{dC}{dt} = -\frac{V_m{}' C}{K_m + C}, \quad V_m{}' = V_m/V$
(ii) One-Compartment 1st-order absorption (Oral)	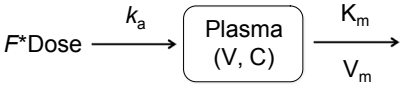 $\frac{dC}{dt} = \frac{k_a FD}{V} e^{-k_a t} - \frac{V_m{}' C}{K_m + C}$
(iii) Two- Compartment IV-Bolus administration	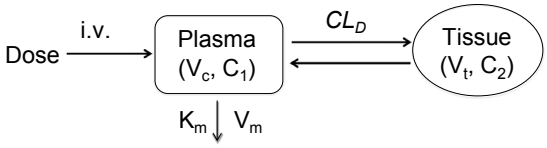 $\frac{dC_1}{dt} = k_{21}C_2 - k_{12}C_1 - \frac{V_m{}' C_1}{K_m + C_1}$ $\frac{dC_2}{dt} = k_{12}C_1 - k_{21}C_2$
(iv) Two-Compartment 1st-order absorption (Oral)	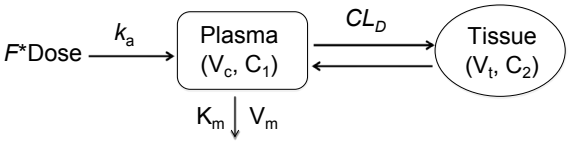 $\frac{dC_1}{dt} = \frac{KaFDe^{-Ka\cdot t}}{V_1} + \frac{CL_D}{V_t}C_2 - \frac{CL_D}{V_c}C_1 - \frac{V_m{}' \cdot C_1}{K_m + C_1}$ $\frac{dC_2}{dt} = \frac{CL_D}{V_c}C_1 - \frac{CL_D}{V_t}C_2$

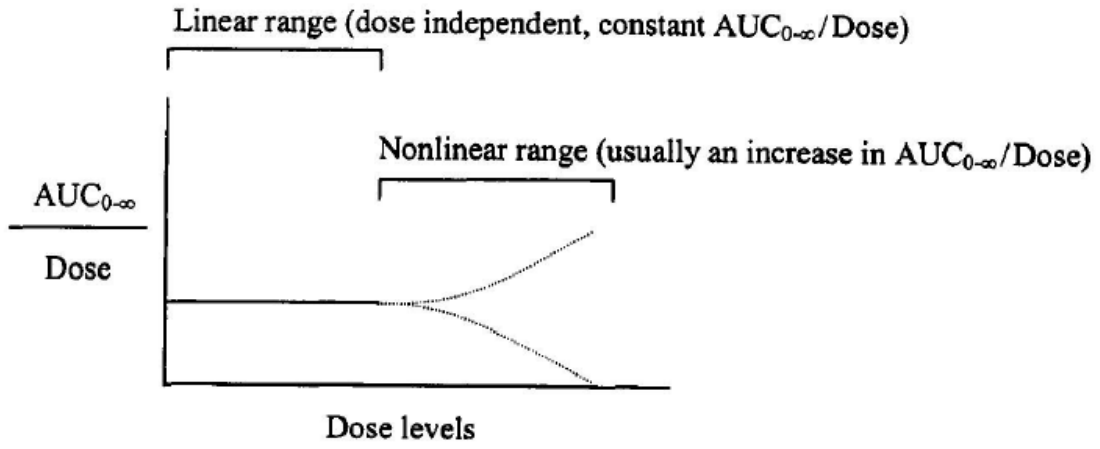

Figure 1-1. Schematic description of the relationship between dose-normalized $AUC_{0-\infty}$ and dose levels of a drug. At high dose levels, the dose-normalized $AUC_{0-\infty}$ can increase or decrease depending on the disposition properties of the drug.

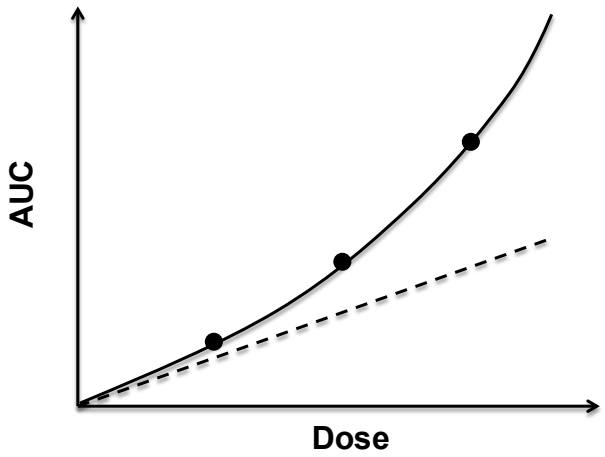

Figure 1-2. Relationship between *AUC* and dose for a compound with nonlinear pharmacokinetic properties (solid line). A drug with linear metabolism would exhibit *AUC* proportional to dose (broken line).

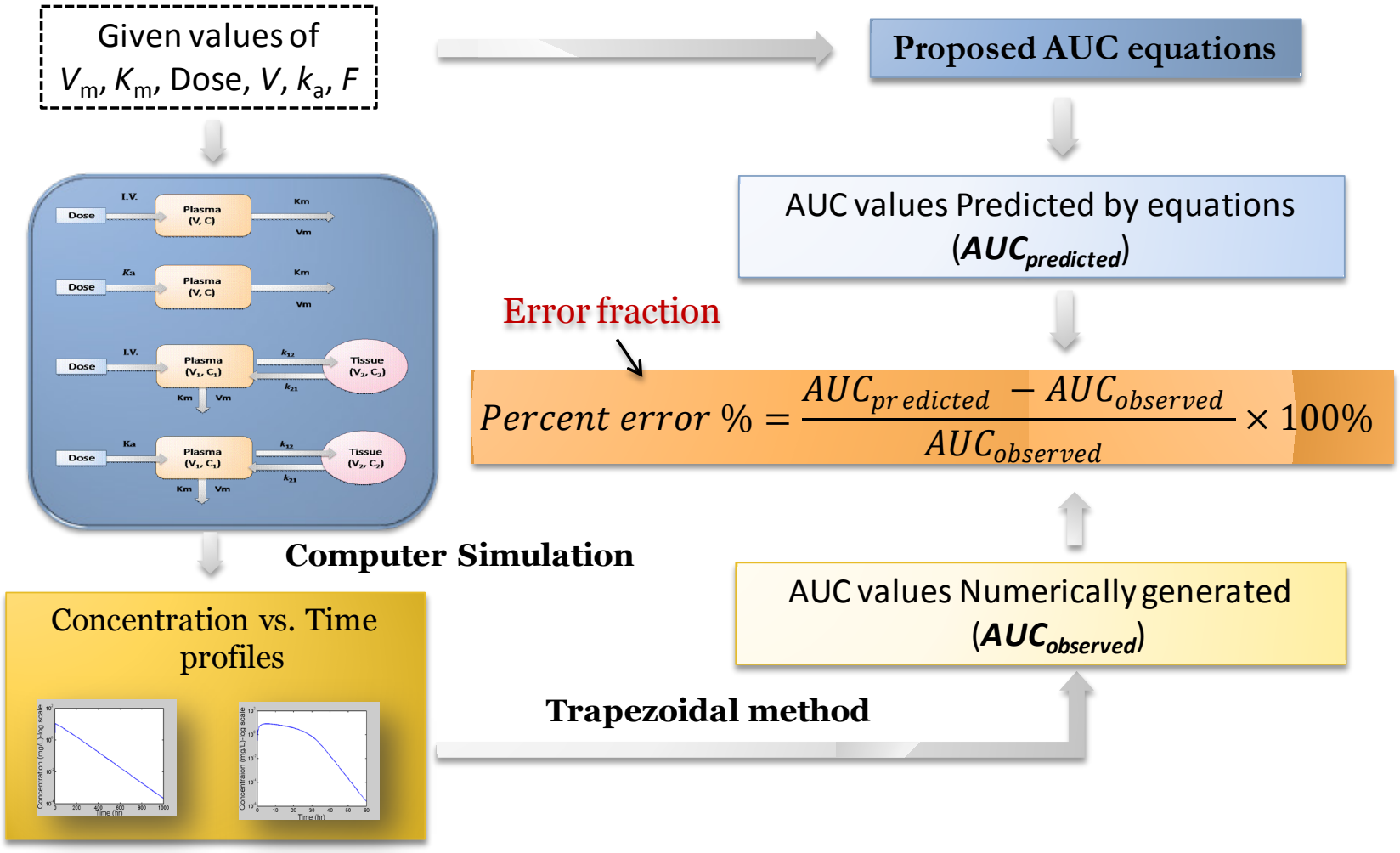

Figure 1-3. Study workflow.

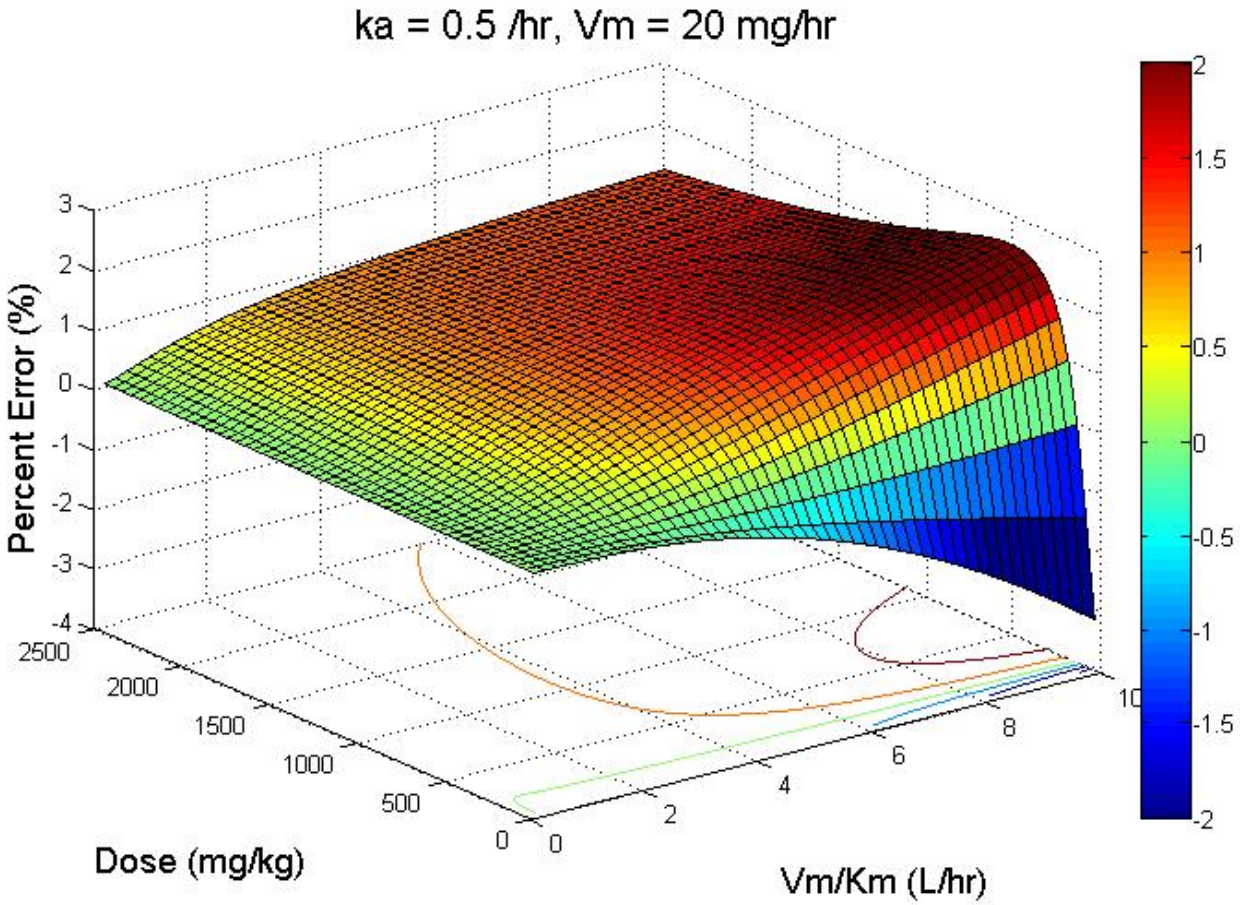

(To be continued)

Figure 1-4-A. 3D surface plot of the effect of both dose and clearance ratio (V_m/K_m) on the percent error in *AUC* determined from simulation data analysis following one-compartment 1st-Order absorption model. (k_a = 0.5 hr^{-1}, V_m = 20 mg/hr)

(Continued from last page)

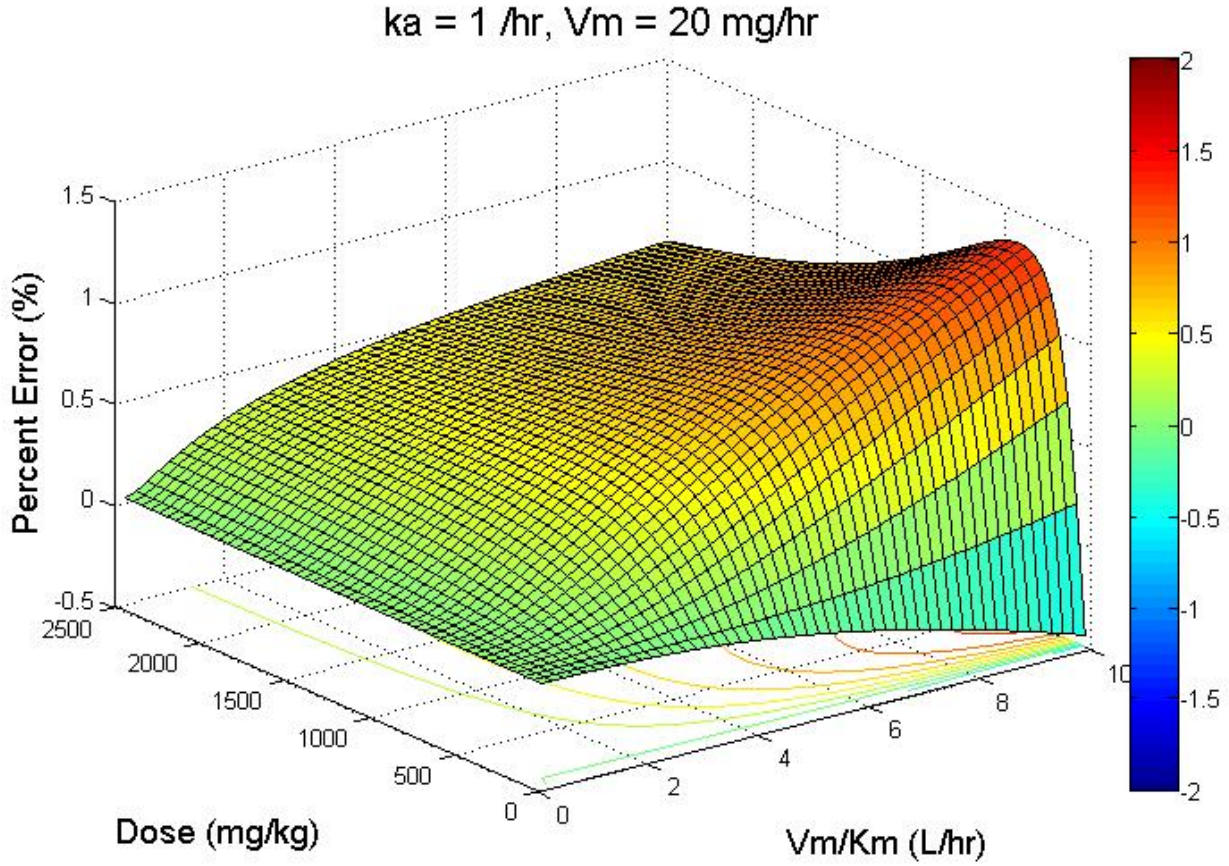

(To be continued)

Figure 1-4-B. 3D surface plot of the effect of both dose and clearance ratio (V_m/K_m) on the percent error in *AUC* determined from simulation data analysis following one-compartment 1st-Order absorption model. (k_a = 1 hr^{-1}, V_m = 20 mg/hr)

(Continued from last page)

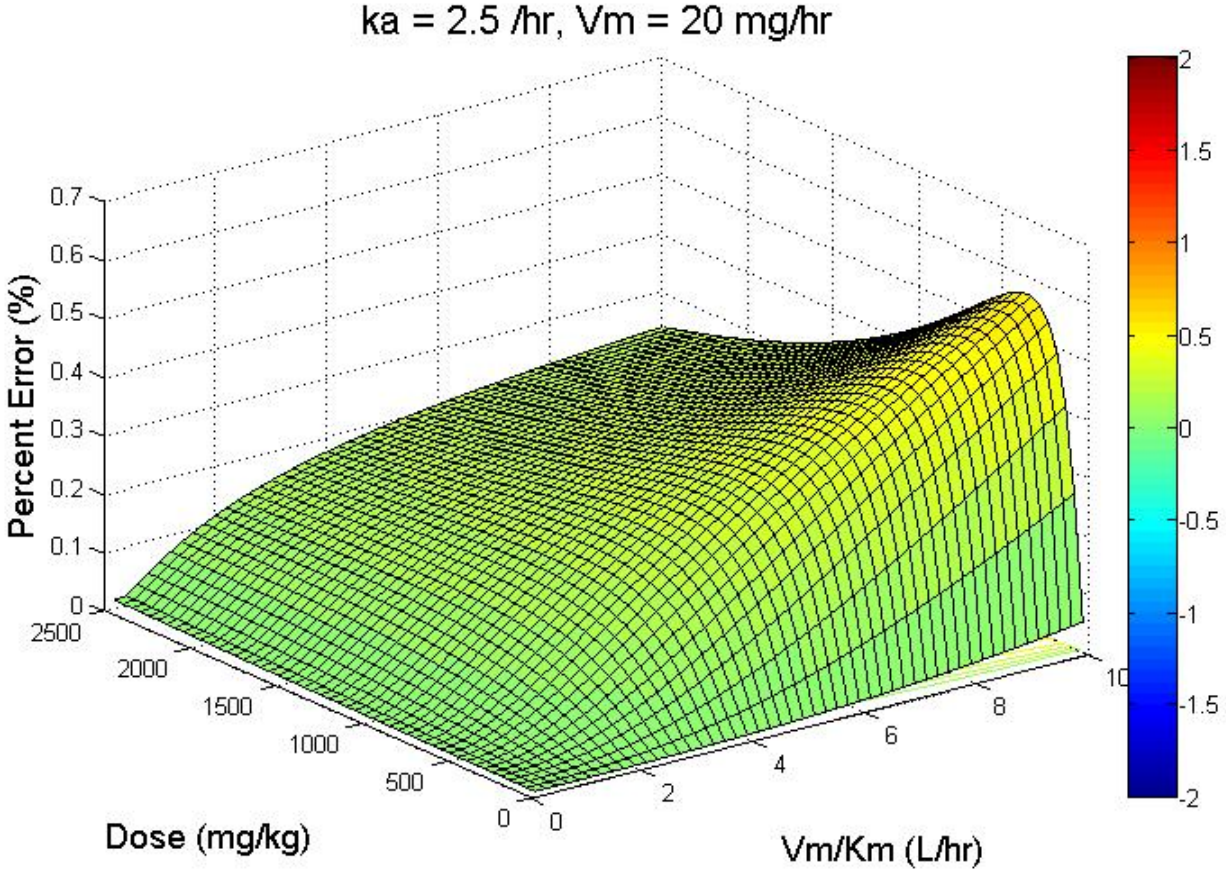

(To be continued)

Figure 1-4-C. 3D surface plot of the effect of both dose and clearance ratio (V_m/K_m) on the percent error in *AUC* determined from simulation data analysis following one-compartment 1st-Order absorption model. (k_a = 2.5 hr^{-1}, V_m = 20 mg/hr)

(Continued from last page)

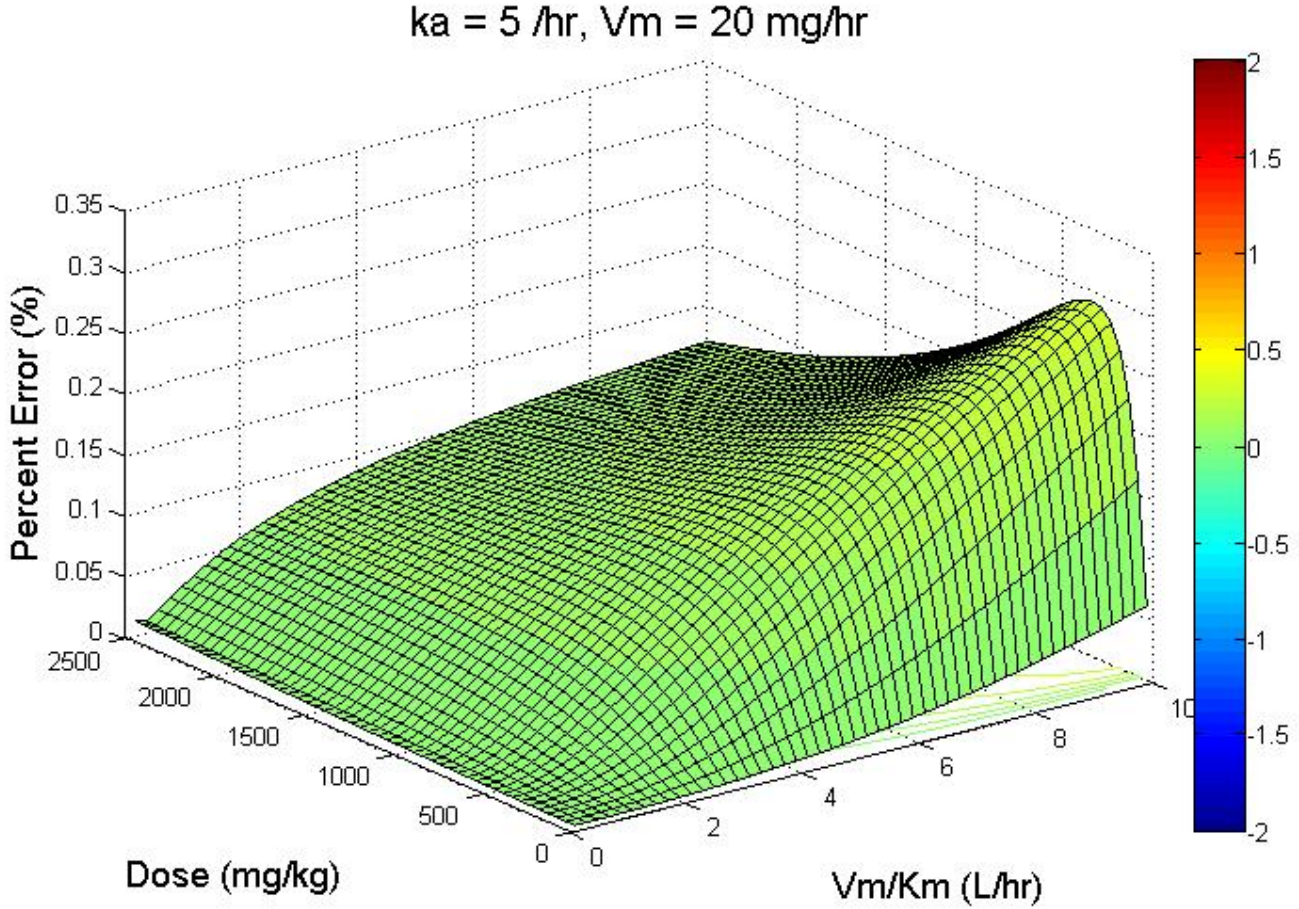

Figure 1-4-D. 3D surface plot of the effect of both dose and clearance ratio (V_m/K_m) on the percent error in *AUC* determined from simulation data analysis following one-compartment 1st-Order absorption model. (k_a = 5 hr^{-1}, V_m = 20 mg/hr)

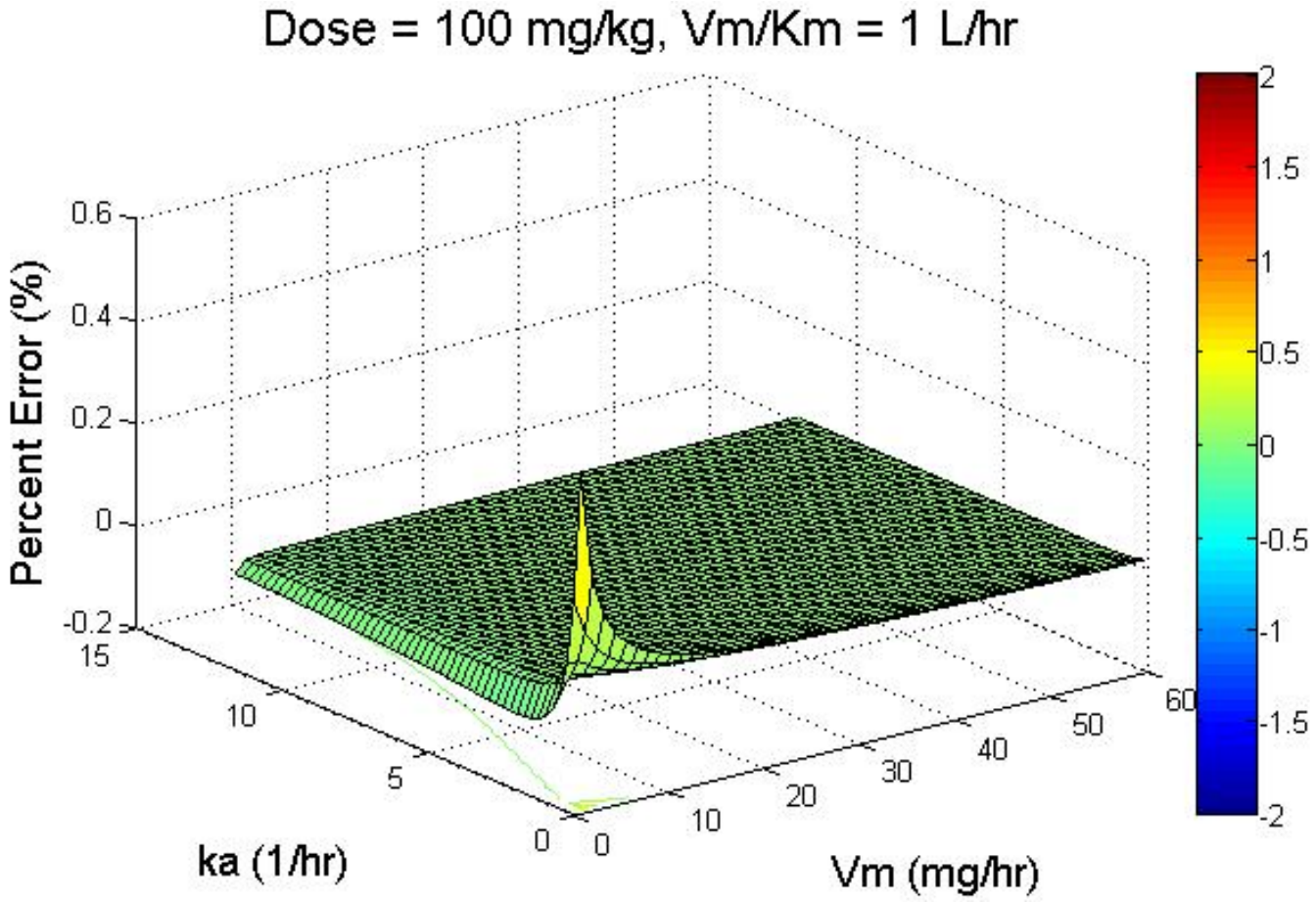

(To be continued)

Figure 1-5-A. 3D surface plot of the effect of absorption rate constant (k_a) and V_m value on the percent error in AUC determined from simulation data analysis following one-compartment 1st-order absorption model. (V_m/K_m=1 L/hr, Dose=100mg/kg)

(Continued from last page)

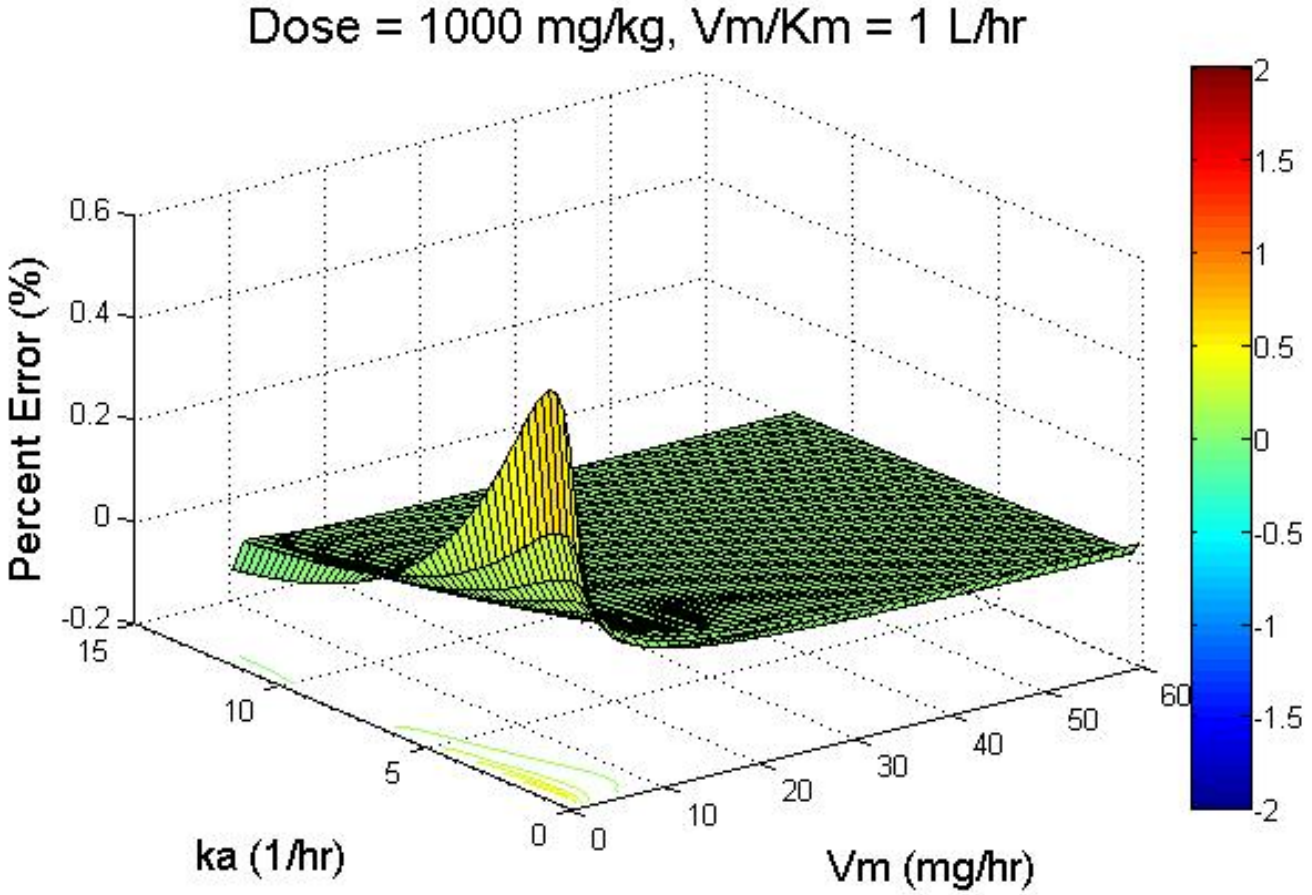

(To be continued)

Figure 1-5-B. 3D surface plot of the effect of absorption rate constant (k_a) and V_m value on the percent error in AUC determined from simulation data analysis following one-compartment 1st-order absorption model. (V_m/K_m=1 L/hr, Dose=1000 mg/kg)

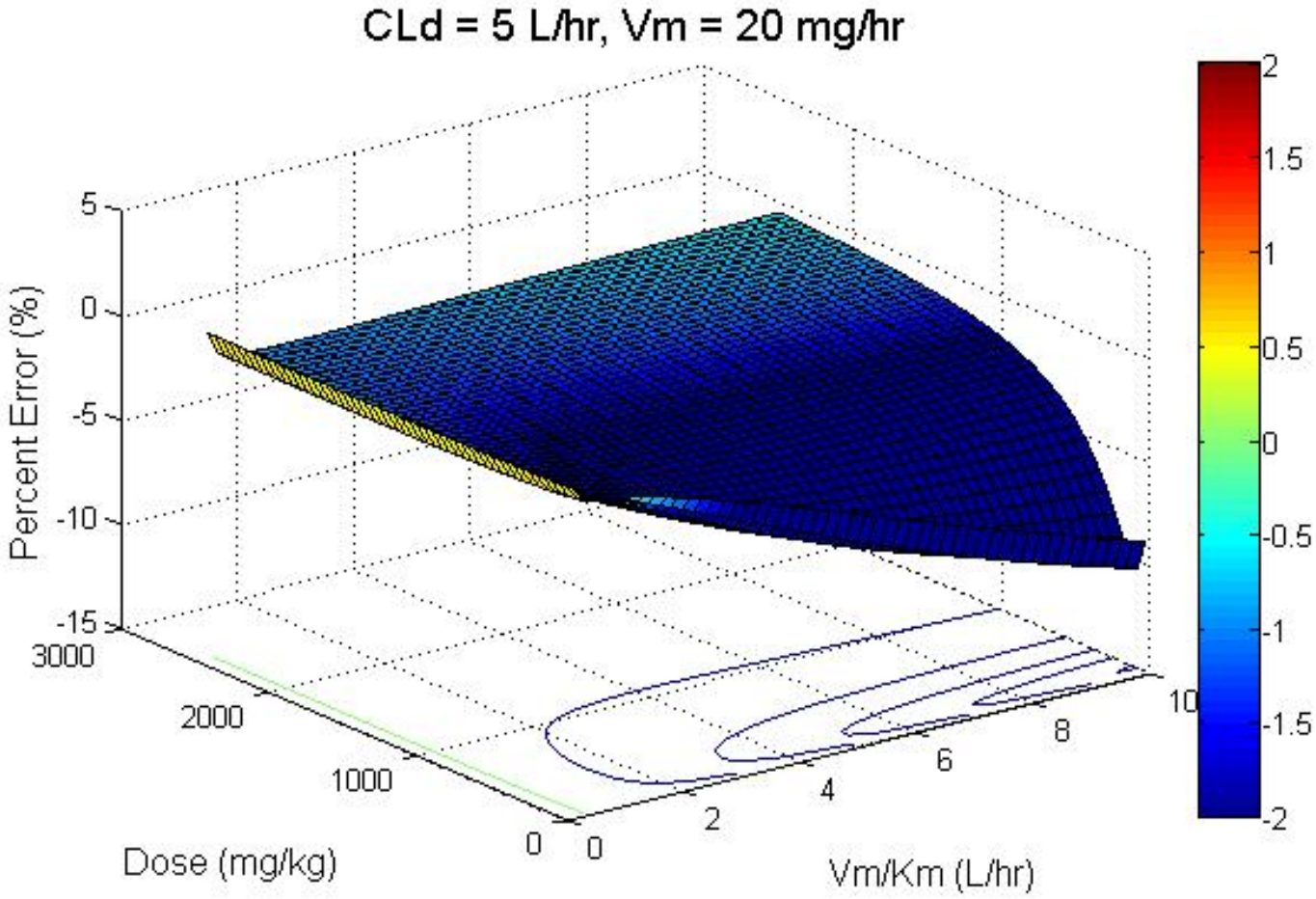

(To be continued)

Figure 1-6-A. 3D surface plot of the effect of Dose and *V*m/*K*m ratio on the percent error in *AUC* determined from simulation data analysis following two-compartment IV-Bolus administration. (CL_D = 5 L/hr, V_m = 20mg/hr).

(Continued from last page)

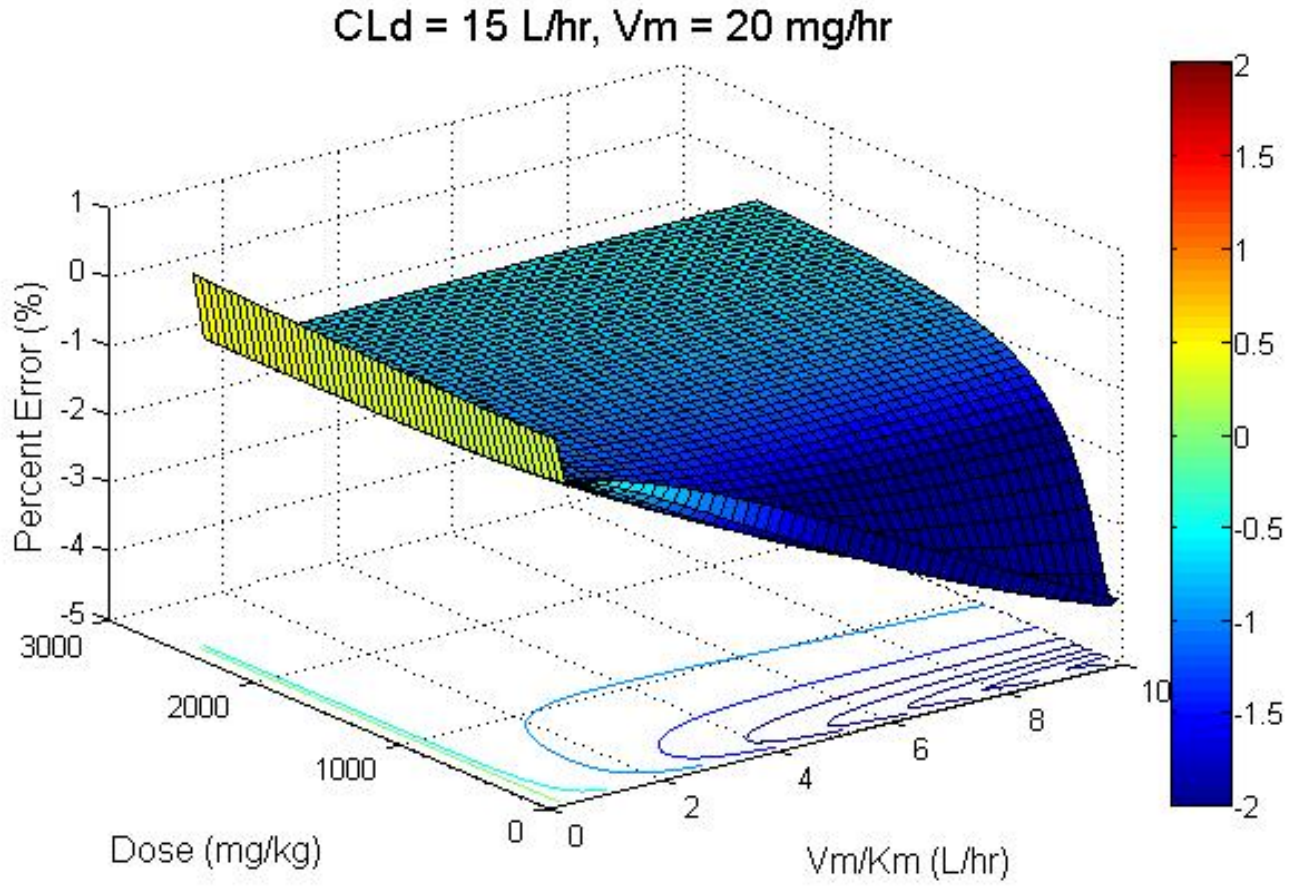

(To be continued)

Figure 1-6-B. 3D surface plot of the effect of Dose and *V*m/*K*m ratio on the percent error in *AUC* determined from simulation data analysis following two-compartment IV-Bolus administration. (CL_D = 15 L/hr, V_m = 20 mg/hr).

(Continued from last page)

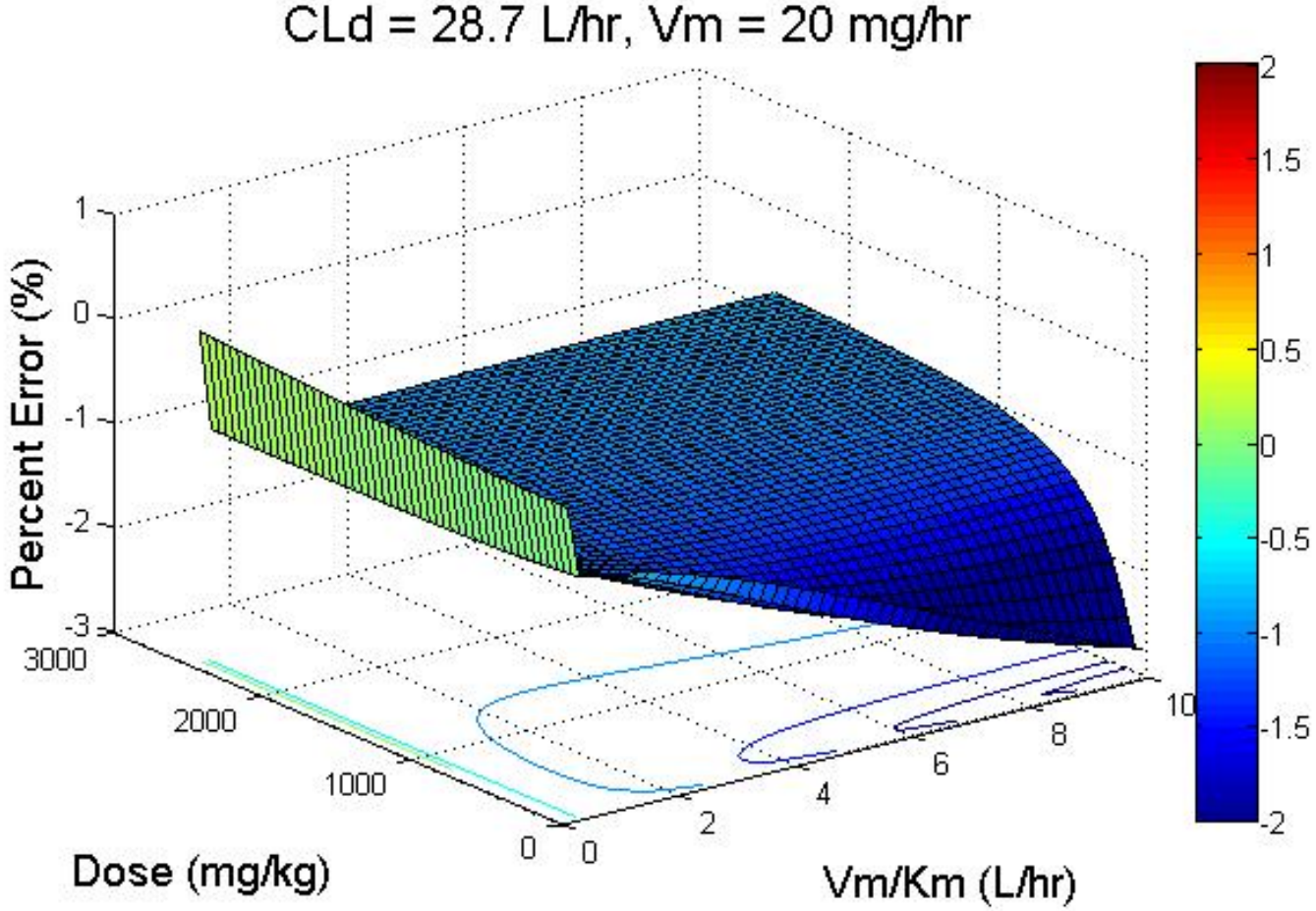

(To be continued)

Figure 1-6-C. 3D surface plot of the effect of Dose and *V*m/*K*m ratio on the percent error in *AUC* determined from simulation data analysis following two-compartment IV-Bolus administration. (CL_D = 28.7 L/hr, V_m = 20 mg/hr).

(Continued from last page)

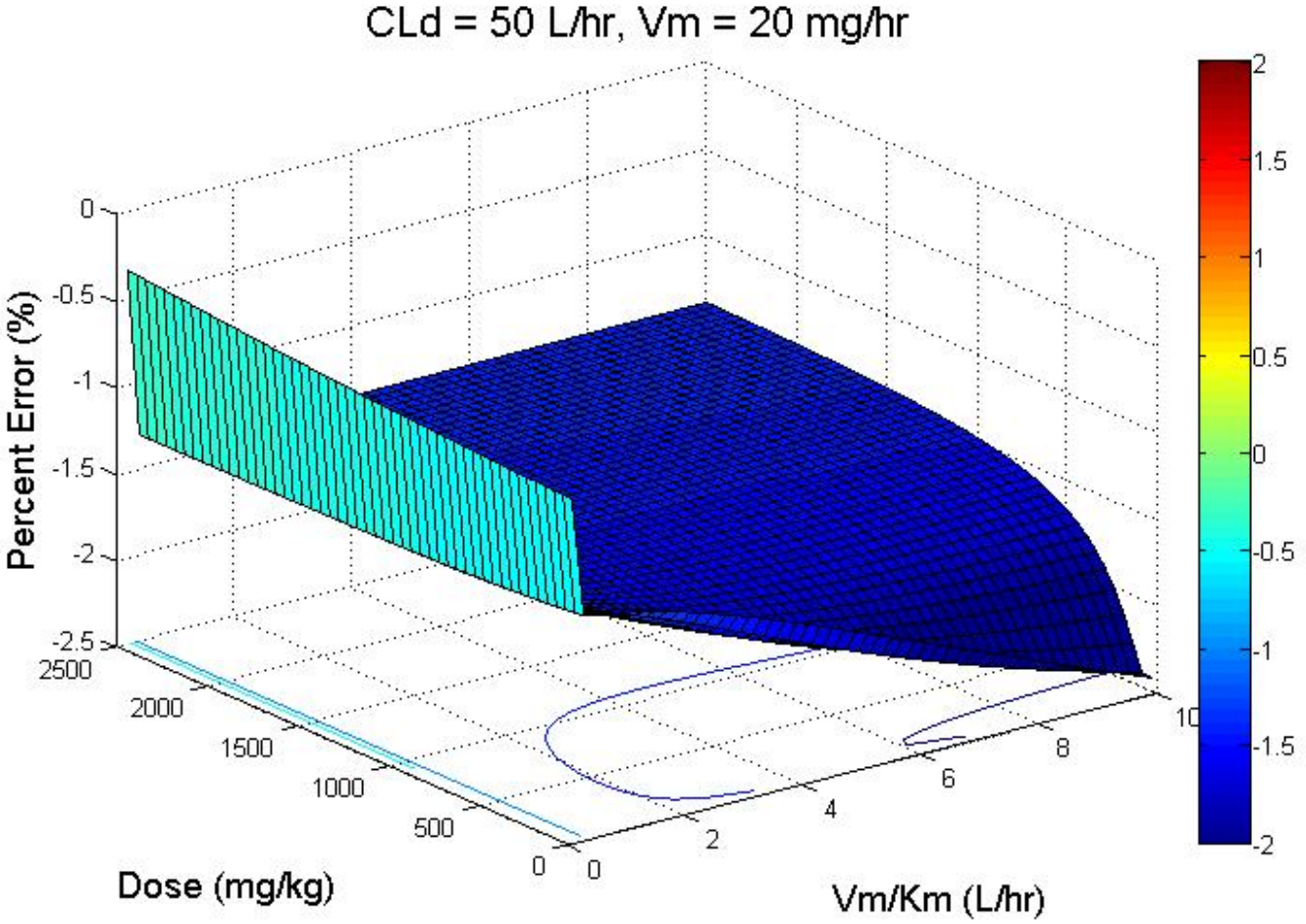

Figure 1-6-D. 3D surface plot of the effect of Dose and *V*m/*K*m ratio on the percent error in *AUC* determined from simulation data analysis following two-compartment IV-Bolus administration. (CL_D = 50 L/hr, V_m = 20 mg/hr).

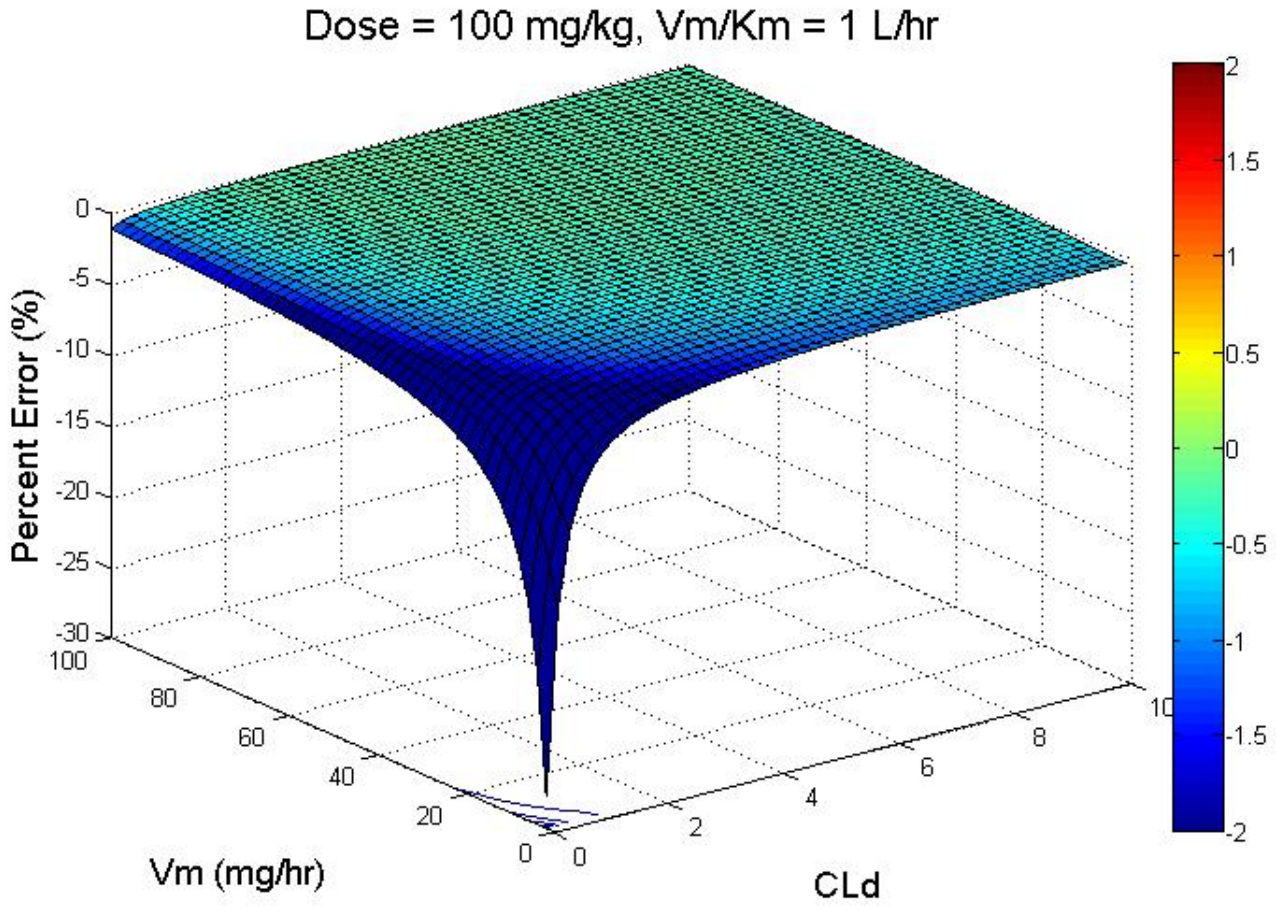

(To be continued)

Figure 1-7-A. 3D surface plot of the effect of inter-compartment distribution clearance (CL_D) and V_m value on the percent error in *AUC* determined from simulation data analysis following two-compartment IV-Bolus administration (V_m/K_m=1 L/hr, Dose=100 mg/kg).

(Continued from last page)

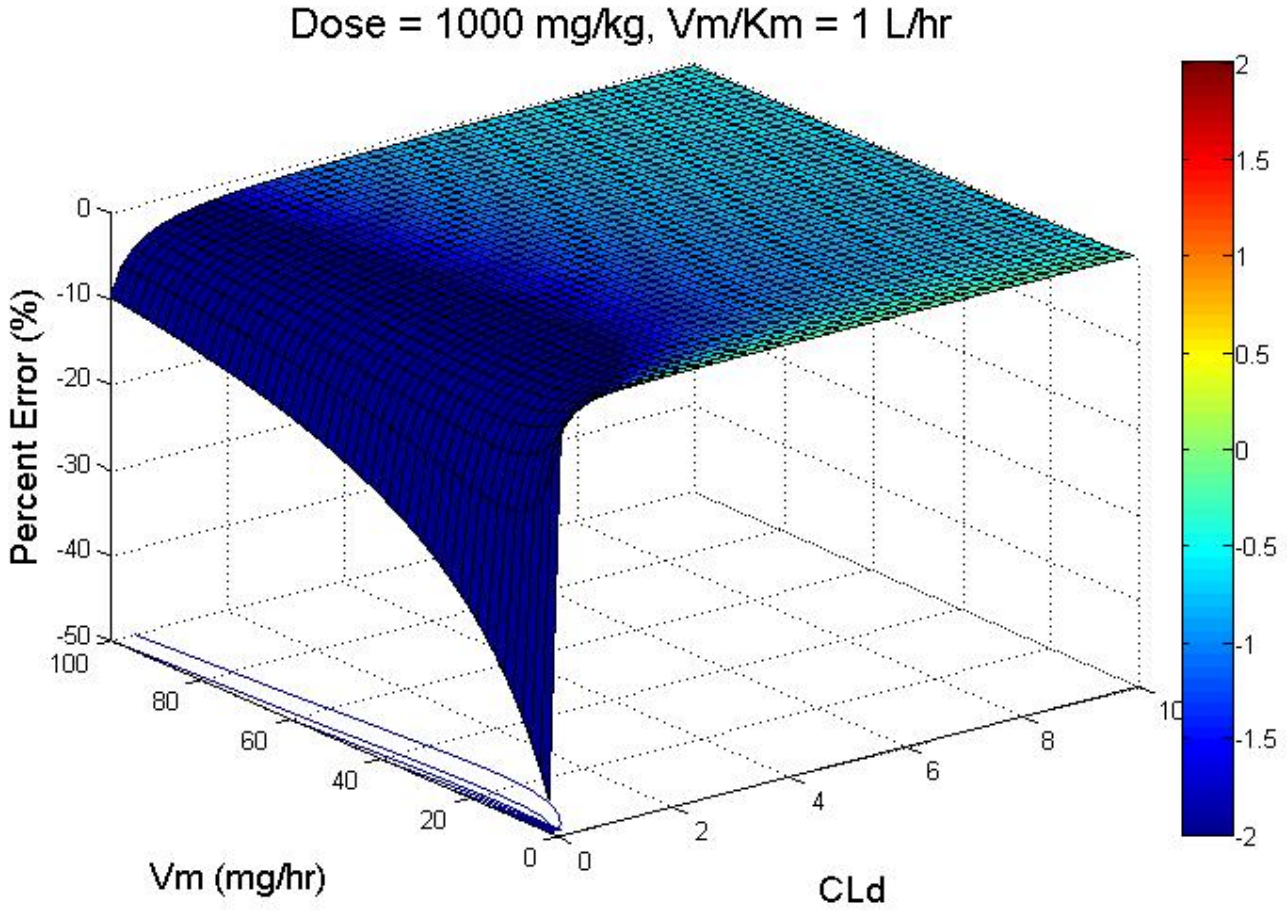

Figure 1-7-B. 3D surface plot of the effect of inter-compartment distribution clearance (CL_D) and V_m value on the percent error in *AUC* determined from simulation data analysis following two-compartment IV-Bolus administration (V_m/K_m=1 L/hr, Dose=1000 mg/kg).

APPENDICE

Runge-Kutta 4th order method

Runge-Kutta 4th order method is a numerical technique used to solve ordinary differential equation of the form

$$\frac{dy}{dx} = f(x, y), \quad y(0) = y_0$$

Runge-Kutta 4th order method is give by

$$y_{i+1} = y_i + \frac{1}{6}(k_1 + 2k_2 + 2k_3 + k_4)h$$

Where

$$k_1 = f(x_i, y_i)$$

$$k_2 = f(x_i + \frac{1}{2}h,\ y_i + \frac{1}{2}k_1 h)$$

$$k_3 = f(x_i + \frac{1}{2}h,\ y_i + \frac{1}{2}k_2 h)$$

$$k_4 = f(x_i + \frac{1}{2}h,\ y_i + k_3 h)$$

REFERENCE

Browne, T. R., G. K. Szabo, C. McEntegart, J. E. Evans, B. A. Evans, J. J. Miceli, C. Quon, C. L. Dougherty, J. Kres and H. Davoudi (1993). "Bioavailability studies of drugs with nonlinear pharmacokinetics: II. Absolute bioavailability of intravenous phenytoin prodrug at therapeutic phenytoin serum concentrations determined by double-stable isotope technique." J Clin Pharmacol **33**(1): 89-94.

Browne, T. R., G. K. Szabo, G. E. Schumacher, D. J. Greenblatt, J. E. Evans and B. A. Evans (1992). "Bioavailability studies of drugs with nonlinear pharmacokinetics: I. Tracer dose *AUC* varies directly with serum concentration." J Clin Pharmacol **32**(12): 1141-1145.

Chow, A. T. and W. J. Jusko (1987). "Application of moment analysis to nonlinear drug disposition described by the Michaelis-Menten equation." Pharm Res **4**(1): 59-61.

Jusko, W. J. (1989). "Pharmacokinetics of capacity-limited systems." J Clin Pharmacol **29**(6): 488-493.

Pancorbo, S., J. Benson, D. Goetz, K. Moore, A. Vaida and D. Johnson (1983). "Evaluation of the effect of nonlinear kinetics on dosage adjustments of theophylline." Ther Drug Monit **5**(2): 173-177.

Soiffer, R. J., C. Murray, P. Mauch, K. C. Anderson, A. S. Freedman, S. N. Rabinowe, T. Takvorian, M. J. Robertson, N. Spector, R. Gonin and et al. (1992). "Prevention of graft-versus-host disease by selective depletion of CD6-positive T lymphocytes from donor bone marrow." J Clin Oncol **10**(7): 1191-1200.

Straka, R. J., R. L. Lalonde, J. A. Pieper, M. B. Bottorff and D. M. Mirvis (1987). "Nonlinear pharmacokinetics of unbound propranolol after oral administration." J Pharm Sci **76**(7): 521-524.

Toffoli, G., I. Robieux, D. Fantin, M. Gigante, S. Frustaci, G. L. Nicolosi, M. De Cicco and M. Boiocchi (1997). "Non-linear pharmacokinetics of high-dose intravenous verapamil." Br J Clin Pharmacol **44**(3): 255-260.

Wagner, J. G. (1973). "Properties of the Michaelis-Menten equation and its integrated form which are useful in pharmacokinetics." J Pharmacokinet Biopharm **1**(2): 103-121.

Wagner, J. G., G. J. Szpunar and J. J. Ferry (1985). "Michaelis-Menten elimination kinetics: areas under curves, steady-state concentrations, and clearances for compartment models with different types of input." Biopharm Drug Dispos **6**(2): 177-200.

Wilkinson, P. K., G. Reynolds, O. D. Holmes, S. Yang and L. O. Wilkin (1980). "Nonlinear pharmacokinetics of ethanol: the disproportionate AUC-dose relationship." Alcohol Clin Exp Res **4**(4): 384-390.

CHAPTER 2

PHARMACOKINETIC ANALYSIS FOR POTENTIAL DRUG INTERACTION BETWEEN PHENYLBUTAZONE AND RANITIDINE IN THOROUGHBRED HORSES

Lian Ma, John Mark Christensen, Shun-wen Chang, Linda L. Blythe, and A. Morrie Craig

ABSTRACT

Phenylbutazone was administered to six thoroughbred horses in a cross-over design in which the horses received co-administration of ranitidine or control treatment. The study started with single-dose oral administrations of 2.2, 4.4, and 8.8 mg/kg phenylbutazone, and then multiple-dose administrations of twice daily dose of 2.2, 4.4, and 8.8 mg/kg phenylbutazone with a 1-week washout period between trials.

Blood samples were collected at various times up to 24 hr. after single-dose and up to 72 hr. after multiple-dose phenylbutazone administration. Pharmacokinetic analyses were performed for phenylbutazone, and its major metabolites oxyphenbutazone and γ-hydroxyphenylbutazone.

Twelve-hr single-dose and 72-hr multiple-dose plasma concentration profiles of phenylbutazone with concomitant ranitidine treatment were not significantly different from the control. The observed pharmacokinetic parameters were not altered by ranitidine treatment either.

The results suggest that concurrent treatment with ranitidine and phenylbutazone does not result in elevations of plasma phenylbutazone concentrations. Ranitidine should be safe to be co-administered with phenylbutazone in thoroughbred horses.

INTRODUCTION

Phenylbutazone, a pyrazolone nonsteroidal anti-inflammatory drug (Murray and Brater), works primarily through inhibition of the arachidonic acid cascade to decrease production of prostaglandins and thromboxane. It is a potent pain reliever, antipyretic, and anti-inflammatory agent (Figure 2-1).

Phenylbutazone has been used in veterinary medicine for more than 50 years and for 30 years it was the drug of choice as an analgesic and anti-inflammatory agent in companion and farm animal medicine. It has also been used in racing animals to treat bone and joint inflammation, laminitis, and soft-tissue inflammation.

The major metabolites so far identified in the horse include oxyphenbutazone (ring hydroxylation) and γ-hydroxyphenylbutazone (side-chain hydroxylation), accounting for some 25-30% of administered dose over 24 hr (Figure 2-2). Less than 2% is excreted in the urine as parent phenylbutazone over 24 h (Maylin 1974; Lees, Creed et al. 1983). The plasma half-life of phenylbutazone and termination of its pharmacological action are determined primarily by its rate of hepatic metabolism.

Side effects of phenylbutazone are similar to that of other NSAIDs. Overdose or prolonged use can cause gastrointestinal ulcers, blood dyscrasia, kidney damage, oral lesions, and internal hemorrhage. The primary toxicities of this drug in horses are oral and gastrointestinal ulceration and a protein losing gastroenteropathy (Snow, Bogan et al. 1979; Snow, Douglas et al. 1980; Traub 1982; Collins and Tyler 1984). While phenylbutazone dosage varies with the treatment regime, 8.8 mg/kg/day is reported to be the maximum safe dose by Collins & Tyler (1984).

Ranitidine is a Histamine H2-receptor antagonist that inhibits stomach acid production. It can be co-administered with NSAIDs to reduce the risk of ulceration. The elevated gastric pH caused by ranitidine may increase

dissolution and absorption of phenylbutazone, as phenylbutazone's dissolution and absorption from the stomach and small intestine are influenced by gastric pH (Mooney, Rodriguez-Gaxiola et al. 1981). Concurrent use of these two agents may cause enhanced phenylbutazone absorption from the gastrointestinal track resulting in higher plasma concentration.

In addition, there is increasing evidence that ranitidine interferes with the hepatic elimination of several drugs (Smith and Kendall 1988; Klotz and Kroemer 1991). Ranitidine has been reported to be an inhibitor of microsomal P-450 enzymes in the liver responsible for drug metabolism, especially hydroxylation and oxidation reactions (Kirch, Hoensch et al. 1984). Phenylbutazone is metabolized by the same mixed function oxidase system (Van Peer, Belpaire et al. 1980). Thus, there may be a concurrent reduction in clearance of phenylbutazone when these two drugs are used simultaneously.

Both effects could result in higher plasma phenylbutazone concentrations, especially with long term use, that may exceed the concentrations permitted in racing horses and cause potential toxic effects. The current study was performed to evaluate the pharmacokinetics of phenylbutazone as well as its major metabolites with the concurrent administration of ranitidine for potential drug interaction.

MATERIALS AND METHODS

Animals and study design

Six mature racing Thoroughbred mares ranging in weight from 436 to 604 kg were used in the study. Physical examination of each horse was performed prior to the start of study. They were fed alfalfa pellets twice a day (8 a.m. and 4 p.m.) at 2% body weight/day and had free access to water.

The study follows a single cross-over design. The horses were initially placed into two groups (A and B) by randomization. Phenylbutazone tablets (Sigma Chemical Co., St Louis, MO) were crushed, mixed with 1 L of water and administered via a stomach tube. Horses in group A received single and multiple oral doses of 2.2 mg/kg, 4.4 mg/kg and 8.8 mg/kg phenylbutazone, with co-treatment of 150 mg/70kg ranitidine via a stomach tube at the same time when phenylbutazone was given. Multiple dose was given at 8 a.m. on the first day, and then at 12, 24, 36, 48, 60 hr following the first dose. Treatments were given subsequentially 7 days apart.

Horses in group B received single and multiple oral doses of phenylbutazone at 2.2 mg/kg, 4.4 mg/kg and 8.8 mg/kg in the same fashion as in group A, only without co-administration of ranitidine. A week later, each group switched treatments receiving the same materials and techniques described above for the other treatments. With the cross-over treatment regime, each horse served as its own control.

Single i.v. dose of 2.2 mg/kg phenylbutazone was also administered in 6 horses with or without 150mg/70kg of Ranitidine administration.

Heparinized blood samples (~10 mL) were collected at 0, 0.25, 0.5, 0.75, 1, 1.5, 2, 4, 6, 8, 10, 12 and 24 hr following single-dose phenylbutazone administration. Samples for multiple doses were collected at 0, 0.25, 0.5, 0.75, 1, 1.5, 2, 4, 6, 8, 10, 12, 14, 24, 26, 36, 38, 48, 48.25, 48.5, 48.75, 49, 49.5,

50, 52, 54, 56, 58, 60 and 72 hr post-administration. The collection time was extended to 168 hr for multiple dosing of 8.8 mg/kg. At 1 hr following blood collection, samples were centrifuged, and plasma was harvested and stored at -20°C until analyses.

Analytical analysis

Plasma concentrations of phenylbutazone, oxyphenbutazone and γ-hydroxyphenylbutazone were determined by a high performance liquid chromatographic (HPLC) method based on that of Shargel et al. (L Shargel, P.J. Breen & S. Ponichpol, personal communication). The HPLC system (Water Associates, Milford, MA) consisted of an automatic liquid chromatographic injector (Linear Systems Corp., Irvine, CA), a U.V. spectrophotometer detector set at 254 nm and a strip chart recorder with integrator. Acetonitrile (J.T. Baker, Phillipsburg, NJ) and methanol were the HPLC solvents used. A precolumn (Altec Associates, Arlington Heights, IL) packed with Bondapak, C_{18}/corasil, 37-50 μm particle size and a chromatographic column (Bondapak, C_{18}, 5 μm particle size; Waters Associates, Milford, MA) were used. The mobile phase was maintained at 25°C and consisted of 50% (v/v) 0.05 M KH_2PO_4 at pH 5.5 and methanol. The mobile phase was filtered and degassed using a Millipore filter. Flow rate was 1.8 mL/min. Injection volumes were 25 or 50 μL.

Known phenylbutazone, oxyphenbutazone, and γ-hydroxy-phenylbutazone standards (Ciba-Geigy Pharmaceuticals, Summit, NJ, and Basel, Switzerland) were compared to plasma samples. These standards were dissolved in acetonitrile to give a solution containing 1 mg/5 mL of each. Two-milliliter aliquots of equine plasma were spiked with this solution to give samples containing 0, 0.1, 0.2, 0.5, 1, 2.5, 5, 10, 15, 20, 30 and 50 μg/mL of each component. The standard phenylbutazone, oxyphenbutazone and γ-hydroxyphenylbutazone concentration curves were prepared daily by processing control plasma samples containing known concentrations

concurrently with the unknown plasma samples. A control sample containing 10 μg/mL of phenylbutazone and its metabolites in methanol was run once every ten injections.

To each plasma sample containing known or unknown concentrations of phenylbutazone and its metabolites was added an equal volume of acetonitrile containing antipyrine (internal standard). The antipyrine concentration in the acetonitrile was 5 μg/mL. The deproteinized mixture was centrifuged to 12000 r.p.m. for 15 min. The supernatant solution was removed and subjected to HPLC.

Standard curves for phenylbutazone were obtained by comparing the integrated area of phenylbutazone to antipyrine plotted against the phenylbutazone concentration. The oxyphenbutazone and γ-hydroxy-phenylbutazone standard curves were prepared by comparing the integrated area of the respective metabolite concentrations. Unknown plasma phenylbutazone and metabolite concentrations were calculated by comparison to standard curves. A linear relationship between absorbance and phenylbutazone concentration occurred between 0.2 and 50 μg/mL. A linear relationship also existed for the phenylbutazone metabolites. Within and between assay variation was 4.7 and 7.1%, respectively. The metabolites of phenylbutazone (oxyphenbutazone and γ-hydroxyphenylbutazone) were only detectable at concentrations greater than 0.2 μg/mL using this method.

Pharmacokinetic analysis

The phenylbutazone plasma concentration profiles of control and ranitidine treated horses were analyzed according to a one-compartment open model with first-order absorption and elimination (Gibaldi 1975). A scheme depicting this model is shown below (Scheme 2-1):

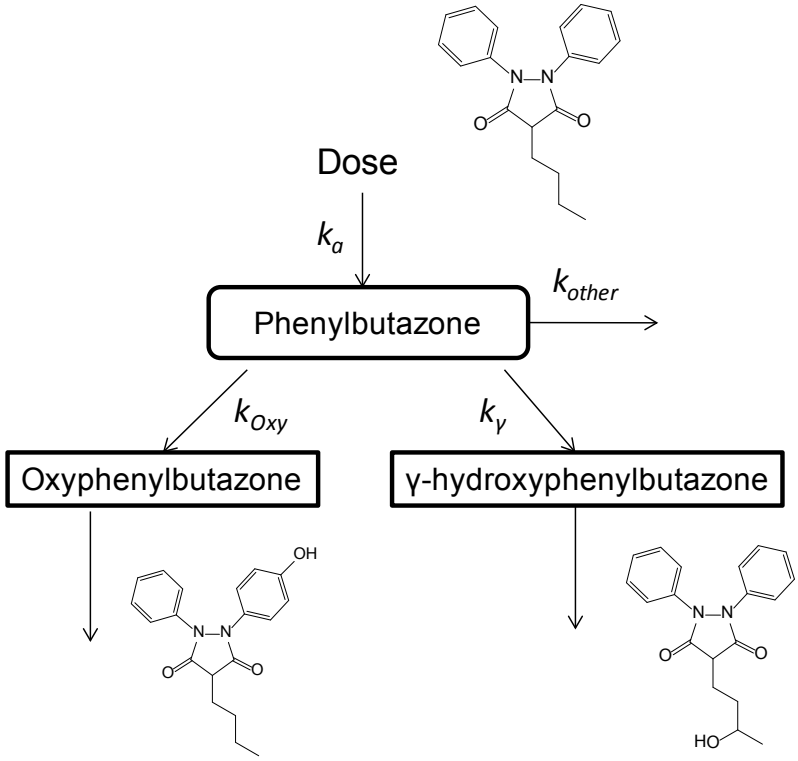

$$K_{el} = k_{Oxy} + k_\gamma + k_{other}$$

Scheme 2-1. Pharmacokinetic model for phenylbutazone in horses

Pharmacokinetic parameters k_a, k_{el}, volume of distribution (*V/F*), clearance (*CL/F*), time to peak plasma concentration (T_{max}), peak plasma concentrations (C_{max}). half-life ($t_{1/2}$) and the area under the plasma concentration time curve (*AUC*) were estimated by fitting this model to the experimental results obtained from i.v.-dosed and oral-dosed animals. Non-compartmental analysis was used for oxyphenbutazone and γ-hydroxyphenylbutazone. $t_{1/2}$, *CL/F*, T_{max}, C_{max}, *AUC, MRT* were determined for oxyphenbutazone and γ-hydroxyphenylbutazone. The plasma concentration profiles of ranitidine were also analyzed based on a two-compartment open model with first-order absorption and biexponential elimination. Optimized estimates for the model parameters were obtained by using nonlinear regression analysis (WinNonlin 5.3; Pharsight, Mountain View, CA).

Statistical analysis

The pharmacokinetic parameters for control and ranitidine treatment were compared using Wilcoxon Signed-Rank Test for statistical significant differences (R version 2.13.2). One-way ANOVA Tests were performed to assess dose-dependency of major pharmacokinetic parameters across three dosing levels.

RESULTS

Plasma concentration profiles

The mean plasma concentration profiles for phenylbutazone, oxyphenbutazone and γ-hydroxyphenylbutazone following single doses (2.2 mg/kg, 4.4 mg/kg and 8.8 mg/kg) of phenylbutazone are depicted in Figure 2-4, 2-5 and 2-6, respectively. Plasma concentration profiles following multiple doses (b.i.d.) are shown in Figure 2-7, 2-8 and 2-9. Plasma concentrations of phenylbutazone were higher than the metabolites at each time. This is in agreement with the findings of other investigators (Maylin 1974; Gerring, Lees et al. 1981; Soma, Gallis et al. 1983). The mean plasma concentration profiles for ranitidine following single and multiple doses (2.14 mg/kg) of ranitidine and co-administration of phenylbutazone are shown in Figure 2-10 and 2-11.

The phenylbutazone plasma concentrations for the ranitidine treatment are higher than control at the times near peak plasma concentrations. Over the first 4 hr, averaged plasma concentrations of ranitidine-treated horses ranged from 51-125%, 21-55% and 30-49% greater than the control values, after single oral dosing of 2.2 mg/kg, 4.4 mg/kg and 8.8 mg/kg phenylbutazone respectively (Figure 2-4). However, these differences were not statistically significant after accounting for the variability between individual horses. For multiple dosing, similar trend is observed with horses receiving 2.2 mg/kg and 4.4 mg/kg of phenylbutazone, but not with the ones receiving 8.8 mg/kg (Figure 2-7).

The mean plasma concentrations of oxyphenbutazone and γ-hydroxyphenylbutazone with ranitidine treatment (Figure 2-5, 2-6) were also higher than control during the first 4 hr after administration of phenylbutazone. The differences were 33-98% and 31-114% following the 2.2 mg/kg doses, and 33-100% and 37-227% following the 4.4 mg/kg doses. For the 8.8 mg/kg dosing groups, the plasma concentrations appear to be equivalent with control

values. There was no difference between ranitidine-treated horses and control in the concentration profile following multiple doses (Figure 2-8, 2-9).

There were no significant difference in ranitidine's concentration profile following multiple co-administrations of 2.2 mg/kg and 8.8 mg/kg phenylbutazone (Figure 2-11).

Pharmacokinetic parameters

The estimated pharmacokinetic parameters for i.v. and oral administered phenylbutazone are presented in Table 2-1. Parameter estimates from Non-compartmental analyses for oxyphenbutazone and γ-hydroxyphenylbutazone are presented in Table 2-2 to Table 2-3. The observed values compare favorably with the values previously reported for phenylbutazone in horses (Gerring, Lees et al. 1981; Soma, Gallis et al. 1983; Tobin, Chay et al. 1986).

For 2.2 mg/kg doses, the peak phenylbutazone concentration was observed at 5.02 ± 2.05 and 5.41 ± 1.6 hr for ranitidine treatment and controls, whereas $t_{1/2}$ was 3.53 ± 1.20 and 4.06 ± 4.38 hr for ranitidine treatment and controls, respectively. For 4.4 mg/kg doses, the peak phenylbutazone concentration was observed at 5.22 ± 2.15 and 4.79 ± 1.60 hr, whereas $t_{1/2}$ was 3.59 ± 1.30 and 3.67 ± 4.80 hr for ranitidine treatment and controls. For the 8.8 mg/kg doses, the phenylbutazone concentration reached peak levels earlier at 2.47 ± 0.72 and 2.51 ± 0.43 hr, with $t_{1/2}$ equals to 2.10 ± 0.44 and 1.96 ± 0.51 hr for ranitidine treatment and controls, respectively.

For further comparison, boxplots of pharmacokinetic parameters between treatment groups are shown in Figures 2-12 to 2-14. No statistical difference was seen in the shown pharmacokinetic parameters between control and ranitidine treatments among three dose levels.

The dose-normalized C_{max} and *AUC* values for phenylbutazone at 8.8 mg/mL doses were significantly higher compared to the ones at lower dose

levels (p-value < 0.05 from one-way ANOVA test). This confirmed that phenylbutazone follows nonlinear pharmacokinetics in horses (Tobin, Chay et al. 1986). The $t_{1/2}$ at 8.8 mg/mL was also found shorter than the other two dose groups. It is probably due to the terminal phase of elimination was not captured for the 2.2 and 4.4 mg/mL groups (concentration lower than LOD). Since the terminal phase should be linear, the rate of elimination is higher than the earlier phase where the elimination was still saturated, therefore resulting in a shorter half-life.

The dose-dependent pharmacokinetics was also observed for oxyphenbutazone and γ-hydroxyphenylbutazone (Figures 2-13, 2-14). There were significant increases of dose-normalized C_{max} and AUC values at 8.8 mg/mL compared to the lower levels.

The estimated pharmacokinetic parameters for orally dosed 2.14 mg/kg ranitidine with co-administration of 8.8 mg/kg phenylbutazone are presented in Table 2-4. The results differed from those reported previously from single dose study of ranitidine in horses (Holland, Ruoff et al. 1997). The values of clearance (3.12 L/hr/kg), apparent volume of distribution (25.6 L/kg) and terminal half-life (4.58 hr) obtained from the current study, were all higher than that reported (0.58 L/hr/kg, 1.12 L/kg and 1.4 hr). The time to peak, however, was similar in the horses currently used with co-administered phenylbutazone (1.2 hr), compared to the value obtained from horses under ranitidine alone treatment (1.25 hr).

DISCUSSION

There have been reports that ulcers are the most common pathological feature of phenylbutazone overdose or toxicity in horses (Snow, Bogan et al. 1979; Traub 1982; Collins and Tyler 1984). It is also becoming common practice to use H2 receptor antagonists in veterinary medicine for the prophylactic, short-term, and maintenance therapy of equine gastric ulcers (Becht and Byars 1986; MacAllister, Qualls et al. 1987; Furr and Murray 1989; Murray 1992). The extension of the use of this therapeutic agent to race horses receiving high doses (8.8 mg/kg) of phenylbutazone over extended periods of time is predicted.

However, by mechanism there is potential drug interaction between these two agents. Firstly, H2-antagonists bind to cytochrome P450 and may inhibit the metabolism of phenylbutazone, which mediated by the mixed function oxygenase system. Secondly, H2-antagonists inhibit gastric acid production and may alter the rate of gastric emptying, and hence the rate of phenylbutazone's dissolution and absorption, which has been shown to be influenced by gastric pH (Mooney, Rodriguez-Gaxiola et al. 1981). H2-antagonists may also have some effect on portal vein and hepatic artery flow. However, these effects are small and probably not clinically relevant (Smith and Kendall 1988).

There are three H2-receptor antagonists available for the treatment of peptic ulcer disease – cimetidine, famotidine and ranitidine. Cimetidine is well known to interact with a number of concurrently administered drugs (Smith and Kendall 1988). The interactive effect between cimetidine and phenylbutazone in horses has been reported previously (Christensen, Blythe et al. 1985). Cimetidine pretreatment was found to elevate phenylbutazone plasma concentrations during the first 8 hr after phenylbutazone administration. The absorption rate, maximum phenylbutazone plasma

concentrations and *AUC* were also significantly greater with cimetidine pretreatment.

Similar to cimetidine, by elevating the gastric pH, ranitidine could enhance absorption and thereby increase plasma concentration of phenylbutazone. However, this study has shown that horses receiving a single and multiple therapeutic dose of phenylbutazone with concurrent administration of ranitidine did not have higher plasma phenylbutazone concentrations compared to horses not treated with ranitidine. The pharmacokinetic parameters of phenylbutazone did not differ between control and ranitidine treatment. And there was only negligible influence shown on the production of oxyphenbutazone or γ-hydroxyphenylbutazone in this study.

The reason for absence of effect for ranitidine is probably due to potency difference between cimetidine and ranitidine. It has been reported that ranitidine exert an inhibitory effect on cytochrome P-450 in the liver, but to a lesser extent than cimetidine (Figure 2-13). Several drugs which are known to interact with cimetidine have been found not to interact significantly with ranitidine, including propranolol, lidocaine, phenytoin and diazepam (Kirch, Hoensch et al. 1984).

During the first 4 hr after single dose, however, the mean plasma concentrations of phenylbutazone in ranitidine treated horses were higher compared to control values. After 6 hr and up to 72 hr, plasma phenylbutazone concentrations for both ranitidine treated and untreated horses were equivalent. Although the differences were not statistically significant, the initial increase in phenylbutazone plasma concentrations in some horses was probably due to the ability of ranitidine to inhibit gastric acid secretion, resulting in a rise in gastric acid pH in these horses. Increasing the gastric pH above 5.5 may have increased the rate of phenylbutazone dissolution and absorption from the gastrointestinal tract, since it has a p*K*a of 4.50.

The higher-than-proportional increase of γ-hydroxyphenylbutazone exposure at high doses suggest further investigation on the toxicity of this metabolite in horses, as it may contribute to the side effects of phenylbutazone occurred at high dose level.

The pharmacokinetics of ranitidine in the current study show difference compared to previously reported values from horses given ranitidine alone. This indicates that the clearance of ranitidine might be altered by concurrent phenylbutazone, which requires further investigation.

CONCLUSION

Phenylbutazone and its metabolites, oxyphenbutazone and γ-hydroxyphenylbutazone showed dose-dependent pharmacokinetics with increasing dose in horses. Plasma concentrations of phenylbutazone appear to be higher with ranitidine; however, this difference did not reach statistically significant level ($p < 0.05$). Overall, concurrent ranitidine treatment has negligible influence on the pharmacokinetics of phenylbutazone and its major metabolites in thoroughbred horses.

Table 2-1. Pharmacokinetic parameters for plasma phenylbutazone with or without co-administration of ranitidine

Parameters	Units	IV	Oral					
			2.2 with R	2.2 Control	4.4 with R	4.4 Control	8.8 with R	8.8 Control
V/F	L/kg	0.12 ± 0.02	0.51 ± 0.19	0.77 ± 0.48	0.52 ± 0.09	0.89 ± 0.49	0.09 ± 0.02	0.10 ± 0.01
k_a	1/hr	N/A	0.28 ± 0.20	0.26 ± 0.14	0.26 ± 0.18	0.29 ± 0.10	0.57 ± 0.26	0.48 ± 0.15
k_{el}	1/hr	0.20 ± 0.05	0.20 ± 0.06	0.17 ± 0.07	0.19 ± 0.06	0.19 ± 0.09	0.33 ± 0.07	0.35 ± 0.09
AUC	hr*µg/mL	95.62 ± 29.67	24.95 ± 5.70	26.39 ± 13.49	49.86 ± 11.19	43.77 ± 25.31	332.12 ± 119.74	251.47 ± 48.63
$t_{1/2}$	hr	3.40 ± 1.03	3.53 ± 1.20	4.06 ± 4.38	3.59 ± 1.30	3.67 ± 4.80	2.10 ± 0.44	1.96 ± 0.51
CL/F	mL/hr/kg	18.46 ± 2.68	94.08 ± 31.35	129.43 ± 116.32	93.74 ± 29.78	147.69 ± 109.42	29.34 ± 9.84	36.21 ± 7.73
T_{max}	hr	N/A	5.02 ± 2.05	5.41 ± 1.60	5.22 ± 2.15	4.79 ± 1.60	2.47 ± 0.72	2.51 ± 0.43
C_{max}	µg/mL	N/A	2.01 ± 0.92	1.61 ± 0.71	3.92 ± 1.84	3.08 ± 1.88	49.73 ± 24.51	35.86 ± 6.52

Data represents mean ± S.D. for n = 6.

Table 2-2. Pharmacokinetic parameters for plasma oxyphenylbutazone with or without co-administration of ranitidine

Parameters	Units	2.2 with R	2.2 Control	4.4 with R	4.4 Control	8.8 with R	8.8 Control
T_{max}	hr	6.50 ± 1.91	6.00 ± 2.00	6.50 ± 1.91	6.00 ± 1.63	7.00 ± 2.45	6.00 ± 0.00
C_{max}	µg/mL	0.29 ± 0.07	0.27 ± 0.17	0.60 ± 0.14	0.45 ± 0.33	5.89 ± 1.48	5.04 ± 0.63
AUC	hr*µg/mL	14.02 ± 2.51	5.05 ± 3.93	19.29 ± 4.29	8.41 ± 7.17	85.56 ± 0.36	84.93 ± 19.30
$t_{1/2}$	hr	10.80 ± 9.13	7.33 ± 2.47	9.97 ± 5.07	7.66 ± 2.02	6.74 ± 2.46	8.53 ± 3.65
CL/F	L/hr/kg	0.16 ± 0.06	0.44 ± 0.28	0.23 ± 0.06	0.52 ± 0.23	0.10 ± 0.04	0.01 ± 0.03
MRT	hr	24.36 ± 13.32	13.98 ± 3.64	22.44 ± 7.09	14.37 ± 2.99	13.47 ± 3.39	15.78 ± 5.06

Data represents mean ± S.D. for n = 6.

Table 2-3. Pharmacokinetic parameters for plasma γ-hydroxyphenylbutazone with or without co-administration of ranitidine

Parameters	Units	2.2 with R	2.2 Control	4.4 with R	4.4 Control	8.8 with R	8.8 Control
T_{max}	hr	3.33 ± 1.03	2.92 ± 1.74	3.17 ± 1.33	3.58 ± 2.42	3.00 ± 0.10	3.00 ± 1.10
C_{max}	μg/mL	0.42 ± 0.19	0.34 ± 0.10	0.95 ± 0.38	0.64 ± 0.25	12.52 ± 5.19	11.03 ± 3.80
AUC	hr*μg/mL	3.34 ± 1.38	2.44 ± 0.90	6.78 ± 2.56	4.49 ± 1.80	65.39 ± 15.25	57.82 ± 19.53
$t_{1/2}$	hr	3.91 ± 2.55	3.67 ± 1.50	3.96 ± 2.54	3.26 ± 1.14	2.51 ± 1.33	2.62 ± 0.97
CL/F	L/hr/kg	0.66 ± 0.35	0.90 ± 0.34	0.65 ± 0.31	0.98 ± 0.45	0.13 ± 0.03	0.15 ± 0.08
MRT	hr	7.78 ± 3.17	6.85 ± 2.64	7.67 ± 3.33	6.51 ± 2.27	5.05 ± 1.34	4.87 ± 0.90

Data represents mean ± S.D. for n = 6.

Table 2-4. Pharmacokinetic parameters for plasma ranitidine following 2.14mg/kg oral dose of ranitidine with co-administration of 8.8 mg/kg phenylbutazone

Parameter	Units	Mean ± S.D.
A	μg/mL	1.49 ± 1.06
B	μg/mL	0.08 ± 0.03
k_a	1/hr	2.15 ± 1.15
α	1/hr	1.18 ± 0.16
β	1/hr	0.15 ± 0.08
AUC	hr*μg/mL	0.69 ± 0.34
half-life $t_{1/2,\alpha}$	hr	0.59 ± 0.08
half-life $t_{1/2,\beta}$	hr	4.58 ± 3.76
CL/F	L/hr/kg	3.12 ± 1.89
T_{max}	hr	1.17 ± 0.33
C_{max}	μg/mL	0.08 ± 0.02
V_{ss}/F	L/kg	25.57 ± 7.08

Data represents mean ± S.D. for n = 6.

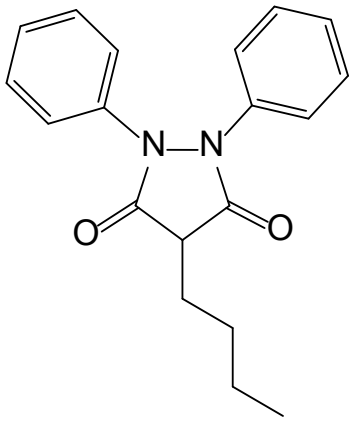

Figure 2-1. Chemical structure of phenylbutazone

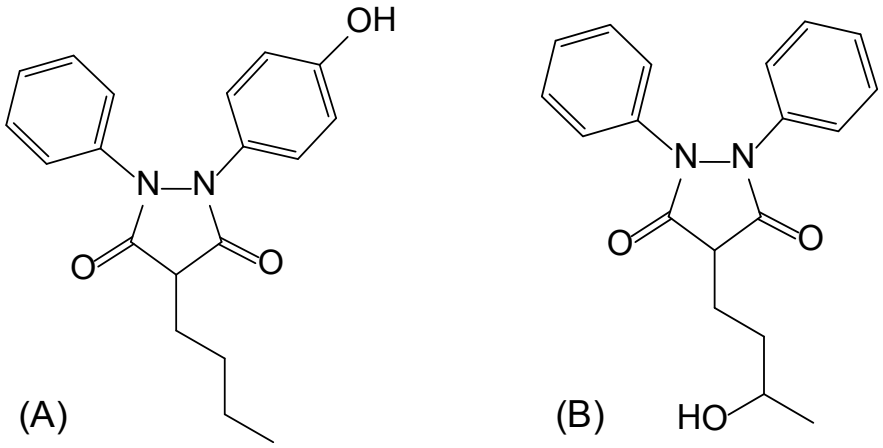

Figure 2-2. Chemical structure of oxyphenbutazone (A) and γ-hydroxyphenylbutazone (B)

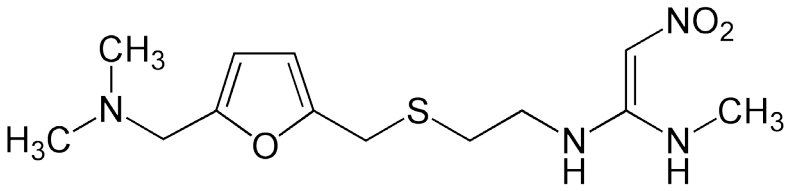

Figure 2-3. Chemical structure of ranitidine

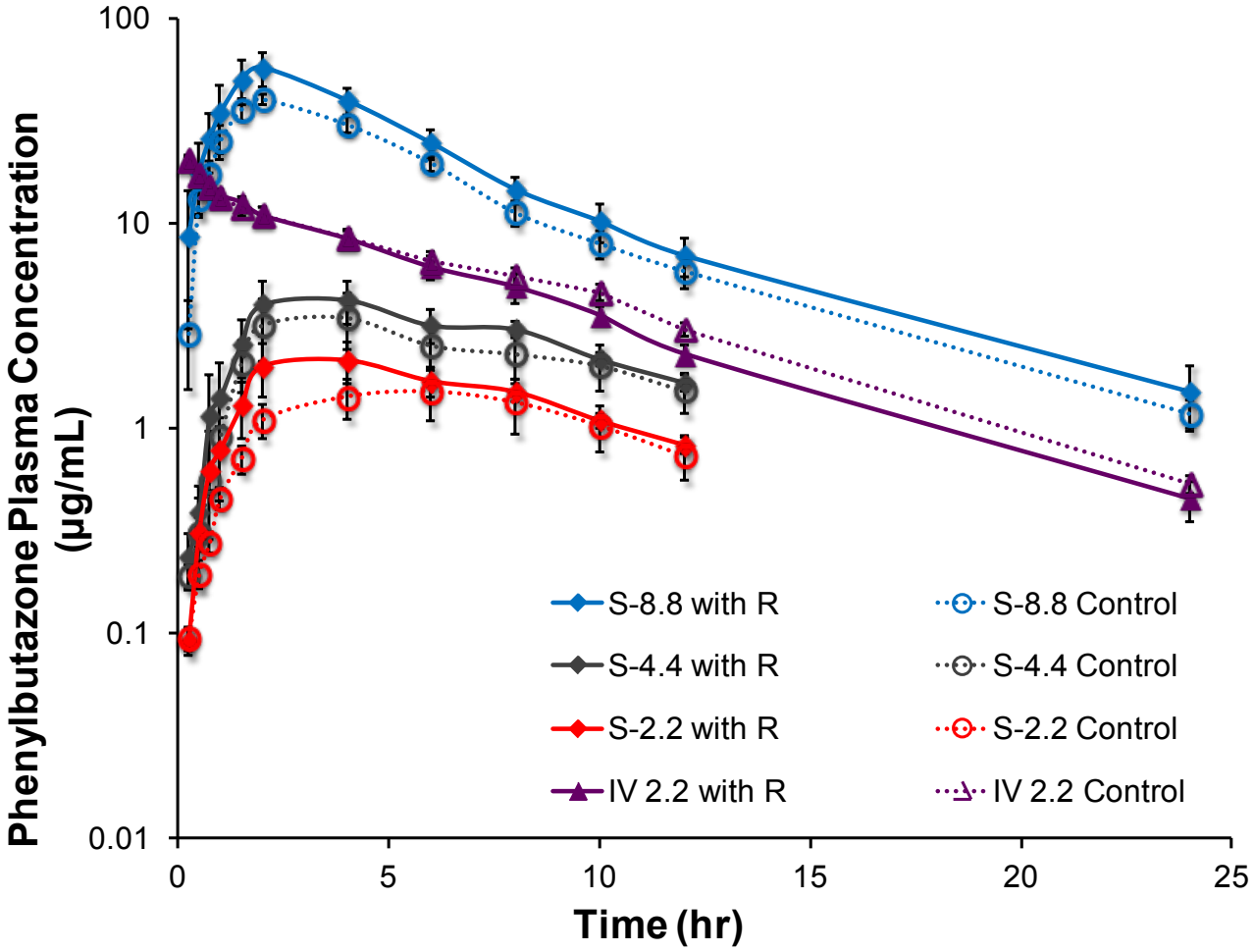

Figure 2-4. Mean (± S.E.) plasma concentration profiles for phenylbutazone following single doses with or without co-administration of ranitidine

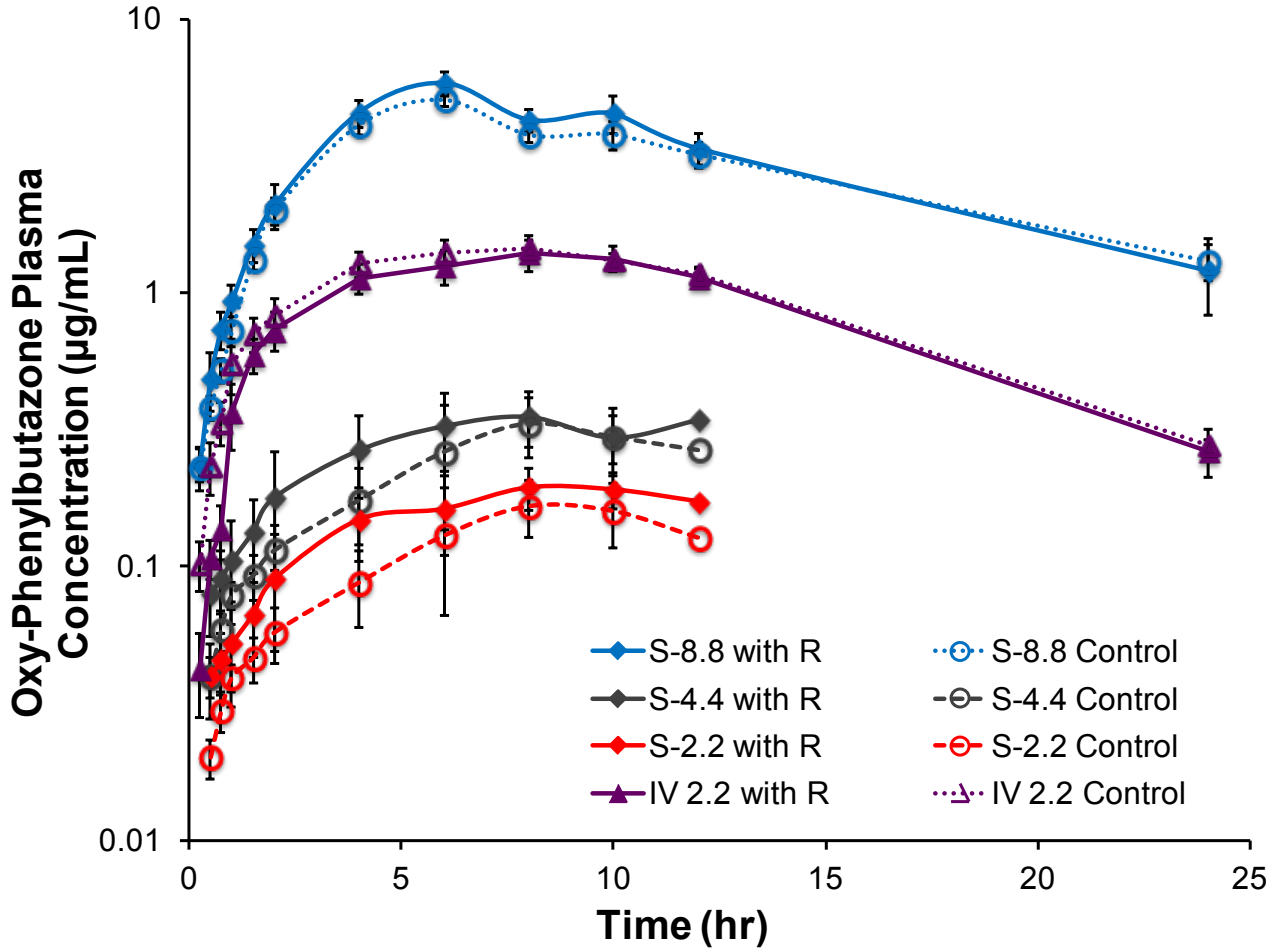

Figure 2-5. Mean (± S.E.) plasma concentration profiles for oxyphenbutazone following single doses with or without co-administration of ranitidine

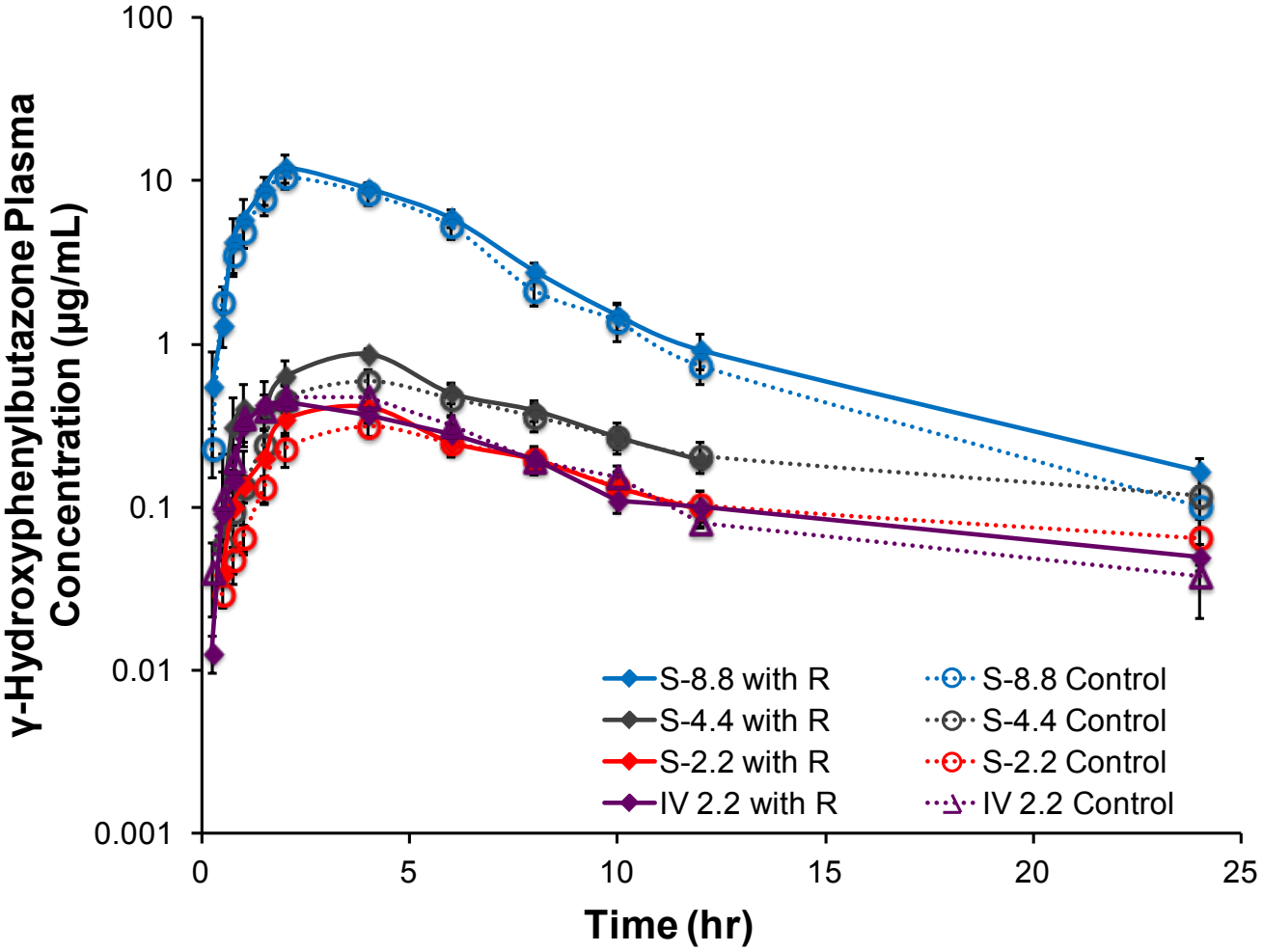

Figure 2-6. Mean (± S.E.) plasma concentration profiles for γ-hydroxyphenylbutazone following single doses with or without co-administration of ranitidine

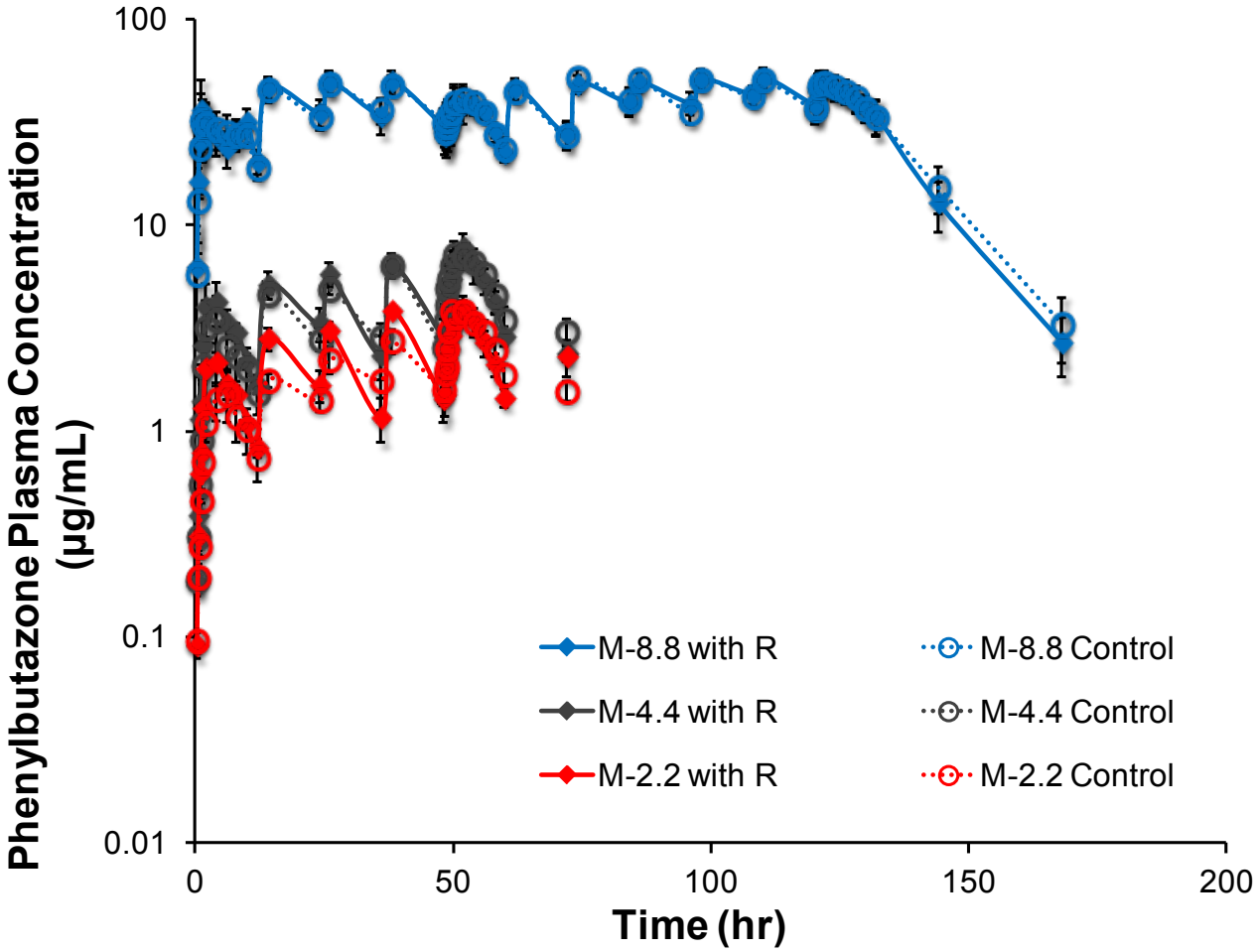

Figure 2-7. Mean (± S.E.) plasma concentration profiles for phenylbutazone following multiple doses (b.i.d.) with or without co-administration of ranitidine

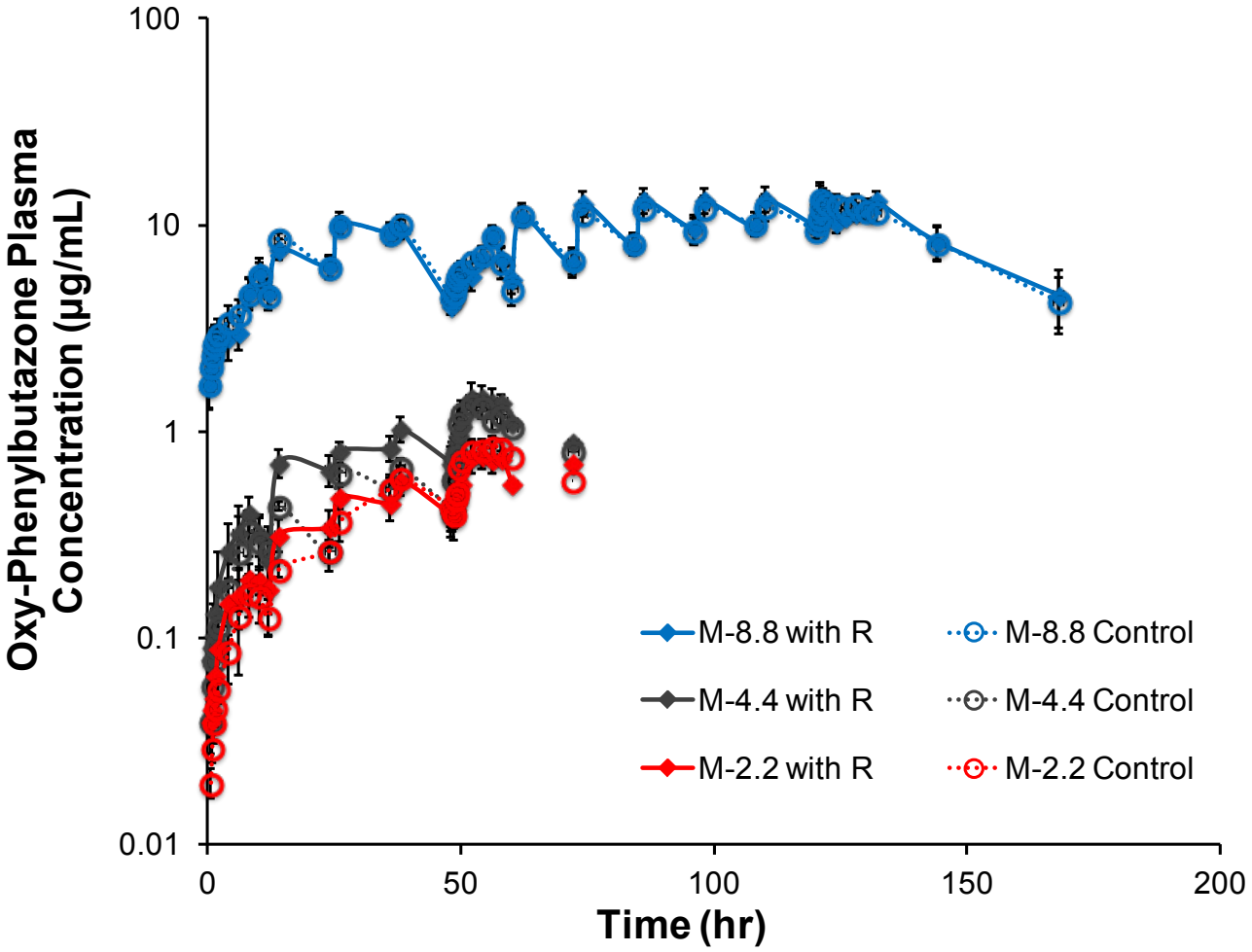

Figure 2-8. Mean (± S.E.) plasma concentration profiles for oxyphenbutazone following multiple doses (b.i.d.) with or without co-administration of ranitidine

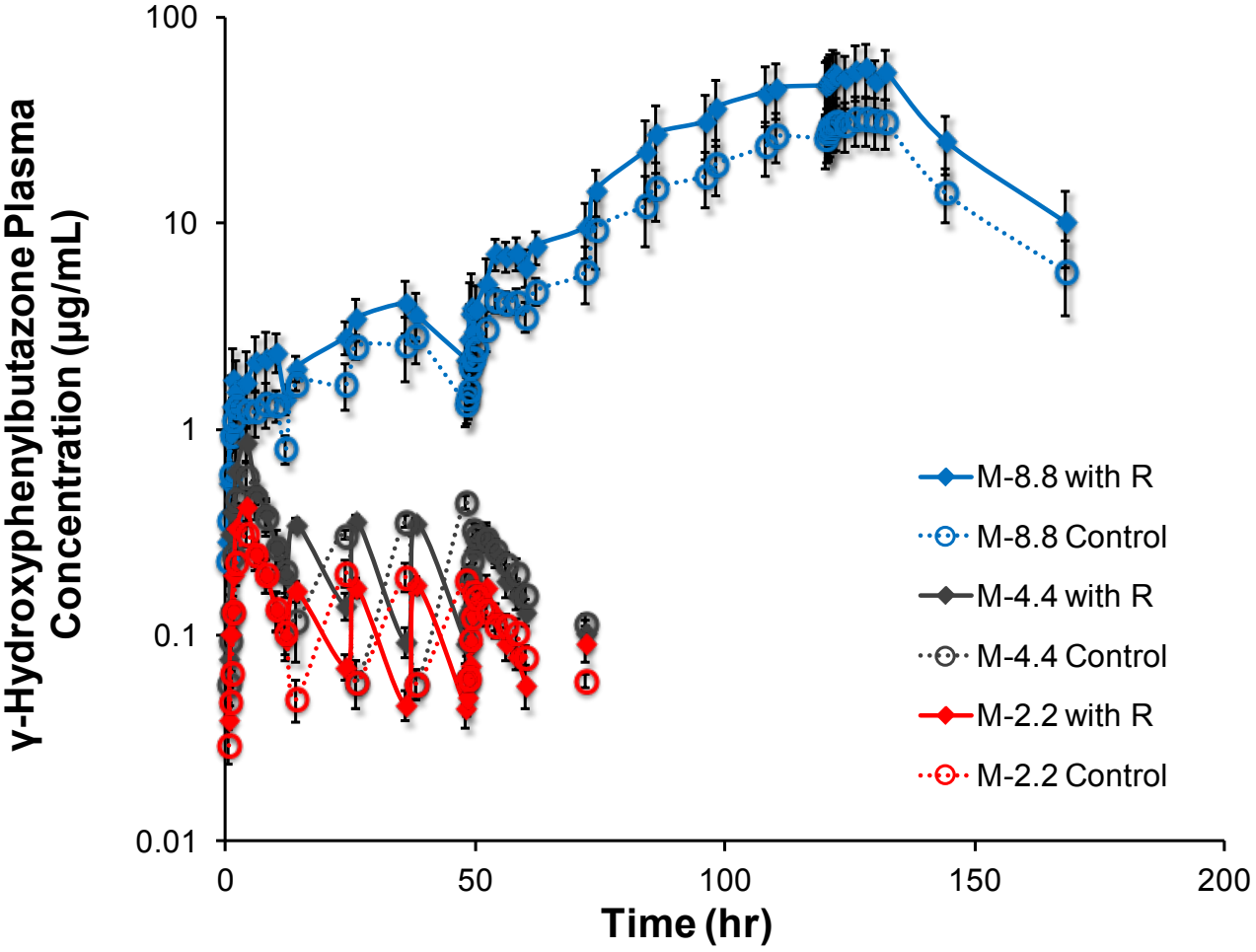

Figure 2-9. Mean (± S.E.) plasma concentration profiles for γ-Hydroxyphenylbutazone following multiple doses (b.i.d.) with or without co-administration of ranitidine

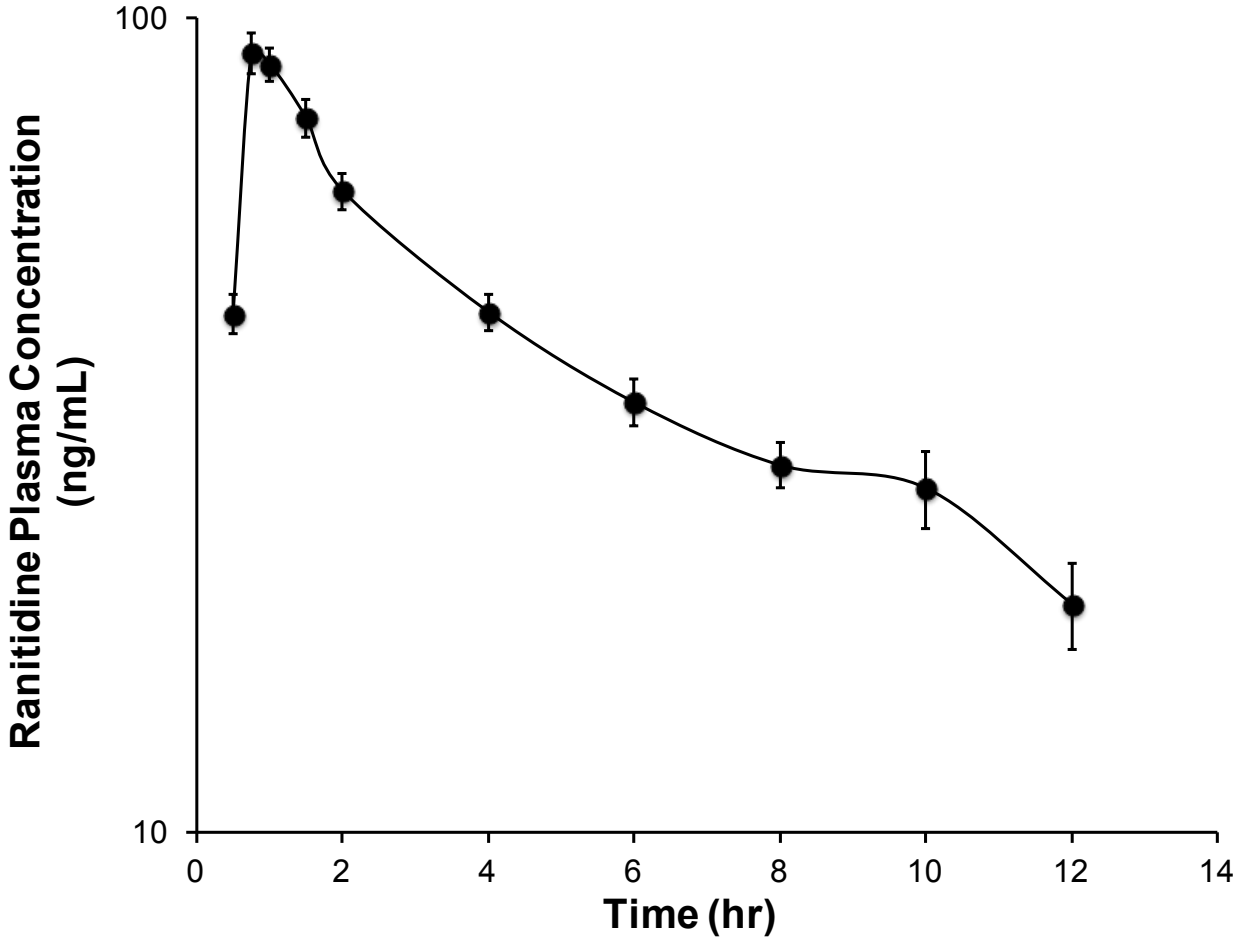

Figure 2-10. Mean (± S.E.) plasma concentration profiles for ranitidine following 2.14 mg/kg ranitidine and co-administration of 8.8 mg/kg phenylbutazone

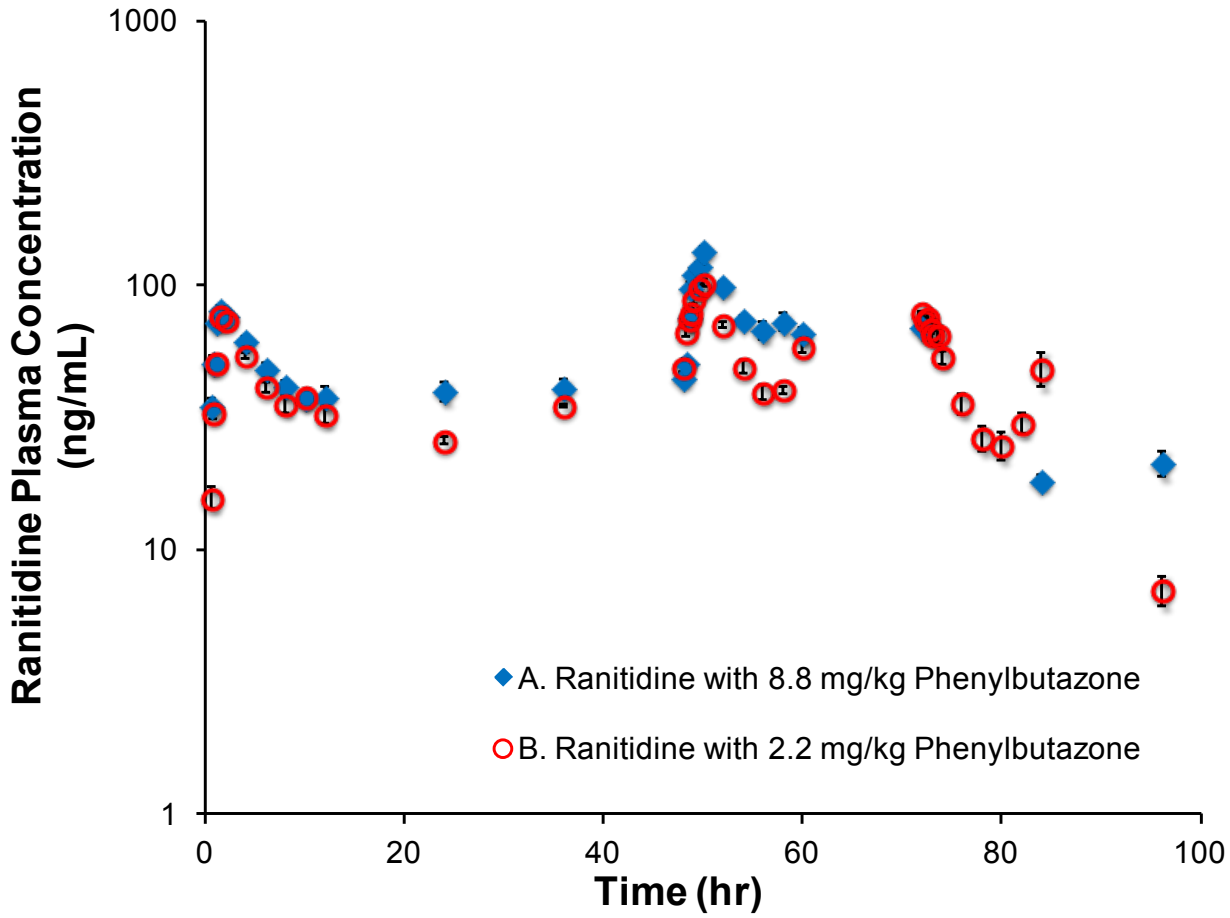

Figure 2-11. Mean (± S.E.) plasma concentration profiles for ranitidine following: A. oral administration of seven 8.8 mg/kg phenylbutazone and six 2.14 mg/kg ranitidine; B. oral administration of five 2.2 mg/kg phenylbutazone and five 2.14 mg/kg ranitidine, then i.v. administration of 2.2 mg/kg phenylbutazone at 72-hr.

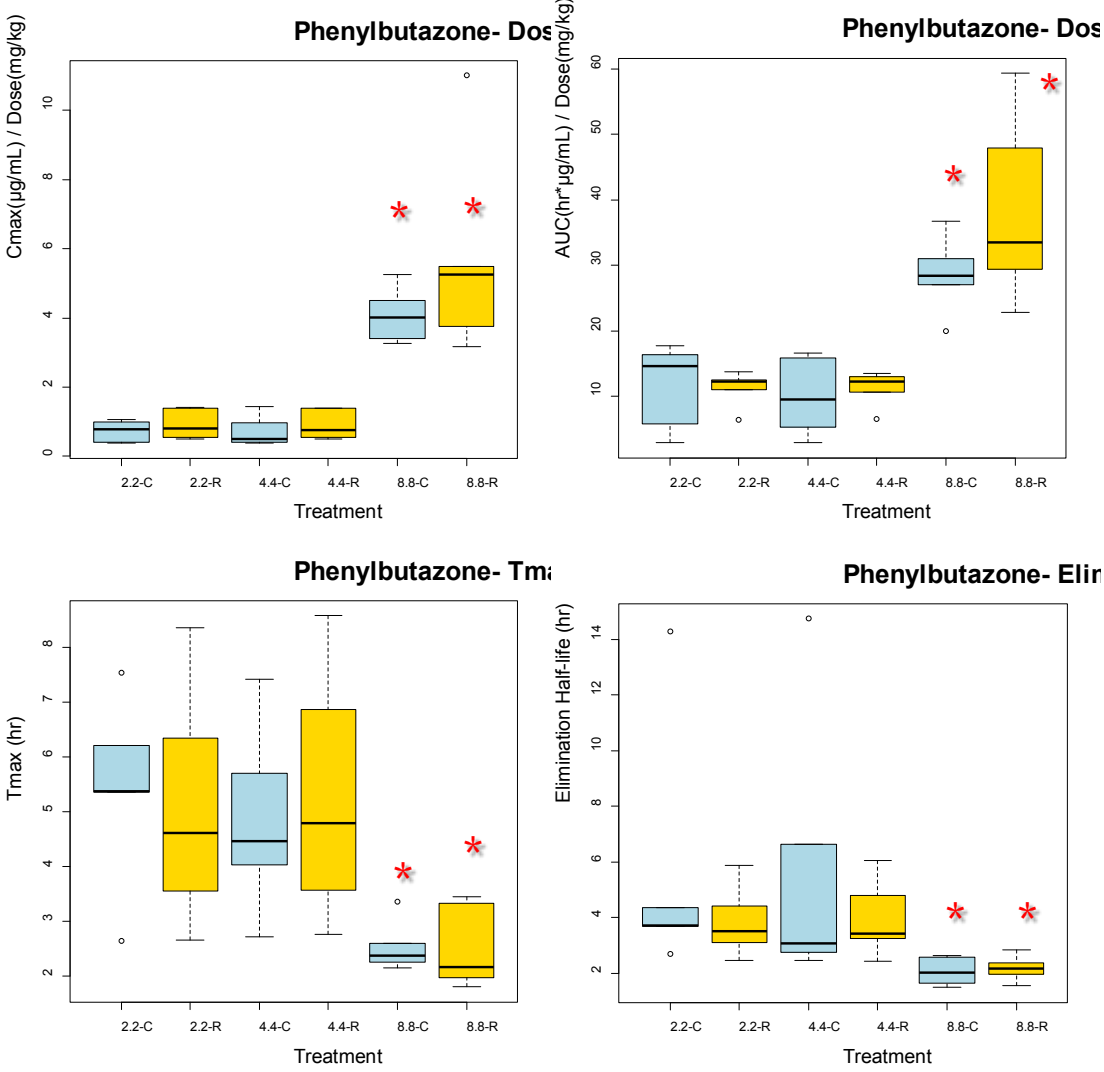

Figure 2-12. Boxplot comparing pharmacokinetic parameters of phenylbutazone between treatment groups. (yellow: with concomitant ranitidine; blue: control)
* : Significant difference compared to lower doses (*p*-value < 0.05 from one-way ANOVA test)

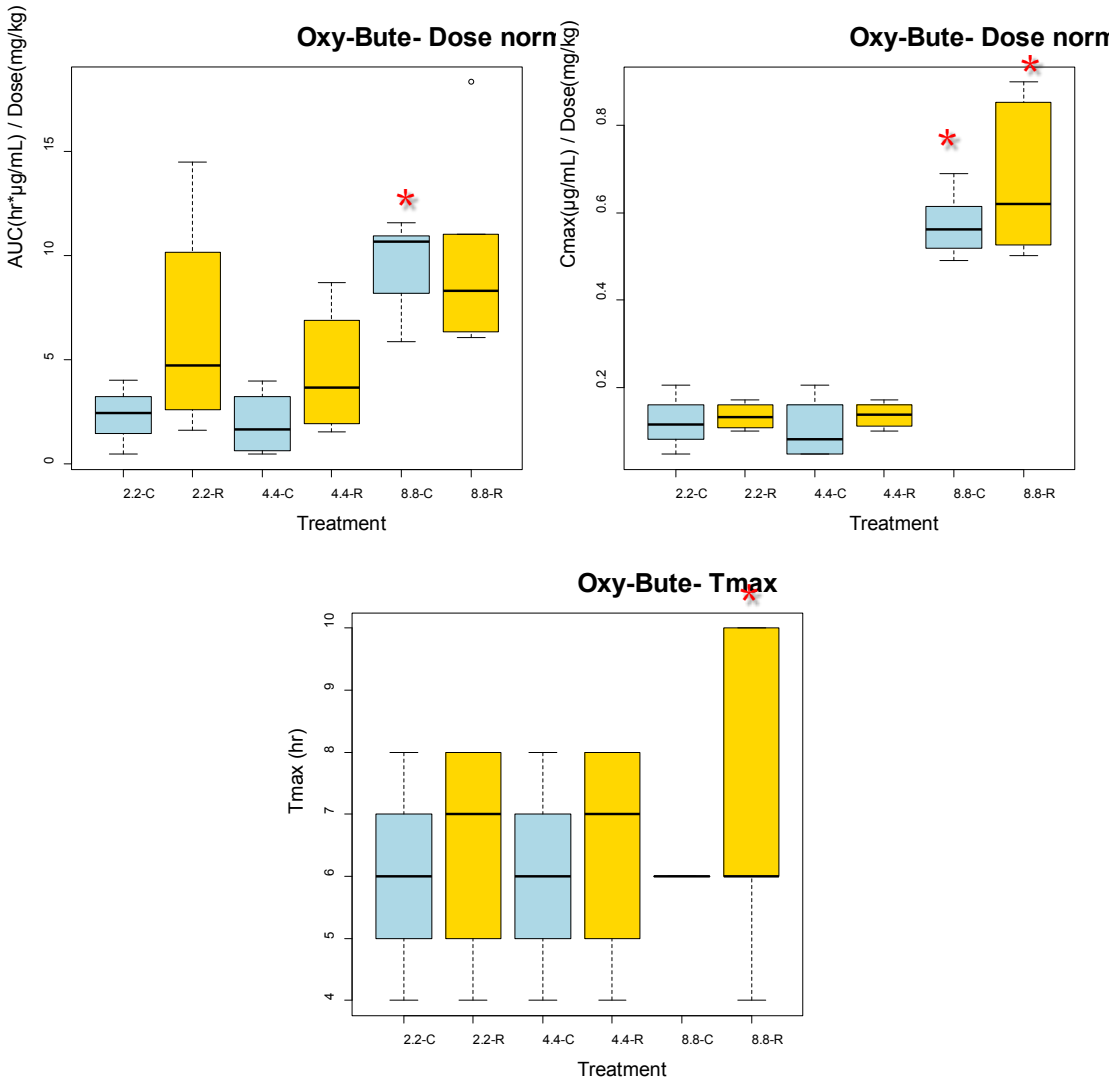

Figure 2-13. Boxplot comparing pharmacokinetic parameters of oxy-phenylbutazone between treatment groups. (yellow: with concomitant ranitidine; blue: control)
* : Significant difference compared to lower doses (*p*-value < 0.05 from one-way ANOVA test)

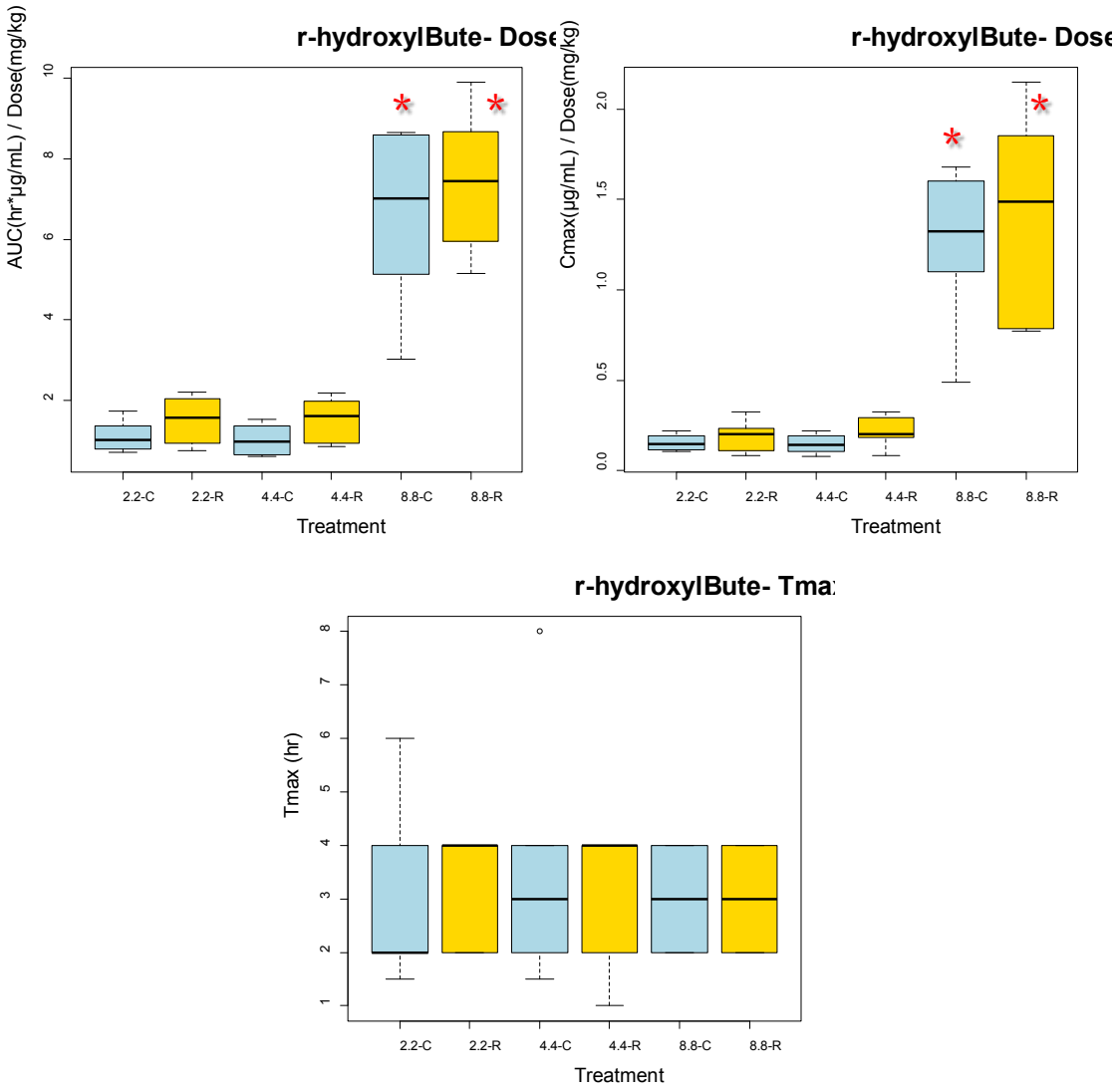

Figure 2-14. Boxplot comparing pharmacokinetic parameters of γ-hydroxyl-phenylbutazone between treatment groups. (yellow: with concomitant ranitidine; blue: control)
* : Significant difference compared to lower doses (*p*-value < 0.05 from one-way ANOVA test)

REFERENCE

Becht, J. L. and T. D. Byars (1986). "Gastroduodenal ulceration in foals." Equine Vet J 18(4): 307-312.

Christensen, J. M., L. L. Blythe and A. M. Craig (1985). "Effects of oral cimetidine on plasma concentrations of phenylbutazone in horses." J Vet Pharmacol Ther 8(4): 404-412.

Collins, L. G. and D. E. Tyler (1984). "Phenylbutazone toxicosis in the horse: a clinical study." J Am Vet Med Assoc 184(6): 699-703.

Furr, M. O. and M. J. Murray (1989). "Treatment of gastric ulcers in horses with histamine type 2 receptor antagonists." Equine Vet J Suppl(7): 77-79.

Gerring, E. L., P. Lees and J. B. Taylor (1981). "Pharmacokinetics of phenylbutazone and its metabolites in the horse." Equine Vet J 13(3): 152-157.

Gibaldi, M., Perrier, D. (1975). Bioavailability. Pharmacokinetics. New York, Marcel and Decker: 145-150.

Holland, P. S., W. W. Ruoff, G. W. Brumbaugh and S. A. Brown (1997). "Plasma pharmacokinetics of ranitidine HCl in adult horses." J Vet Pharmacol Ther 20(2): 145-152.

Kirch, W., H. Hoensch and H. D. Janisch (1984). "Interactions and non-interactions with ranitidine." Clin Pharmacokinet 9(6): 493-510.

Klotz, U. and H. K. Kroemer (1991). "The drug interaction potential of ranitidine: an update." Pharmacol Ther 50(2): 233-244.

Lees, P., R. F. Creed, E. E. Gerring, P. W. Gould, D. J. Humphreys, T. E. Maitho, A. R. Michell and J. B. Taylor (1983). "Biochemical and haematological effects of phenylbutazone in horses." Equine Vet J 15(2): 158-167.

MacAllister, C., C. Qualls, Jr., R. Tyler and C. R. Root (1987). "Multiple myeloma in a horse." J Am Vet Med Assoc 191(3): 337-339.

Maylin, G. A. (1974). "Editorial: Pre-race drug testing." Cornell Vet 64(3): 325-334.

Mooney, K. G., M. Rodriguez-Gaxiola, M. Mintun, K. J. Himmelstein and V. J. Stella (1981). "Dissolution kinetics of phenylbutazone." J Pharm Sci 70(12): 1358-1365.

Murray, M. D. and D. C. Brater (1990). "Nonsteroidal anti-inflammatory drugs." Clin Geriatr Med 6(2): 365-397.

Murray, M. J. (1992). "Gastric ulceration in horses: 91 cases (1987-1990)." J Am Vet Med Assoc 201(1): 117-120.

Smith, S. R. and M. J. Kendall (1988). "Ranitidine versus cimetidine. A comparison of their potential to cause clinically important drug interactions." Clin Pharmacokinet 15(1): 44-56.

Snow, D. H., J. A. Bogan, T. A. Douglas and H. Thompson (1979). "Phenylbutazone toxicity in ponies." Vet Rec 105(2): 26-30.

Snow, D. H., T. A. Douglas, H. Thompson, J. J. Parkins and P. H. Holmes (1980). "Phenylbutazone toxicity in ponies." Vet Rec 106(3): 68.

Soiffer, R. J., C. Murray, P. Mauch, K. C. Anderson, A. S. Freedman, S. N. Rabinowe, T. Takvorian, M. J. Robertson, N. Spector, R. Gonin and et al. (1992). "Prevention of graft-versus-host disease by selective depletion of CD6-positive T lymphocytes from donor bone marrow." J Clin Oncol 10(7): 1191-1200.

Soma, L. R., D. E. Gallis, W. L. Davis, T. A. Cochran and C. B. Woodward (1983). "Phenylbutazone kinetics and metabolite concentrations in the horse after five days of administration." Am J Vet Res 44(11): 2104-2109.

Tobin, T., S. Chay, S. Kamerling, W. E. Woods, T. J. Weckman, J. W. Blake and P. Lees (1986). "Phenylbutazone in the horse: a review." J Vet Pharmacol Ther 9(1): 1-25.

Traub, W. H. (1982). "Combined serum bactericidal and phagocytic activities of defibrinated human blood against Serratia marcescens. Use of phenylbutazone to selectively block phagocytic killing activity and of Group A (phage tail) bacteriocins to kill extraphagocytic bacteria." Chemotherapy 28(5): 355-362.

Van Peer, A. P., F. M. Belpaire and M. G. Bogaert (1980). "In vitro hepatic oxidative metabolism of antipyrine, phenytoin and phenylbutazone in uraemic rabbits." J Pharm Pharmacol 32(2): 135-136.

CHAPTER 3

ORGANOPHOSPHORUS PESTICIDE DEGRADATION PRODUCT IN VITRO METABOLIC STABILITY AND TIME-COURSE UPTAKE AND ELIMINATION IN RATS FOLLOWING ORAL AND INTRAVENOUS DOSING

N. D. Forsberg, R. Rodriguez-Proteau, L. Ma, J. Morré, J. M. Christensen, C. S. Maier, J. J. Jenkins, and K. A. Anderson

Manuscript in: (2001) Xenobiotica. 41(5): 422-429

ABSTRACT

Levels of urinary dialkylphosphates (DAPs) are currently used as a biomarker of human exposure to organophosphorus insecticides (OPs). It is known that OPs degrade on food commodities to DAPs at levels that approach or exceed those of the parent OP. However, little has been reported on the extent of DAP absorption, distribution, metabolism and excretion.

The metabolic stability of *O,O*-dimethylphosphate (DMP) was assessed using pooled human and rat hepatic microsomes. Time-course samples were collected over two hours and analyzed by LC-MS/MS. It was found that DMP was not metabolized by rat or pooled human hepatic microsomes.

Male Sprague-Dawley rats were administered DMP at 20 mg/kg via oral gavage and I.V. injection. Time-course plasma and urine samples were collected and analyzed by LC-MS/MS. DMP bioavailability was found to be 107 $\pm$ 39 % and the amount of the orally administered dose recovered in the urine was 30 $\pm$ 9.9 % by 48 hrs.

The *in vitro* metabolic stability, high bioavailability and extent of DMP urinary excretion following oral exposure in a rat model suggests that measurement of DMP as a biomarker of *O,O*-dimethyl organophosphorus insecticide exposure may lead to overestimation of human exposure.

INTRODUCTION

Organophosphorus insecticides (OPs) are among the most widely used insecticides in US and global agriculture. An estimated 60 million pounds of the roughly 40 currently registered OPs are applied annually to US agriculture (Barr, Bravo et al. 2004; Zhang, Driver et al. 2008). They share a common mode of toxicity through the non-species specific inhibition of acetylcholinesterase (AChE) (Mileson, Chambers et al. 1998; Casida and Quistad 2004). The association between low-level lead exposure in children and the development of subtle neurologic effects in children led scientists to develop and investigate parallel hypotheses for OPs (Whitney, Seidler et al. 1995; Chanda and Pope 1996; Fenske, Kissel et al. 2000). Recognition of these ideas aided in the passage of the 1996 Food Quality Protection Act that charged the US Environmental Protection Agency with assessing the aggregate and cumulative exposure of OPs to humans with careful attention being paid to childhood exposure (Loewenherz, Fenske et al. 1997).

The majority of OP insecticides registered with the US Environmental Protection Agency are metabolized to at least one of six dialkylphosphate (DAP) metabolites (Figure 3-1) (Wessels, Barr et al. 2003). Following human OP exposure and metabolism, DAPs are eliminated from the body in the urine (Shafik, Bradway et al. 1971; Shafik, Bradway et al. 1973; Bradway and Shafik 1977; Fenske, Kissel et al. 2000; Bicker, Lämmerhofer et al. 2005). Monitoring the levels of these six common dialkylphosphate urinary metabolites, rather than the individual parent OPs, has allowed researchers to develop a single analytical method with which to monitor human spatial and temporal exposure to OPs (Aprea, Sciarra et al. 1996; Loewenherz, Fenske et al. 1997; Aprea, Strambi et al. 2000; Fenske, Kissel et al. 2000; Lu, Knutson et al. 2001; Barr, Bravo et al. 2004; Bradman, Eskenazi et al. 2005). Additionally, it is becoming more and more common for researchers to employ the biomonitoring of DAPs to investigate associations between human OP exposure and the risk of

developing adverse health effects (Castorina, Bradman et al. 2003; Eskenazi, Harley et al. 2004; Young, Eskenazi et al. 2005; Eskenazi, Marks et al. 2007). Though the measurement of DAPs offers several analytical and cost-effective advantages, their use as human biomarkers of OP exposure has limitations.

It has been demonstrated that OPs can degrade in the environment to DAPs and that DAPs are present in raw food at molar levels that approach or exceed those of the parent OP (Hong and Pehkonen 1998; Sakellarides, Siskos et al. 2003; Lu, Bravo et al. 2005; Zhang, Driver et al. 2008; Slotkin, Seidler et al. 2009). It has also been demonstrated that the ethylated DAP hydrolysis products of chlorpyrifos are excreted in the urine of rats orally dosed with *O,O*-diethylphosphate, DEP, and *O,O*-diethylthiophosphate, DETP (Shafik, Bradway et al. 1971; Timchalk, Busby et al. 2007; Busby-Hjerpe, Campbell et al. 2010). Additionally, the aforementioned ethyl DAP toxicokinetic studies demonstrated that exposure to equal molar levels of ethylated DAPs and chlorpyrifos consistently resulted in higher urinary ethyl DAP excretion rates and cumulative urine levels in rats receiving oral doses of ethyl DAPs (Timchalk, Busby et al. 2007).

There were three objectives in the current study; (1) to assess the metabolic stability of methyl DAPs to rat and human hepatic microsomes, (2) to investigate the absorption, metabolism and elimination of methyl DAPs in a rat model and (3) determine methyl DAP pharmacokinetic parameters following oral and I.V. dosing. Integration of results from the current study with those for the ethyl DAPs will provide quantitative information necessary for interpretation of biomonitoring data that employ the DAPs as chemical markers of OP insecticide exposure.

MATERIALS AND METHODS

Chemicals

O,O-dimethylphosphoric acid sodium salt (DMP, ≥ 95%) and O,O-dimethylthiophosphoric acid sodium salt (DMTP, ≥ 96%) were purchased from AppliChem GmbH (Darmstradt, Germany) and O,O-dimethlyphosphoric acid was purchased from AccuStandard (New Haven, CT, USA). Tramadol-hydrochloride (T-HC) was obtained from Sigma-Aldrich Corp (St. Louis, MO, USA). HPLC-grade solvents were purchased from Fisher Scientific Co. (Fairlawn, NJ, USA). All other reagent chemicals were obtained from commercial sources and used without further purification.

Metabolic stability assays

The metabolic stability of DMP was determined using rat and pooled human hepatic microsomes (BD Biosciences, San Jose, CA, USA). Incubation mixtures were prepared starting with 2455 µL of phosphate buffer (50 mM, pH = 7.4) and adding sequentially 225 µL of microsomal protein (20 mg mL^{-1}), 300 µL of NADPH (10 mM) and 20 µL of DMP (75 mM) to yield a solution with a final volume of 3 mL and DMP concentration of 0.5 mM. After a 0, 0.25, 0.5, 1, 2-h incubation at 37 °C with shaking, the reaction was terminated with an equal volume solution of ice-cold methanol with 0.5% (v/v) formic acid and DMTP (internal standard) at 0.5 mM. Proteins were precipitated by centrifugation at 12 000 g for 15 min. Supernatant was diluted 1:50 for a final dilution of 1:100 with methanol and the resulting solutions were stored at -20 °C until analysis. The experiment was carried out with four replicates. Positive control incubations were conducted with T-HC, a drug with a known metabolic profile, in the presence of all other reported incubation components (metabolism expected), while negative controls were conducted in the absence of NADPH (no metabolism expected). DMP and control incubations were carried out in tandem and underwent similar sample preparation.

Animal study

All procedures using animals were reviewed and approved by the Institutional Animal and Care Use Committee of Oregon State University. Male Sprague-Dawley rats with jugular catheters attached were purchased from Charles River Laboratories and Simonsen Laboratories and were acclimated to laboratory conditions for three to four days in metabolic cages designed to separate feces from urine. Rats were maintained on a 12-h light/dark cycle at the Oregon State University Laboratory Animal Resource Center. During acclimation rats were allowed free access to water and food. At the time of dosing, weight among rats ranged from 233 – 274 g.

Dose selection and preparation

Weight specific dosing solutions (20 mg/kg) were prepared by dissolving DMP in an appropriate amount of normal saline (0.9 % NaCl) such that rats received 100 µL and 500 µL dosing volumes during I.V. and oral dose administration respectively. Control rats were administered normal saline vehicle at the same dosing volumes as DMP treated rats. The 20 mg/kg dose level was chosen to increase the ability to detect chemicals in rat blood and urine over the time-course of the study.

Pharmacokinetic study

Rats were denied access to food from 1-hr prior to dosing to 2-hr post-dosing. DMP was administered intravenously via jugular catheter to manually restrained rats or by gavage to rats lightly anesthetized with isoflurane in a controlled chamber. Blood samples (~100 µL) from I.V. and orally dosed animals were collected at 0, 5, 10, 20, 30, 40, 60, 75, 90, 120 min and 0, 20, 30, 40, 60, 90, 120, 150, 180, 240 min post-dosing respectively from jugular vein catheters. The blood volume removed was replaced with an equal volume of normal saline followed by cannula blocking solution. Time-course urine samples were collected at 0, 1.5, 4.5, 7.5, 14, 24, 36 and 48-hr post dosing

into 15 mL screw-top vials and excretion volumes were recorded. Urine was collected for all animals in the study. The urine collection volumes ranged from no sample (one rat at time point 1.5 hr and a different rat at time point 7.5 h) to 9.25 mL. Average urine collection volumes for time points 1.5 – 4.5 hr and 7.5 – 48 hr were 1.1 $\pm$ 0.9 mL and 2.7 $\pm$ 2.0 mL respectively. Rats were humanely sacrificed via CO_2 asphyxiation following the final urine time point collection. Plasma and urine samples were placed on ice during sample collection and subsequently stored at -20 °C until sample preparation.

Plasma and urine sample preparation

Time-course blood samples were dispensed into heparinized microcentrifuge tubes (50 units of heparin mL^{-1} blood) and underwent plasma separation via centrifugation at 10 000 g for 15 min. Plasma proteins were precipitated via a 1:5 dilution with methanol, vortexing for 10 s and centrifugation at 15 000 g for 15 min. Plasma samples were subsequently diluted with methanol for a final dilution of 1:100 – 1:1000 and spiked with DMTP as an internal standard.

Urine samples were vortexed for 10 s and centrifuged for 10 min at 10 000 g. One hundred µL of the supernatant was diluted 1:10 with methanol, vortexed for 10 s and centrifuged for 10 min at 10 000 g. The resulting supernatant's final dilution with methanol was 1:100 – 1:1000 and spiked with DMTP as an internal standard. Prepared samples were stored at -20 °C until analysis.

Analytical instrumentation

All samples were analyzed using an Applied Biosystems/MDS Sciex 4000 Q-trap mass spectrometer (Applied Biosystems, Foster City, CA) equipped with a TurboV electrospray ionization source, Shimadzu Prominence HPLC solvent delivery system and a Shimadzu SIL-HTc autosampler (Columbia, MD, USA). Optimization of instrument sensitivity was achieved by

performing infusion experiments with DMP, DMTP and T-HC and generating enhanced product ion mass spectrums in combination with Applied Biosystems Analyst 1.4.2 software (Foster City, CA, USA). The analytical methods for DMP, DMTP and T-HC and T-HC metabolites were adapted from Hernandez et al. and Wu et al. respectively (2002; 2004). Optimized instrument parameters are presented in Table 1. Samples were chromatographically resolved using a 150 x 3 mm Phenomenex Luna C18 column with a 4.6 µm internal diameter and 100 Å particle size (Torrence, CA, USA).

LC-MS/MS analyses

Microsome incubation samples

DMP and DMTP, an internal standard, were chromatographically resolved from microsome samples using gradient elution with aqueous (A) and methanol (B) solutions of formic acid (0.1%, v/v). The elution program was as follows: 0 – 6 min, 20 – 50% B; 6 – 7 min, 50 – 90% B; 7 – 10 min, 90 – 90% B; 10 – 10.1 min, 90 – 20% B; 10.1 – 15 min, 20 – 20% B at a flow rate of 300 µL min^{-1} and an injection volume of 1 µL. DMP standard curves were prepared in methanol and spiked with the DMTP internal standard similarly to samples.

T-HC and its major metabolites were chromatographically resolved using a 0 – 15 min, 10 – 90% B; 15 – 16 min, 90 – 10% B; 16 – 22 min, 10 – 10% B gradient elution program at a flow rate of 300 µL min^{-1} and an injection volume of 10 µL. Metabolism of T-HC was assessed in terms of % T-HC remaining and presence of T-HC's major metabolite O-desmethyl tramadol-hydrochloride (transition followed m/z 250 → 58). The analysis of DMP, DMTP, T-HC and O-desmethyl tramadol-hydrochloride were performed with the instrument in MRM mode following the transitions presented in Table 3-1.

Rat plasma and urine samples

DMP and DMTP were chromatographically resolved from rat plasma and urine samples using the microsome gradient elution program modified to equilibrate from 10.1 to 18 min and with an injection volume ranging from 1 - 10 µL. For quantification, matrix matched standards were prepared from control plasma and blood samples. The instrument was run in MRM mode monitoring transitions described previously. The LC-MS/MS instrumental range for all DMP analyses was 0.001 – 1 µg/mL and yielded correlation coefficients greater than 0.999.

Pharmacokinetic analysis

DMP pharmacokinetic parameters were estimated using a two-compartment model to fit the experimental results following oral and I.V. administration. The oral (Eq. 1) and I.V. (Eq. 2) models were defined by the following equations:

Oral administration:

$$C(t) = Ae^{-\alpha t} + Be^{-\beta t} + Ce^{-k_a t} \quad \text{(Eq. 1)}$$

Intravenous administration:

$$C(t) = Ae^{-\alpha t} + Be^{-\beta t} \quad \text{(Eq. 2)}$$

where α is the first-order distribution rate constant, β is the first-order elimination rate constant and k_a is the absorption rate constant; A and B are the intercepts for the respective phases and C(t) represents the concentration of DMP at a given time t. Maximum plasma concentration (C_{max}) and the time to reach C_{max} (T_{max}) were determined from the plasma concentration-time curves. Optimized estimates for the model parameters were obtained using nonlinear regression analysis (WinNonlin 5.0.1; Pharsight, Mountain View, CA, USA). Estimates were further used to calculate values for apparent volume of distribution (V_d) and the apparent half-life of each phase ($t_{1/2\ \alpha,\beta}$). Additionally,

the total amount of DMP excreted in urine when excretion was complete ($DMP_{U\infty}$) was estimated by Method IIA (Wagner and Ayres 1977). Bioavailability (*F*) was determined as the quotient of total $DMP_{U\infty}$ after oral and I.V. DMP administration, appropriately correcting for dose, and assuming that clearance remained constant.

RESULTS

Metabolic stability

Quality control incubations were carried out in tandem with DMP incubations. In positive controls, the % T-HC decreased 41 – 50% over the 2-h rat hepatic microsome incubation and the total peak area for T-HC decreased by ~ 35%, while it increased for its major reported O-desmethyl metabolite. Conversely, there was no statistically significant decrease in T-HC over the 2-h incubation and no metabolites detected in negative rat controls. The same procedure was carried out for pooled human hepatic microsomes. The percentage of T-HC remaining for positive controls after two hours of incubation was 86 - 90%, while its percentage of total peak area decreased to ~ 95% and its major metabolite increased ~ 5%. Similarly to the rat hepatic microsomes, there was no statistically significant decrease in T-HC over the 2-h incubation and no metabolites detected in negative human controls.

The percentage of DMP remaining in rat hepatic microsome incubation mixtures was followed for two hours and assessed by LC-MS/MS (Fig. 2). No statistically significant difference was detected between time points (p-value = 0.35 from a one-way ANOVA with 19 d.f.). Similarly, the percentage of DMP remaining in pooled human microsome incubations did not display a trend that suggested it was being metabolized (p-value = 0.14 from a one-way ANOVA with 19 d.f.). Additionally, there was no statistically significant difference detected between the mean percentage of DMP remaining in rat and human DMP microsome incubations (p-value = 0.15 from a two sample t-test with 38 d.f.).

DMP pharmacokinetics

The concentrations of DMP in plasma following both oral and I.V. administration are shown in Table 3-2, while the time-course of DMP excreted in urine from both dosing groups are presented in Figures 3A and 3B.

Pharmacokinetic models (two-compartment) were developed to describe the time-course of DMP in plasma and the best fitting model parameter values are listed in Table 3-1. The volume of distribution (V_d) suggested extensive distribution of DMP in the body (6,970 ± 905 mL/kg for I.V. and 6,973 ± 691 mL/kg for oral dose). Following oral administration, peak plasma DMP levels of 3.3 ± 0.27 mg mL^{-1} were reached within 0.5-hr post dosing, and DMP was undetectable 2-h post dosing. The plasma time-course of DMP was bi-exponential with a rapid distribution phase (α) and a slower elimination phase (β). The half-lives for each phase were estimated to be 0.17 hr ($t_{1/2, \alpha}$) and 6.2 hr ($t_{1/2, \beta}$), respectively. The absolute bioavailability (F) of DMP was determined to be 107 ± 39%. In comparison to DMP, we analyzed the DEP and DETP plasma concentration time curve data from Timchalk's et al. (2007) paper using our methods of WinNonlin® software to estimate the pharmacokinetic parameters of these metabolites which are presented in Table 3-2.

The interval urinary excretion rates (dDMP/dt), amount of DMP remaining to be excreted in urine ($DMP_{U\infty}$ - DMP_U), dose normalized cumulative amount of DMP (DMP_U/dose) and cumulative DMP in urine normalized to total mass excreted (DMP_U / $DMP_{U\infty}$) for both administration routes are presented in Figures 3A, 3B, 4A and 4B respectively. In accordance with observed plasma pharmacokinetics, the urinary elimination of DMP following I.V. dosing also appears to be biphasic (Figure 3-3A). Peak urinary DMP excretion rates (104 ± 32 µg/h) were attained between 10 – 20 hr post oral dosing (Figure 3-3A) and excretion is almost complete after 40 – 50 hr for both dosing groups (Figure 3-4A and B). However, the estimated total recovery of DMP ($DMP_{U\infty}$ / Dose) in the urine was relatively low for both oral (30 ± 9.9 %) and I.V. dosing (36 ± 15 %) as compared to the calculated bioavailability. This may indicate that urine is not the only elimination pathway for DMP.

DISCUSSION

General population level exposure to OP insecticides occurs mostly through the diet where the majority of chemical metabolism is facilitated by first pass hepatic metabolism. It is known that hepatic cytochrome P450s, CYP, plays an integral role in phase I metabolism of environmental chemicals and drugs (Yan, Caldwell et al. 2002; Ackley 2004; Wu 2004). While it has been shown that CYP450s participate in the detoxification of OPs via the hydrolysis of the OP phosphoester bond to yield DAPs, it has also been demonstrated that CYP-mediated bioactivation of OPs to oxons is a major contributor to overall OP toxicity (Buratti, Volpe et al. 2003; Poet, Wu et al. 2003; Casida and Quistad 2004; Buratti, D'Aniello et al. 2005; Bharate, Prins et al. 2010; Busby-Hjerpe, Campbell et al. 2010). In light of the importance of CYP-mediated bioactivation to the toxicity of OPs, it was likewise hypothesized that they may play an equally important role in DAP metabolism. However, our results suggest that neither rat nor human hepatic microsomes are major contributors to the metabolism of DMP under CYP-mediated conditions. Additionally, our results provide an initial platform for comparing rat and human DAP metabolism.

All animals orally treated with DMP excreted DMP in their urine. As expected, no DMP was detected in any of the control animal blood or urine samples. These results, in conjunction with data showing extensive and rapid urinary excretion of DEP and DETP within 72 hours following DEP and DETP dosing, suggest that oral exposure to DAPs leads to significant urinary DAP levels (Timchalk, Busby et al. 2007). Evaluation of the time-course cumulative DMP in urine plot (Figure 3-4A) suggests that approximately 30% of the oral dose was excreted in the urine within 48 hours, which could signify that DMP has additional elimination pathways. However, urine sample loss (i.e. DMP loss) occurred for all animals during blood sampling and rats likely received varying doses of DMP due to incomplete delivery of the administered dose.

Observing that animals received variable DMP doses and that urine samples collected after 48 hours had levels of DMP below detection, suggest that comparison of the % cumulative DMP in urine normalized to total amount of DMP measured over 48 hrs (Figure 3-4B) would be appropriate. Assessment of urinary DMP levels under these assumptions demonstrates that the majority of DMP excretion occurs within 24 hours and is terminal by 48 hours.

The distribution phase half-life for DMP (0.17-hr) was comparable to the 0.2-h estimate previously reported for *O,O*-diethylphosphate (DEP), while the reported elimination half-life of DEP was greater (6 hr versus 52 hr) (Timchalk, Busby et al. 2007). The discrepancy in DMP and DEP elimination half-lives may be related to the ethoxy groups of DEP interacting to a greater degree with biomolecules than the methyl groups of DMP. However, this explanation fails to account for differences between DMP, DEP and DETP, where DETP has been reported to display single compartment pharmacokinetics and an elimination half-life that falls intermediate to DMP and DEP (Timchalk, Busby et al. 2007). Observing that DMP, DEP and DETP are partially excreted in the urine, it is reasonable to assume that differences in DAP pharmacokinetics may also be attributed to structure specific incorporation of the DAPs into *in vivo* systems (Timchalk, Busby et al. 2007).

The large volume of distribution, rapid distribution and slow elimination of DMP following oral dosing demonstrate that DMP is efficiently removed from plasma, distributed throughout the body and slowly and partially eliminated in the urine. Though pharmacokinetic results demonstrate that DAPs can remain in the body from hours to days, few studies have been published investigating the toxicity of DAPs. It has been shown that DAPs are cytotoxic and immunotoxic to human peripheral blood mononuclear cells and that DETP and DEDTP induce genotoxic effects in human embryonic hepatic and hepatocarcinoma cells under metabolic conditions when assessed by single cell gel electrophoresis (Lima and Vega 2005; Vega, Valverde et al.

2009). Considering the volume of OPs applied each year in the U.S. and that OPs degrade to DAPs in produce, a better understanding of human DAP pharmacokinetics and toxicodynamics is warranted.

CONCLUSION

The goal of the current work was to investigate the metabolic stability of a model DAP and characterize its pharmacokinetics in an animal model. Toward this end, the extent of DMP metabolism in rats and humans was investigated using hepatic microsomes. Results suggested that DMP was not metabolized over 2-h incubation by rats or humans. Similarities in rat and human DMP metabolic stability profiles also suggest that rats and humans may display similar trends with regards to DMP pharmacokinetics. Additionally, it was demonstrated that DMP has high oral bioavailability and is excreted in the urine of rats following oral environmental exposure. Assuming that humans display similar pharmacokinetics, the measurement of DMP as a biomarker of *O,O*-dimethyl OP exposure may lead to overestimation of human exposure.

Table 3-1. Mass spectrometry parameters used in the determination of DMP, DMTP, tramadol-HCl and *O*-desmethyl tramadol-HCl

Compound	Precursor ion (m/z)	Product ion (m/z)	Declustering potential	Entrance potential	Collision energy	Collision cell exit potential
DMP	125[ac]	79	-35	-10	-35	-5
	125[ad]	63	-35	-10	-35	-5
DMTP	141[ac]	126	-46	-10	-20	-5
	141[ad]	95	-46	-10	-36	-5
	141[ad]	79	-46	-10	-20	-5
Tramadol-HCl	264[bc]	58	46	10	27	9
O-desmethyl tramadol-HCl	250[bc]	58	46	10	27	9

[a] Mass spectrometer operated in negative mode; source temperature, 550 °C; ion spray voltage, -4200 V.
[b] Mass spectrometer operated in positive mode; source temperature, 450 °C; ion spray voltage, 5500 V.
[c] Quantification transition
[d] Confirmation transition

Table 3-2. Concentration of DMP in plasma following single i.v. and oral administration of 20 mg/kg dose to male Sprague-Dawley rats (μg/mL)

Time post-dosing (h)	Plasma concentration (μg/mL)	
	Intravenous	Oral
0.08	138 ± 99.6	-
0.17	93.7 ± 57.7	ND
0.33	36.1 ± 21.9	2.05 ± 0.65
0.5	18.9 ± 11.8	1.54 ± 0.63
0.67	4.71 ± 3.85	0.86 ± 0.55
1	4.05 ± 1.88	1.25 ± 0.66
1.25	1.41 ± 1.15	-
1.5	1.14 ± 0.93	ND
2	0.59 ± 0.53	0.73 ± 0.63
4	ND	ND
8	ND	-

ND, non-detected; (-), no sample
Data represents mean ± S.E. for n = 3-5.

Table 3-3. Pharmacokinetic parameters of DMP following a single I.V. and oral dose of 20 mg kg-1 to male Sprague-Dawley rats in comparison with results from Timchalk *et al.* (2007) DEP (dose = 21.57 mg/kg) and DETP (dose = 23.82 mg/kg) data obtained from male Sprague-Dawley rats

Parameters	Units	Intravenous	Oral	DEP (Oral)†	DETP (Oral)†
α (Distribution)	h^{-1}	4.5 ± 0.79	4.6 ± 0.79	3.5	0.17
$t_{1/2, \alpha}$	h	0.17 ± 0.03	0.17 ± 0.03	0.20	4.2
β (Elimination)	h^{-1}	0.12 ± 0.01	0.12 ± 0.01	0.013	0.12
$t_{1/2, \beta}$	h	6.2 ± 0.62	6.2 ± 0.62	52	5.8
k_a (Absorption)	h^{-1}	NA	0.26 ± 0.08	1.32	4.23
$t_{1/2, a}$	h	NA	3.6 ± 1.0	0.51	0.16
V_d/F	mL/kg	6,970 ± 905	6,973 ± 691	29,680	10,086
C_{max}	Mg/mL	3.3 ± 0.27	NA	0.31	2.0
T_{max}	H	0.39 ± 0.06	NA	1.0	0.80

NA, not applicable. Data represents mean ± S.E. for n = 3 - 5.
† The parameters presented were determined using the plasma concentration time curve data in Timchalk et al. (2007) paper and WinNonlin® software.

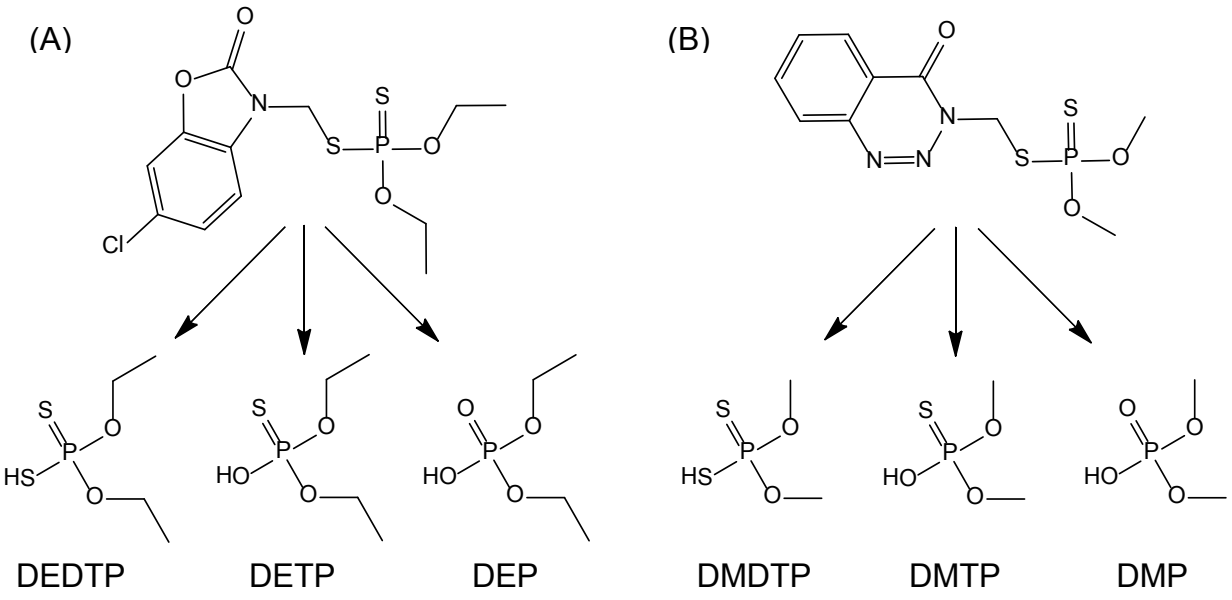

Figure 3-1. DAPs commonly used in biomonitoring studies and specific examples of DAPs found in urine following exposure to the OPs phosalone (A) and azinphos-methyl (B). Abbreviations: DEDTP, *O,O*-diethyldithiophosphate; DETP, *O,O*-diethylthiophosphate; DEP, *O,O*-diethylphosphate; DMDTP, *O,O*-dimethyldithiophosphate; DMTP, *O,O*-dimethylthiophosphate; DMP, *O,O*-dimethylphosphate.

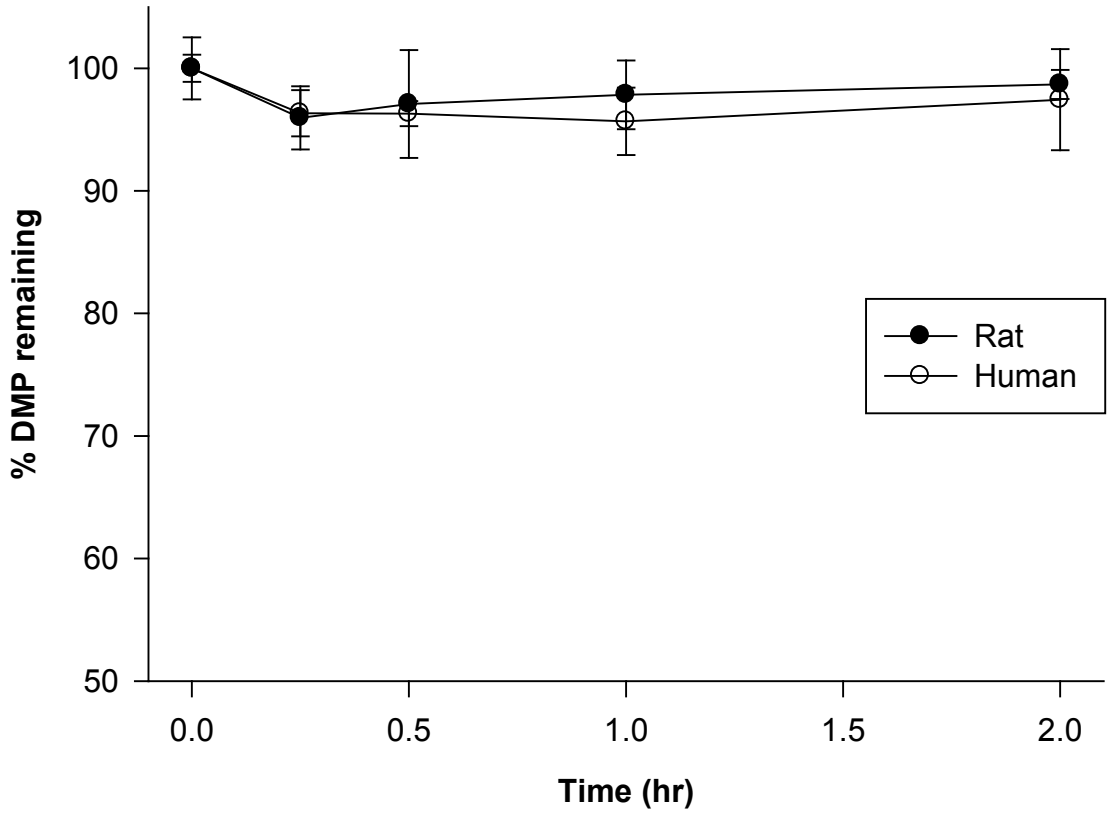

Figure 3-2. Percentage of DMP remaining in male Sprague-Dawley and pooled human hepatic microsome incubations. Error bars represent S.D. of four replicates. Statistical significance for intraspecies and interspecies differences, *p < 0.05.

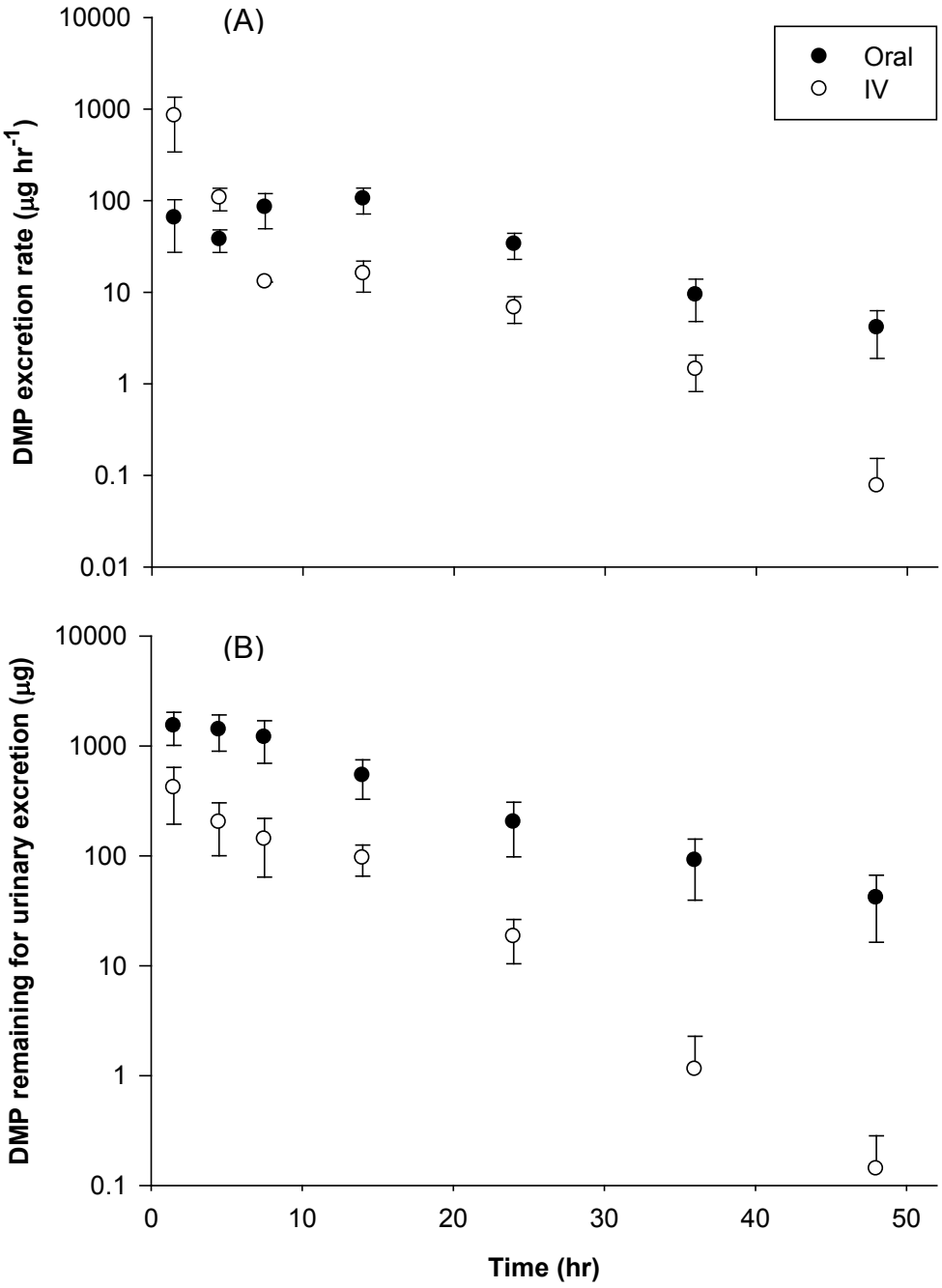

Figure 3-3. Time-course of DMP excretion rates (A) and urine Sigma-Minus DMP plot (B) following oral and i.v. administration of 20 mg/kg dose to male Sprague-Dawley rats. Data represents mean ± S.E. of 3 – 4 rats.

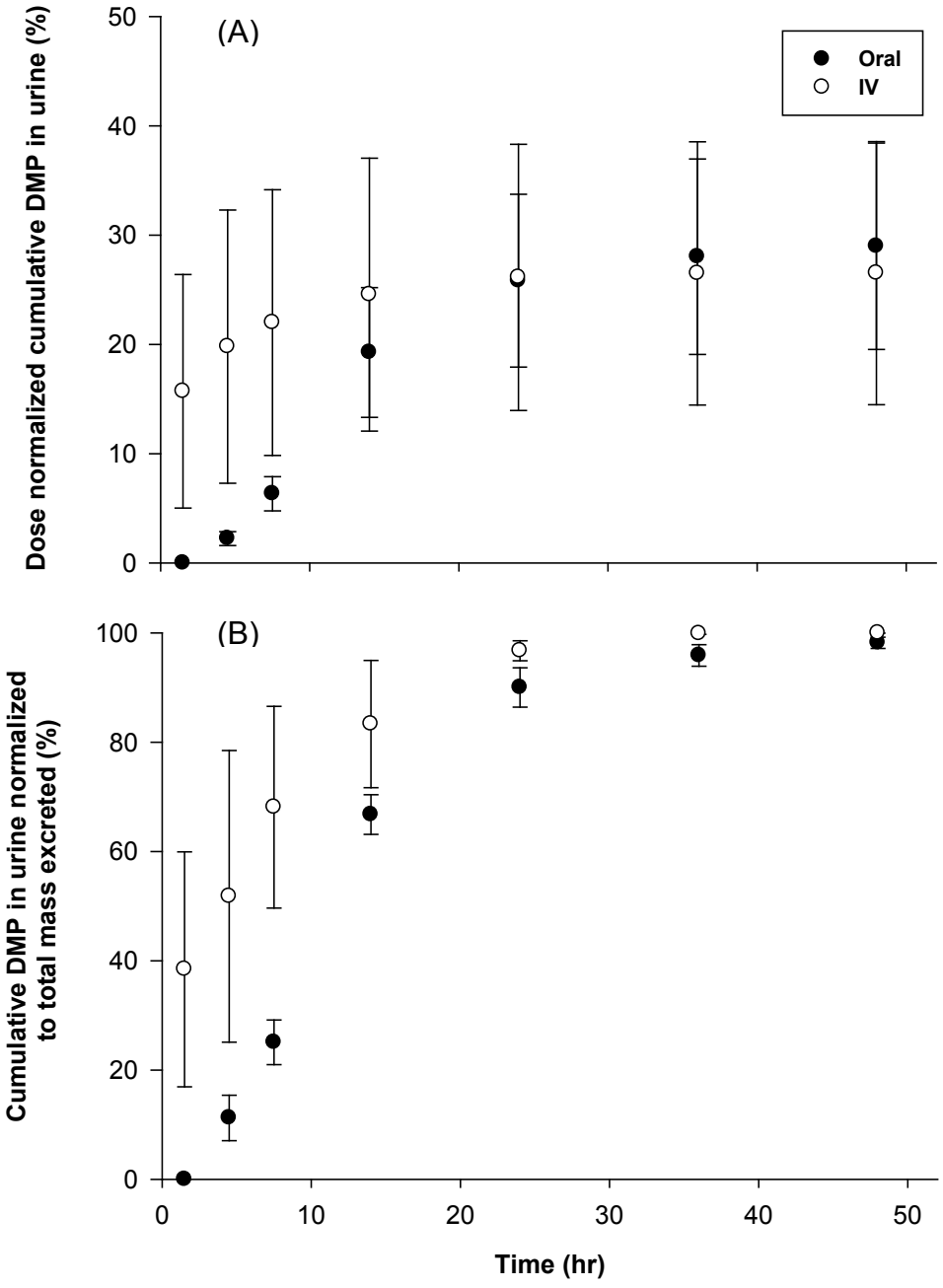

Figure 3-4. Time-course of dose normalized cumulative amount of DMP (A) and cumulative DMP in urine normalized to total mass excreted (B) following oral and i.v. administration of 20 mg/kg dose to male Sprague-Dawley rats. Data represents mean ± S.E. of 3 – 4 rats.

REFERENCE

Ackley, D. C., Rockich, K.T., Baker, T.R. (2004). Metabolic Stability Assessed by Liver Microsomes and Hepatocytes. Methods in Pharmacology and Toxicology Optimization in Drug Discovery: In Vitro Methods. Z. a. C. Yan, G.W. Totowa, NJ, Humana Press Inc.: 151-162.

Aprea, C., G. Sciarra, D. Orsi, P. Boccalon, P. Sartorelli and E. Sartorelli (1996). "Urinary excretion of alkylphosphates in the general population (Italy)." Science of the Total Environment 177(1-3): 37-41.

Aprea, C., M. Strambi, M. T. Novelli, L. Lunghini and N. Bozzi (2000). "Biologic monitoring of exposure to organophosphorus pesticides in 195 Italian children." Environmental Health Perspectives 116(6): 521-525.

Barr, D. B., R. Bravo, G. Weerasekera, L. M. Caltabiano, R. D. Whitehead Jr, A. O. Olsson, S. P. Caudill, S. E. Schober, J. L. Pirkle and E. J. Sampson (2004). "Concentrations of dialkyl phosphate metabolites of organophosphorus pesticides in the US population." Environmental Health Perspectives 112(2): 186-200.

Barr, D. B., R. Bravo, G. Weerasekera, L. M. Caltabiano, R. D. Whitehead, Jr., A. O. Olsson, S. P. Caudill, S. E. Schober, J. L. Pirkle, E. J. Sampson, R. J. Jackson and L. L. Needham (2004). "Concentrations of dialkyl phosphate metabolites of organophosphorus pesticides in the U.S. population." Environ Health Perspect 112(2): 186-200.

Bharate, S. B., J. M. Prins, K. M. George and C. M. Thompson (2010). "Thionate versus oxon: comparison of stability, uptake, and cell toxicity of (14CH3O)2-labeled methyl parathion and methyl paraoxon with SH-SY5Y cells." Journal of Agricultural and Food Chemistry 58(14): 8460-8566.

Bicker, W., M. Lämmerhofer, D. Genser, H. Kiss and W. Lindner (2005). "A case study of acute human chlorpyrifos poisoning: Novel aspects on metabolism and toxicokinetics derived from liquid chromatography-tandem mass spectrometry analysis of urine samples." Toxicology Letters 159(3): 235-251.

Bradman, A., B. Eskenazi, D. B. Barr, R. Bravo, R. Castorina, J. Chevrier, K. Kogut, M. E. Harnly and T. E. McKone (2005). "Organophosphate urinary metabolite levels during pregnancy and after delivery in women living in an agricultural community." Environ Health Perspectives 113(12): 1802-1807.

Bradway, D. E. and T. M. Shafik (1977). "Malathion exposure studies. Determination of mono- and dicarboxylic acids and alkyl phosphates in urine." Journal of Agricultural and Food Chemistry 25(6): 1342-1344.

Buratti, F. M., A. D'Aniello, M. T. Volpe, A. Meneguz and E. Testai (2005). "Malathion bioactivation in the human liver: the contribution of different cytochrome P450 isoforms." Drug Metab Dispos 33(3): 295-302.

Buratti, F. M., M. T. Volpe, A. Meneguz, L. Vittozzi and E. Testai (2003). "CYP-specific bioactivation of four organophosphorothioate pesticides by human liver microsomes." Toxicol Appl Pharmacol 186(3): 143-154.

Busby-Hjerpe, A. L., J. A. Campbell, J. N. Smith, S. Lee, T. S. Poet, D. B. Barr and C. Timchalk (2010). "Comparative pharmacokinetics of chlorpyrifos versus its major metabolites following oral administration in the rat." Toxicology 268(1-2): 55-63.

Casida, J. E. and G. B. Quistad (2004). "Organophosphate toxicology: safety aspects of nonacetylcholinesterase secondary targets." Chemical Research in Toxicology 17: 983-998.

Castorina, R., A. Bradman, T. E. McKone, D. B. Barr, M. E. Harnly and B. Eskenazi (2003). "Cumulative organophosphate pesticide exposure and risk assessment among pregnant women living in an agricultural community: a case study from the CHAMACOS cohort." Environmental Health Perspectives 111(13): 1640-1648.

Chanda, S. M. and C. N. Pope (1996). "Neurochemical and neurobehavioral effects of repeated gestational exposure to chlorpyrifos in maternal and developing rats." Pharmacology Biochemistry and Behavior 53(4): 771-776.

Eskenazi, B., K. Harley, A. Bradman, E. Weltzien, N. P. Jewell, D. B. Barr, C. E. Furlong and N. T. Holland (2004). "Association of in utero organophosphate pesticide exposure and fetal growth and length of gestation in an agricultural population." Environmental Health Perspectives 112(10): 1116-1123.

Eskenazi, B., A. R. Marks, A. Bradman, K. Harley, D. B. Bart, C. Johnson, N. Morga and N. P. Jewell (2007). "Organophosphate pesticide exposure and neurodevelopment in young Mexican-American children." Environmental Health Perspectives 115(5): 792-798.

Fenske, R. A., J. C. Kissel, C. Lu, D. A. Kalman, N. J. Simcox, E. H. Allen and M. C. Keifer (2000). "Biologically based pesticide dose estimates for children in an agricultural community." Environmental Health Perspectives 108(6): 515-520.

Hernández, F., J. V. Sancho and O. J. Pozo (2004). "An estimation of the exposure to organophosphorus pesticides through the simultaneous determination of their main metabolites in urine by liquid chromatography–tandem mass spectrometry." Journal of Chromatography B 808(2): 229-239.

Hong, F. and S. Pehkonen (1998). "Hydrolysis of phorate using simulated environmental conditions: rates, mechanisms, and product analysis." Journal of Agricultural and Food Chemistry 46: 1192-1199.

Lima, A. and L. Vega (2005). "Methyl-parathion and organophosphorous pesticide metabolites modify the activation status and interleukin-2 secretion of human peripheral blood mononuclear cells." Toxicology Letters 158(1): 30-38.

Loewenherz, C., R. A. Fenske, N. J. Simcox, G. Bellamy and D. Kalman (1997). "Biological monitoring of organophosphorus pesticide exposure among children of agricultural workers in central Washington state." Environmental Health Perspectives 105(12): 1344-1353.

Lu, C., R. Bravo, L. M. Caltabiano, R. M. Irish, G. Weerasekera and D. B. Barr (2005). "The presence of dialkylphosphates in fresh fruit juices: implication for organophosphorus pesticide exposure and risk assessments." Journal of Toxicology and Environmental Health, Part A 68(3): 209-227.

Lu, C., D. E. Knutson, J. Fisker-Andersen and R. A. Fenske (2001). "Biological monitoring survey of organophosphorus pesticide exposure among preschool children in the Seattle metropolitan area." Environmental Health Perspectives 109(3): 299-303.

Mileson, B. E., J. E. Chambers, W. L. Chen, W. Dettbarn, M. Ehrich, A. T. Eldefrawi, D. W. Gaylor, K. Hamernik, E. Hodgson, A. G. Karczmar, S. Padilla, C. N. Pope, R. J. Richardson, D. R. Saunders, L. P. Sheets, L. G. Sultatos and K. B. Wallace (1998). "Common mechanism of toxicity: a case study of organophosphorus pesticides." Toxicological Sciences 41(1): 8-20.

Poet, T. S., H. Wu, A. A. Kousba and C. Timchalk (2003). "In vitro rat hepatic and intestinal metabolism of the organophosphate pesticides chlorpyrifos and diazinon." Toxicological Sciences 72(2): 193-200.

Sakellarides, T. M., M. G. Siskos and T. A. Albanis (2003). "Photodegradation of selected organophosphorus insecticides under sunlight in different natural waters and soils." International Journal of Environmental Analytical Chemistry 83(1): 33-50.

Shafik, M. T., D. Bradway and H. F. Enos (1971). "Cleanup procedure for the determination of low levels of alkyl phosphates, thiophosphates, and dithiophosphates in rat and human urine." Journal of Agricultural and Food Chemistry 19(5): 885-889.

Shafik, T., D. E. Bradway, H. F. Enos and A. R. Yobs (1973). "Human exposure to organophosphorus pesticides. Modified procedure for the gas-liquid chromatographic analysis of alkyl phosphate metabolites in urine." Journal of Agricultural and Food Chemistry 21(4): 625-629.

Slotkin, T. A., F. J. Seidler, C. Wu, E. A. MacKillop and K. G. Linden (2009). "Ultraviolet photolysis of chlorpyrifos: developmental neurotoxicity modeled in PC12 cells." Environmental Health Perspectives 117(3): 338-343.

Timchalk, C., A. Busby, J. A. Campbell, L. L. Needham and D. B. Barr (2007). "Comparative pharmacokinetics of the organophosphorus insecticide

chlorpyrifos and its major metabolites diethylphosphate, diethylthiophosphate and 3,5,6-trichloro-2-pyridinol in the rat." Toxicology 237(1-3): 145-157.

Vega, L., M. Valverde, G. Elizondo, J. F. Leyva and E. Rojas (2009). "Diethylthiophosphate and diethyldithiophosphate induce genotoxicity in hepatic cell lines when activated by further biotransformation via Cytochrome P450." Mutation Research/Genetic Toxicology and Environmental Mutagenesis 679(1-2): 39-43.

Wagner, J. G. and J. W. Ayres (1977). "Bioavailability assessment: Methods to estimate total area (AUC0-∞) and total amount excreted and importance of blood and urine sampling scheme with application to digoxin." Journal of Pharmacokinetics and Pharmacodynamics 5(5): 533-557.

Wessels, D., D. B. Barr and P. Mendola (2003). "Use of biomarkers to indicate exposure of children to organophosphate pesticides: implications for a longitudinal study of children's environmental health." Environmental Health Perspectives 111(16): 1939-1946.

Whitney, K. D., F. J. Seidler and T. A. Slotkin (1995). "Developmental Neurotoxicity of Chlorpyrifos: Cellular Mechanisms." Toxicology and Applied Pharmacology 134(1): 53-62.

Wu, W., McKown, L.A. (2004). In Vitro Drug Metabolite Profiling Using Hepatic S9 and Human Liver Microsomes. Optimization in Drug Discovery: In Vitro Methods. Z. a. C. Yan, G.W. Totowa, NJ, Humana Press Inc.: 163-185.

Wu, W. N., L. A. McKown and S. Liao (2002). "Metabolism of the analgesic drug ULTRAM (tramadol hydrochloride) in humans: API-MS and MS/MS characterization of metabolites." Xenobiotica 32(5): 411-425.

Yan, Z., G. W. Caldwell, W. N. Wu, L. A. McKown, B. Rafferty, W. Jones and J. A. Masucci (2002). "In vitro identification of metabolic pathways and cytochrome P450 enzymes involved in the metabolism of etoperidone." Xenobiotica 32(11): 949-962.

Young, J. G., B. Eskenazi, E. A. Gladstone, A. Bradman, L. Pedersen, C. Johnson, D. B. Barr, C. E. Furlong and N. T. Holland (2005). "Association between in utero organophosphate pesticide exposure and abnormal reflexes in neonates." Neurotoxicology 26(2): 199-209.

Zhang, X., J. H. Driver, Y. Li, J. H. Ross and R. I. Krieger (2008). "Dialkylphosphates (DAPs) in fruits and vegetables may confound biomonitoring in organophosphorus insecticide exposure and risk assessment." J Agric Food Chem 56(22): 10638-10645.

Zhang, X., J. H. Driver, Y. Li, J. H. Ross and R. I. Krieger (2008). "Dialkylphosphates (DAPs) in fruits and vegetables may confound biomonitoring in organophosphorus insecticide exposure and risk

assessment." Journal of Agricultural and Food Chemistry 56(22): 10638-10645.

CHAPTER 4

PHARMACOKINETICS OF XANTHOHUMOL AND METABOLITES IN RATS AFTER ORAL AND INTRAVENOUS ADMINISTRATION

LeeCole Legette, Lian Ma, Ralph L. Reed, Cristobal L. Miranda, John Mark Christensen, Rosita Rodriguez-Proteau and Jan F. Stevens

Manuscript in: (2012) Mol. Nutr. Food Res. 56(3):466-74

ABSTRACT

Recent evidence suggests that xanthohumol (XN), a dietary flavonoid found in hops, may have health protective actions against cardiovascular disease and type II diabetes. Yet, there are limited data on the pharmacokinetics of XN. This study provides basic pharmacokinetics (PK) parameters for XN and its major metabolites in rats.

A pharmacokinetic study was conducted in male jugular vein-cannulated Sprague-Dawley rats. Rats (n=12/group) received an intravenous (IV) injection (1.86 mg/kg BW) or an oral gavage of a low (1.86 mg/kg BW), medium (5.64 mg/kg BW), or high (16.9 mg/kg BW) dose of XN. Plasma samples were analyzed for XN and its metabolites using LC-MS/MS. The maximum concentration (C_{max}) and area under the curve ($AUC_{0-\infty}$) of total XN (free and conjugated) were 2.9 ± 0.1 mg/L and 2.5 ± 0.3 h*mg/L in the i.v. group, 0.019 ± 0.002 mg/L and 0.84 ± 0.17 h*mg/L in the oral low group, 0.043 ± 0.002 mg/L and 1.03 ± 0.12 h*mg/L in the oral medium group, and 0.15 ± 0.01 mg/L and 2.49 ± 0.10 h*mg/L in the oral high group.

The bioavailability of XN is dose-dependent and approximately 0.33, 0.13 and 0.11 in rats, for the low, medium and high dose groups, respectively.

Abbreviations: **6PN**, 6-prenylnaringenin; **8PN**, 8-prenylnaringenin; **AIN93G**, 1993 American Institute of Nutrition dietary guidelines for growing rodents; **DHC**, 4,2'-dihydroxychalcone**; IX**, isoxanthohumol; **SRM**, selective reaction monitoring; **XN**, xanthohumol

INTRODUCTION

The flowers of the female hop plant (*Humulus lupulus* L.) are used in the brewing industry to add bitterness and flavor to beer. The bitter principles of the hop flowers (commonly referred to as 'hops' or 'hop cones') are prenylated acylphloroglucinol derivatives in a biogenetic sense, and they can be classified as humulones (α-bitter acids) or lupulones (β-bitter acids). Structurally related to the bitter acids are the prenylated flavonoids, which are produced by hops in specialized glands together with the bitter acids and secreted as a sticky resin called 'lupulin'. The principal prenylated flavonoid of hops is xanthohumol (XN) (Stevens, Ivancic et al. 1997), a yellow substance also found in beer (Stevens, Taylor et al. 1999), which may have health-promoting properties as an antioxidant (Miranda, Stevens et al. 2000), an anti-inflammatory agent (Lupinacci, Meijerink et al. 2009; Peluso, Miranda et al. 2010), a cancer chemopreventive agent (Miranda, Stevens et al. 1999; Miranda, Aponso et al. 2000; Miranda, Yang et al. 2000; Gerhauser, Alt et al. 2002; Dietz, Kang et al. 2005; Gerhauser 2005; Colgate, Miranda et al. 2007; Plazar, Filipic et al. 2008), a modulator of the immune system (Xuan, Shumilina et al. 2010), an antimicrobial agent (Gerhauser 2005), and as an inhibitor of osteoporosis in post-menopausal women (Stevens and Page 2004).

Recent evidence suggests that dietary bioactives could aid in prevention and/or halt the progression of several chronic diseases (Kris-Etherton, Hecker et al. 2002; Ferrari 2004; Heber 2004; Milner 2004). Nearly 50 million Americans have metabolic syndrome and are at increased risk for cardiovascular disease and type 2 diabetes (Ford, Giles et al. 2002). In particular, daily oral administration of XN for one month has been shown by Nozawa (Nozawa 2005) to lower plasma triacylglycerols and glucose levels in KK-A^y mice, a model for obesity and type 2 diabetes. Nozawa's study also demonstrated a decrease in wet epididymal weight and an increase in plasma

adiponectin levels. In a study conducted by Mendes *et al.* (Mendes, Monteiro et al. 2008), XN reduced differentiation, decreased proliferation, and increased apoptosis in the murine preadipocyte cell line, 3T3-L1, at concentrations in the range of 1-10 μM. Similar effects of XN were observed by Rayalam *et al.* (Rayalam, Yang et al. 2009) and also by Yang *et al.* (Yang, Della-Fera et al. 2007), who found that the XN-induced apoptosis of 3T3-L1 cells resulted from increased production of reactive oxygen species. In cultured hepatoma HepG2 cells, XN inhibited triacylglycerol synthesis by 62% at 15 μM and dose-dependently decreased apolipoprotein B secretion by 13 - 43 % at 5 - 15 μM (Casaschi, Maiyoh et al. 2004). The decrease in triacylglycerol synthesis was attributed to inhibition of cellular diacylglycerol acyltransferase activity (Casaschi, Maiyoh et al. 2004). *In vitro* and *in vivo* studies have also shown that XN may reduce the risk for non-alcohol steatohepatits, a serious liver condition associated with obesity and type 2 diabetes (Dorn, Kraus et al.). Dorn *et al.* observed inhibition of hepatic inflammation and fibrosis with 3 week feeding of XN (1% w/w XN in diet) in BALB/c mice (Dorn, Kraus et al.). Taken together, these studies suggest that XN may exert beneficial effects in dyslipidemia and its complications.

The question that remains to be answered is whether sufficient plasma and tissue levels of XN or its active metabolites can be reached by oral intake of XN in order obtain the biological effects observed in cell culture studies. *In vitro* and animal studies have established that the chalcone XN is non-enzymatically converted into its flavanone isomer, isoxanthohumol (IX), and enzymatically into 6- and 8-prenylnaringenin (6PN and 8PN) (Figure 1). The conversion of IX into 8PN is mediated by hepatic CYP1A2 (Guo, Nikolic et al. 2006) or by gut microflora enzymes (Possemiers, Heyerick et al. 2005; Possemiers, Bolca et al. 2006; Bolca, Possemiers et al. 2007). XN and its metabolites are found in the free form or as conjugates (mainly as glucuronides and sulfates) (Yilmazer, Stevens et al. 2001; Yilmazer, Stevens

et al. 2001; Jirasko, Holcapek et al. 2010). Minor metabolites of XN include chalcones or flavanones with oxygenation of the prenyl substituent, the olefin carbons between the A- and B-rings, and the B-ring itself (Nikolic, Li et al. 2004; Nookandeh, Frank et al. 2004).

Very few studies have been published on the quantitative aspects of XN absorption, distribution, metabolism, and excretion *in vivo*. Hanske *et al*. (Hanske, Loh et al. 2010) administered XN intragastrically (48 μmol/kg body weight = 17 mg/kg BW) to germ-free and human microbiota-associated Sprague-Dawley rats. The microbiota adequate rats showed maximal blood concentrations of 0.65 μM (free XN), 0.11 μM (conjugated XN), 1.04 μM (free IX), and 4.87 μM (conjugated IX), while 8PN was not detected. The recovery of the administered XN dose from the urine and the feces amounted to 4.2% in the form of XN, IX, 8PN, and their conjugates (Hanske, Loh et al. 2010). Other studies also indicate low recovery of XN and its metabolites. Bolca *et al.* (Bolca, Possemiers et al. 2007) reported that the mean recovery of free and conjugated XN was 0.32 % from the 24 hr urine of post-menopausal women after 5 days of daily intake of 1.38 mg XN. These data show that XN is absorbed and metabolized *in vivo*, but the bioavailability of XN has not yet been established in quantitative terms.

The aim of the present study was to determine basic aspects of the absorption, distribution, and metabolism of XN in male jugular vein-cannulated Sprague-Dawley rats. A single-dose pharmacokinetics (PK) study was conducted at three oral dose levels and one i.v. dose level in order to determine bioavailability and dependence of PK parameters on dose level. The PK parameters from this study make it possible to estimate plasma levels of XN and its metabolites (IX, 6PN and 8PN) for any dosage regimen at steady-state, a necessary step in the evaluation of potential of XN as an agent in the prevention/treatment of dyslipidemia and possibly other metabolic disorders.

MATERIALS AND METHODS

Animals

Six week old male Sprague Dawley rats were purchased from Harlan (Livermore, CA, USA) and underwent jugular catheter implantation surgery two days before shipment. Rats were maintained on an American Institute of Nutrition rodent diet (AIN 93G) (Reeves, Nielsen et al. 1993) with corn oil replacing soy oil and deionized water *ad libitum* throughout the study. Animals were housed in individual cages in temperature and humidity controlled rooms with a 12:12 on-off light cycle. All procedures were approved by Oregon State University's Institutional Animal Care and Use Committee (Protocol #3689).

Treatment Groups

After a two day acclimation period, animals were divided into four treatment groups (n = 12/group): i.v. (1.86 mg XN / kg BW), oral low (1.86 mg XN / kg BW), oral medium (5.64 mg XN / kg BW), and oral high (16.9 mg XN / kg BW). These oral dose levels were selected to correspond to oral doses of 20, 60 and 180 mg XN in humans by using allometric interspecies scaling (2005). Animals were selected to ensure similar body weight average across treatment groups.

Dose and sampling

XN powder was a gift from Anheuser-Busch Companies, Inc., St. Louis, MO, USA and checked for identity and purity (> 99%) by ^{1}H NMR and HPLC with photodiode detection. For each oral dose level, appropriate amounts of XN powder were dissolved in a self-emulsifying isotropic mixture of oleic acid, propylene glycol, and Tween 80. After a 12 hr fast, animals received a single oral gavage solution (1.86, 5.64, or 16.9 mg/kg BW). The animals in the i.v. group were given an intravenous (IV) injection (1.86 mg/kg BW) of XN dissolved in propylene glycol. The i.v. injection was administered through the

jugular catheter. Before each blood draw, the flushing solution was removed from the catheter and blood was drawn to the end of the catheter before a clean sterile needle was placed on for blood collection. Blood (0.3 mL) was drawn via jugular catheter from each rat at the following time points: 0, 0.2, 0.5, 1, 1.5, 2, 4, 8, 12, 24, 48, 72, and 96 hr. After each blood draw, the jugular catheter was flushed with 0.3 mL heparinized saline (20 U/mL) to maintain constant blood volume. Food was returned to animals after the 4 hr blood collection. Blood samples were placed in collection tubes coated with lithium heparin (Microvette CB 300, Sarstedt Inc., Newton, NC, USA) and stored on ice immediately after collection. Samples were centrifuged for 10 min at 2000 $\times$ g (VWR Microcentifuge Galaxy 7D, VWR, Radnor, PA, USA). Plasma was stored at -80 ^{o}C until analysis for XN and its metabolites.

Sample analysis

Aliquots (10 μL for i.v. and 25 μL for oral groups) of plasma in duplicate were diluted with sodium acetate buffer (0.1 M, pH = 4.7), spiked with of 4,2'-dihydroxychalcone (DHC) (2.4 ng in methanol) (Indofine Chemical Company, Hillsborough, NJ) as internal standard, and treated with 600 U of *Helix pomatia* hydrolases dissolved in sodium acetate buffer (Sigma, St. Louis, MO) for 3 hours at 37 ^{o}C in a total volume of 600 μL to convert glucuronide and sulfate conjugates to their free aglycone forms. Incubation solutions were extracted three times with diethyl ether (1.0 mL) and centrifuged for 1 min at 8500 $\times$ g (VWR Microcentifuge Galaxy 7D, VWR). The combined ether extracts were taken to dryness with a stream of nitrogen gas using a TurboVap LV evaporator (Zymark, Hopkinton, MA). The residues were dissolved in 0.1 mL of methanol containing 0.1 % formic acid, briefly vortexed (10 s) and sonicated (30 s), and analyzed directly by LC-MS/MS.

XN standard was obtained by isolation from hops and IX by isomerization of XN (Stevens, Ivancic et al. 1997; Stevens, Taylor et al. 1999).

Standards of 6PN and 8PN were obtained by chemical prenylation of naringenin (Sigma, St. Louis, MO) and chromatographic separation of the regioisomers (Stevens, Taylor et al. 1999). Calibration curves were prepared by spiking blank rat plasma with known concentrations of XN, IX, 6PN, 8PN, and the internal standard, DHC, using 7 – 10 concentration levels covering the entire concentration range for all analytes in the samples. The plasma-based calibration samples were treated the same as the samples obtained from dosed animals. The method was validated for precision (12% RSD or better), accuracy (90-110% recovery of standards) and for limit of quantitation (0.4-0.5 nM, depending on analyte).

LC-MS/MS was performed on an Applied Biosystems 4000 QTRAP hybrid linear ion trap-triple quadrupole instrument (AB Sciex, Concord, ON, Canada) operated at a source temperature of 600 °C with a needle voltage of -4500 kV. Nitrogen was used as the source gas, curtain gas, and collision gas. Selected reaction monitoring (SRM) experiments were conducted at collision energies ranging from -25 to -40 eV. Concentrations were calculated using the internal calibration method and Analyst Software (Analyst 1.5, AB Sciex).

A Shimadzu Prominence HPLC system (Shimadzu, Columbia, MD), consisting of two LC-20AD pumps, a DQU-20A_5 degasser, and an SIL-HTC autosampler, equipped with switching valves, were used for all chromatography. Chromatographic separations of XN and its metabolites were achieved on a 2 $\times$ 50 mm Zorbax 300SB C8 column (Agilent, Santa Clara, CA) eluted with a gradient of 25 to 60 % solvent B (0.1 % formic acid in ACN) in solvent A (aqueous 0.1 % formic acid) in 2.6 min at a flow rate of 0.5 mL/min after an initial 1.4 min at 25 % solvent B. The column was washed with 100 % solvent B for 1.4 min and re-equilibrated at 25 % solvent B for 9 min prior to each injection. Precursor $\rightarrow$ product ion transitions for SRM were developed using standards. SRM transitions used for quantitation included:

353 → 119 for IX and XN, 339 → 219 for 8PN and 6PN, and 239 → 119 for DHC.

Pharmacokinetic model and parameters

Mean plasma concentration-time profiles for XN and its metabolites (IX, 6PN and 8PN) were generated using GraphPad Prism software (version 4.03, San Diego, CA, USA). The concentration-time profiles were fitted to different compartmental models and the goodness of fit was determined based on Akaike and Schwarz criteria values (Ludden, Beal et al. 1994) using WinNonlin software (version 5.0.1; Pharsight, Sunnyvale, CA, USA). A two-compartment model was selected to describe the data. The models for oral (Eq. 1) and i.v. (Eq. 2) administration were defined by the following equations:

Oral administration:

$$C(t) = Ae^{-\alpha t} + Be^{-\beta t} + Ce^{-kat} \quad \text{(Eq. 1)}$$

Intravenous administration:

$$C(t) = Ae^{-\alpha t} + Be^{-\beta t} \quad \text{(Eq. 2)}$$

where α is the first-order distribution rate constant, β is the first-order elimination rate constant and ka is the absorption rate constant; A, B and C are the coefficients for distribution, elimination and absorption phases, respectively. C(t) represents the concentration of XN at a given time, t. Maximum plasma concentration (C_{max}) and the time to reach C_{max} (T_{max}) were determined from the plasma concentration-time curves. Optimized estimates for the model parameters were obtained using nonlinear regression analysis and WinNonlin software (WinNonlin 5.0.1; Pharsight). Estimates were used to calculate the following values: apparent volume of distribution (V_d), total steady state volume of distribution (V_{ss}), central compartment volume (V_c), peripheral compartment volume (V_p), the apparent distribution and elimination half-lives (t1/2 α and t1/2 β), area under the plasma concentration-time curve

(AUC), and systemic total body clearance (CL). CL was determined using the following equation:

$$CL = F \times Dose / AUC \quad \text{(Eq. 3)}$$

The bioavailability (F) of XN was determined for each oral dose by developing a systemic exposure profile obtained from measuring the concentration of free and conjugated XN over time in samples collected from the systemic circulation as defined by the Food and Drug Administration (FDA) (FDA 2003) and using the following equation:

$$F = (AUC_{0\text{-}\infty}{}^{\text{oral dose}} / AUC_{0\text{–}\infty}{}^{\text{i.v.)}} \times (Dose^{\text{i.v.}} / Dose^{\text{oral dose}}) \quad \text{(Eq. 4)}$$

Steady state peak (Css,max) concentrations were estimated for the three oral doses (D) using the following equation with D = dose and τ = dosing interval = 24 hr:

$$C_{ss,max} = (FD / V_d) \times (1 / 1 - e^{-\kappa\tau}) \times (e^{-kT\max}) \quad \text{(Eq. 5)}$$

RESULTS AND DISCUSSION

Pharmacokinetic parameters of XN and its metabolites

The pharmacokinetic parameters for XN from i.v. (1.86 mg/kg) and three oral doses (1.86 mg/kg, 5.64 mg/kg, 16.9 mg/kg) are listed in Table 4-1. Plasma concentration-time curves of XN are shown in Figures 4-2 and 4-3. Following i.v. administration (Figure 4-2), the plasma concentration-time profile of total XN demonstrated a biphasic decline. It started with a rapid distribution phase, where plasma concentration dropped to 50% in approximately 20 minutes, followed by a slow elimination phase up to 96 hr. Extrapolation of the elimination phase yielded a $t_{1/2,\beta}$ of 33.78 ± 3.15 hr. A low clearance rate (0.87 ± 0.14/Lh/kg) and high steady state volume of distribution (V_{ss}) (32.40 ± 6.16 L/kg) indicates high tissue distribution, which is also supported by observed large V_p values.

Following oral administration (Figure 4-3), peak plasma XN levels were achieved at a similar T_{max} (~ 4 hr post dosing) for low, medium and high XN groups. High plasma concentrations of XN were observed between 0.5 – 2 hr and 8 – 12 hr suggesting both small and large intestinal absorption as well as possible enterohepatic recirculation, as previously reported for other flavonoids (Sfakianos, Coward et al. 1997; Chen, Lin et al. 2003; Jia, Chen et al. 2004). The half-lives for the terminal phase also appear to be long for all oral groups (18 - 30 hr).

Time courses for plasma concentrations of XN metabolites (IX and 8PN) after oral administration are shown in Figures 4-4 and 4-5. There were barely detectable levels of 6PN in all treatment groups. Similar to XN, the elimination of IX also appears to be biphasic. For 8PN however, the elimination process is adequately described with a one-compartment open model. The estimated pharmacokinetic parameters for IX and 8PN are detailed in Tables 4-2 and 4-3. There was also a greater amount of circulating

XN metabolites compared to XN in oral medium and high dose animals at 24 and 48 hr.

Hepatic demethylation of IX

The high amount of circulating IX in early time points (0.2 – 4 hr) as well as 8PN at later time points (12 – 48 hr) compared to barely detectable levels of 6PN suggests rapid isomerization of XN to IX followed by hepatic demethylation of IX to produce 8PN (Figure 4-1). After an oral dose of XN, the peak plasma levels of IX reached a T_{max} around 7 – 8 hr whereas the T_{max} of 8PN is doubled (15 - 24 hr). These findings are consistent with current knowledge of the XN metabolic pathway (Figure 4-1). Hepatic demethylation of IX to form 8PN may contribute to in vivo estrogenicity because 8PN has one of the most potent estrogenic activities among flavonoids (Kitaoka, Kadokawa et al. 1998; Milligan, Kalita et al. 1999; Milligan, Kalita et al. 2000; Coldham and Sauer 2001; Milligan, Kalita et al. 2002; Bovee, Helsdingen et al. 2004). It is generally believed that some health protective actions of flavonoids are due to their estrogenic activities. Previous studies have demonstrated that low micromolar concentrations of XN are associated with protective bone and heart health actions through stimulation of bone formation via osteoblast differentiation (Jeong, Han et al.) and inhibition of LDL protein oxidation (Stevens, Miranda et al. 2003).

Steady-state plasma concentrations

An oral low, medium, and high dose of XN resulted in projected steady state peak concentrations ($C_{ss,max}$) of 0.094, 0.129, and 0.213 μM in rats. Preliminary data from our lab supports this estimate. Daily feeding of the oral high XN dose (16.9 mg/kg BW per day), as a mixture of the oral gavage solution in 3 g of AIN 93G diet, to Sprague Dawley rats (n = 2) resulted in plasma concentrations of 0.2 - 0.3 μM (data not shown).

Bioavailability

The bioavailability of total XN (free and conjugated) was calculated to be 33.1%, 13.4% and 10.8% for low, medium and high dose groups, respectively. XN is similar, in terms of structure and biological activity, to soy isoflavones (Overk, Yao et al. 2005); as expected, our findings on bioavailability are comparable to earlier works examining bioavailability of soy isoflavones. Qiu *et al.* determined the bioavailability of total daidzein (free and conjugated), a soy isoflavone, to be 47% for a low dose (20 mg/kg) in Wistar rats (Qiu, Chen et al. 2005). Both oral medium and high XN groups had similar XN bioavailability which was lower than the oral low group suggesting that XN absorption in the gastrointestinal (GI) tract is dependent on the dissolution of XN. Due to the low solubility of XN, bioavailability will decline as observed between oral low and medium doses. Similar dose-response effects on bioavailability have been observed with other flavonoids as well. Setchell *et al.* reported decreased bioavailability of soy isoflavones genistein and daidzein with increasing isoflavones intake in healthy women (Setchell, Brown et al. 2003). In addition to dose amount, dosage formulation of a flavonoid can also influence its bioavailability (Qiu, Chen et al. 2005) .

CONCLUSION

Our findings on the fate of XN in rats and the dose-dependent bioavailability of XN provide pertinent information for subsequent studies. Pharmacokinetic parameters obtained in this study can be utilized to predict steady state plasma levels for XN and its metabolites at various dose levels and coupled with interspecies scaling could aid tremendously in determining the dosing regimen for clinical studies. Doses administered in this study (1.86, 5.64, 16.9 mg / kg BW) correspond to scaled values of 20, 60, 180 mg XN in humans with a BW of 66 kg. The most prominent flavonoid in beer is IX (due to isomerization of XN in brewery process) and the estimated daily intake of prenylflavonoids for the average American is 0.14 mg (Stevens and Page 2004). This suggests that dietary consumption alone will not be sufficient to attain health benefits of XN and highlights the need for future work to determine optimal therapeutic doses of XN. The dose-dependent bioavailability of XN observed in this study also emphasizes the importance of additional investigation of XN metabolism in order to elucidate and optimize the potential health benefits of XN and its metabolites.

Table 4-1. Pharmacokinetic (PK) parameters for total free and conjugated xanthohumol for i.v. and oral treated rats (n = 12/group)

Parameter	Units	IV	Oral		
		1.86 mg/kg	1.86 mg/kg	5.64 mg/kg	16.9 mg/kg
A	mg/L	2.85 ± 1.12	0.107 ± 0.045	0.126 ± 0.058	1.25 ± 0.43
B	µg/L	21.2 ±3.3	4.46 ±1.28	10.5 ± 6.6	15.1 ± 12.9
k_a	h^{-1}	N/A	1.08 ± 0.32	0.61 ± 0.16	0.58 ± 0.22
α	h^{-1}	2.09 ± 0.20	0.40 ± 0.26	0.10 ± 0.01	0.15 ± 0.04
β	h^{-1}	0.021 ± 0.005	0.035 ± 0.016	0.023 ± 0.008	0.04 ± 0.01
AUC	h*mg/L	2.54 ± 0.34	0.839± 0.168	1.03 ± 0.12	2.49 ± 0.10
half-life $t_{1/2,\alpha}$ a)	h	0.33 ± 0.03	1.75 ± 0.38	7.18 ± 1.16	4.55 ± 0.97
half-life $t_{1/2,\beta}$ a)	h	33.8 ± 3.2	20.1 ± 5.8	30.4 ± 4.9	18.2 ± 2.0
V_c/F	L/kg	1.16 ± 0.19	72.8 ± 12.1	88.2 ± 5.7	96.0 ± 51.2
V_p/F	L/kg	31.2 ± 6.0	80.2 ± 25.0	168 ± 57	64.9 ± 7.2
CL/F a)	$L\ h^{-1}kg^{-1}$	0.87±0.14	1.00 ± 0.22	0.80 ± 0.08	1.30 ± 0.65
T_{max}	h	N/A	3.61 ± 0.74	4.51 ± 0.54	4.50 ± 0.59
C_{max}	mg/L	2.87 ± 0.11	0.019 ± 0.002	0.043 ± 0.002	0.15 ± 0.01
V_{ss}	L/kg	32.4 ± 6.2	50.6 ± 8.6	34.2 ± 7.4	17.4 ± 5.4
F			0.33	0.13	0.11

All values are expressed as mean ± S.E.
a) Values were calculated using harmonic means.

Table 4-2. Pharmacokinetic parameters for total free and conjugated isoxanthohumol for i.v. and oral treated rats (n = 12/group)

Parameter	Units	IV	Oral		
		1.86 mg/kg	1.86 mg/kg	5.64 mg/kg	16.9 mg/kg
α	h^{-1}	1.45 ± 0.18	0.09 ± 0.01	0.10 ± 0.01	0.08 ± 0.01
β	h^{-1}	0.11 ± 0.05	0.07 ± 0.03	0.08 ± 0.01	0.07 ± 0.01
AUC	h*µg/L	195± 41	79.3 ± 8.4	196 ± 26	820 ± 109
half-life $t_{1/2,\alpha}$ a)	h	0.48 ± 0.06	8.1 ± 1.2	7.2 ± 2.4	8.4 ± 2.3
half-life $t_{1/2,\beta}$ a)	h	6.4 ± 1.9	10.2 ± 3.9	8.6 ± 1.2	10.5 ± 3.7
CL/F a)	$L\ h^{-1}kg^{-1}$	13.8 ± 3.0	23.5 ± 2.9	28.7 ± 3.0	20.6 ± 1.9
T_{max}	h	N/A	7.81 ± 1.31	7.30 ± 1.00	8.14 ± 0.96
C_{max}	µg/L	81.1 ± 11.7	3.27 ± 0.29	8.15 ± 1.09	31.1 ± 4.4
V_{ss}	L/kg	312 ± 81	312 ± 84	393 ± 104	334 ± 86

All values are expressed as mean ± S.E.
a) Values were calculated using harmonic means.

Table 4-3. Pharmacokinetic parameters for total free and conjugated 8-prenylnaringenin for i.v. and oral treated rats (n = 12/group)

Parameter	Units	IV	Oral		
		1.86 mg/kg	1.86 mg/kg	5.64 mg/kg	16.9 mg/kg
V/F	L/kg	499 ± 113	570 ± 124	654 ± 183	507 ± 67
k_a	h^{-1}	0.047 ± 0.003	0.077 ± 0.014	0.097 ± 0.033	0.042 ± 0.002
AUC	h*µg/L	121± 24	76.5 ± 12.4	284 ± 53	986 ± 169
half-life, $t_{1/2}$	h	16.2 ± 1.7	9.8 ± 1.6	9.3 ± 2.9	16.6 ± 0.8
CL/F a)	L $h^{-1}kg^{-1}$	15.4 ± 3.2	24.3 ± 3.9	19.8 ± 5.8	17.1 ± 3.2
T_{max}	h	23.2 ± 1.4	17.2 ± 3.2	15.8 ± 1.9	24.3 ± 1.2
C_{max}	µg/L	2.2 ± 0.3	1.6 ± 0.2	5.1 ± 0.7	14.7 ± 2.2

All values are expressed as mean ± S.E.

a) Values were calculated using harmonic means.

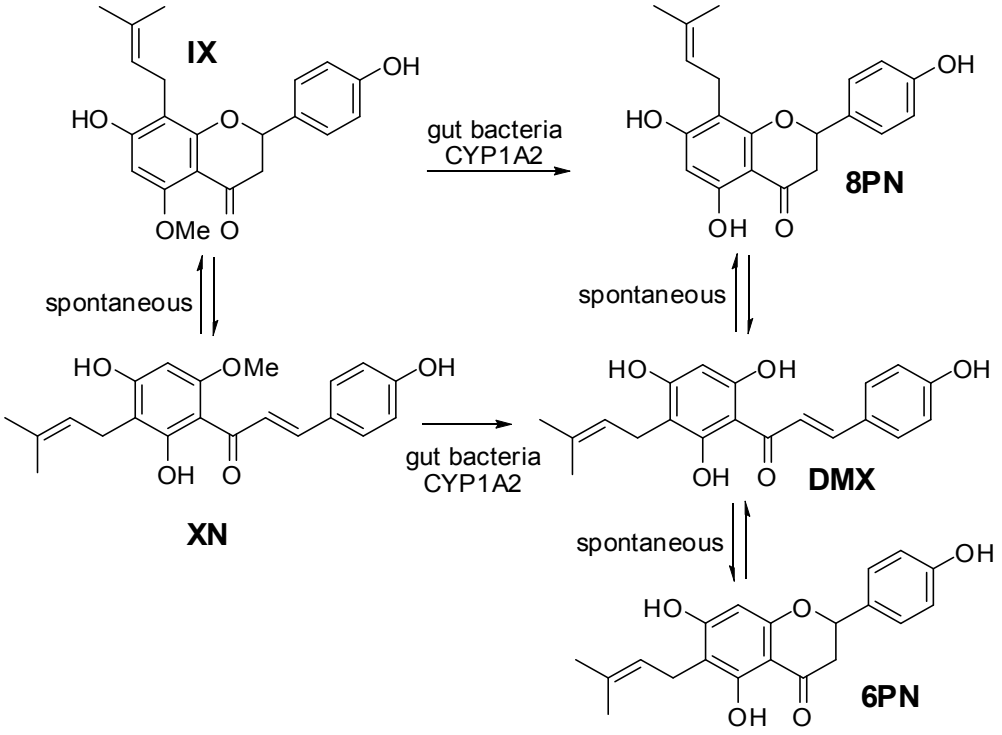

Figure 4-1. Metabolic conversion of XN into desmethylxanthohumol (DMX) and 6- and 8-prenylnaringenin (6PN and 8PN). XN is spontaneously converted into isoxanthohumol (IX) by intramolecular Michael addition. 6-Prenylnaringenin (6PN) is formed from DMX. 8-Prenylnaringenin is formed from DMX or from IX by CYP-mediated demethylation.

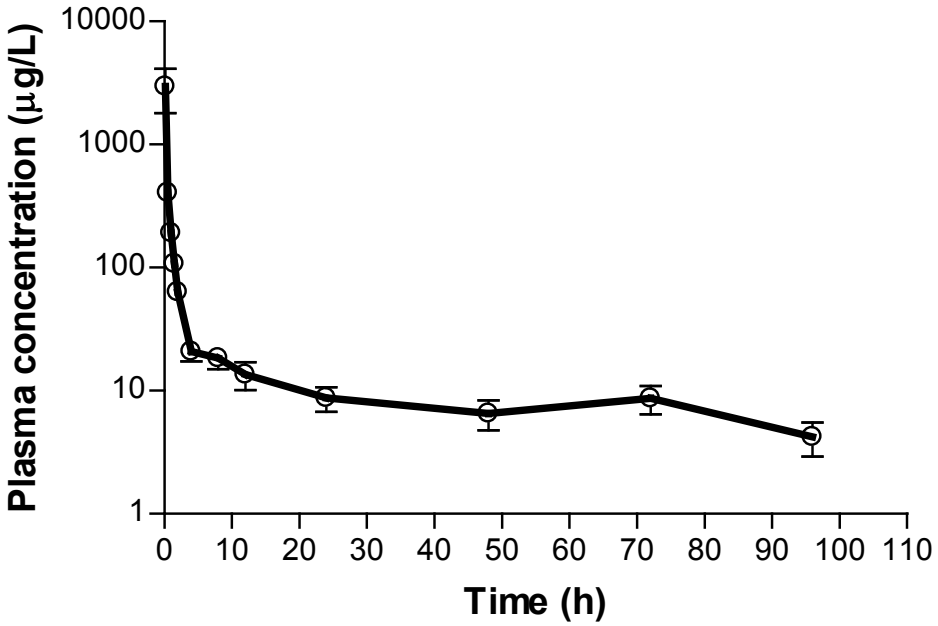

Figure 4-2. Semilogarithmic plot of mean plasma concentration–time data of xanthohumol obtained from Sprague Dawley rats (n = 12) given a single intravenous injection dose of 1.86 mg / kg BW.

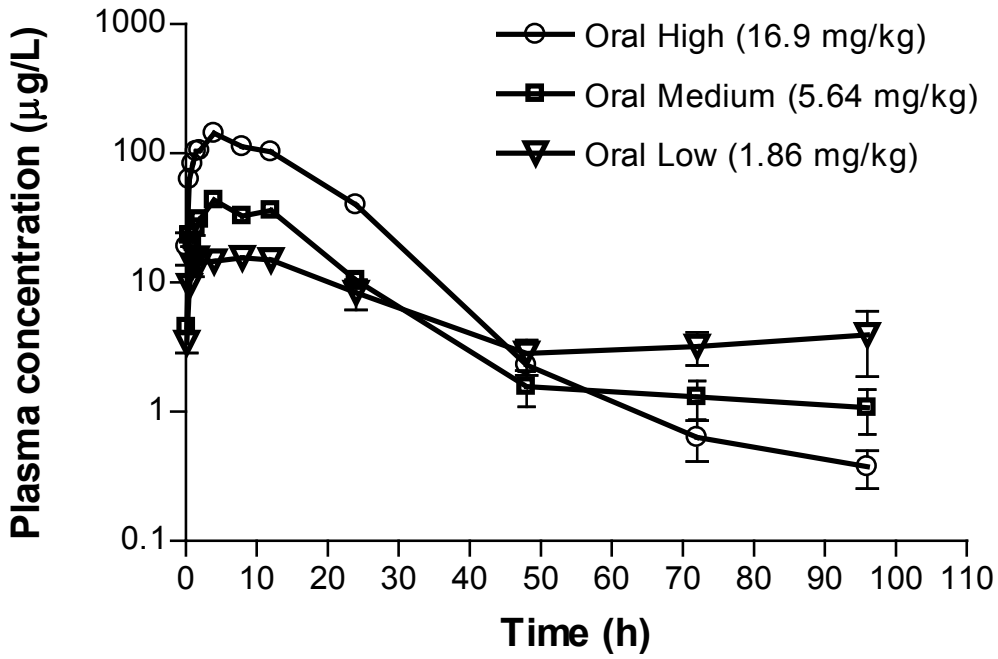

Figure 4-3. Semilogarithmic plot of mean plasma concentration–time data of xanthohumol obtained from Sprague Dawley rats (n = 12/dose) given a single oral low, med, or high dose (1.86, 5.64 or 16.9 mg / kg BW).

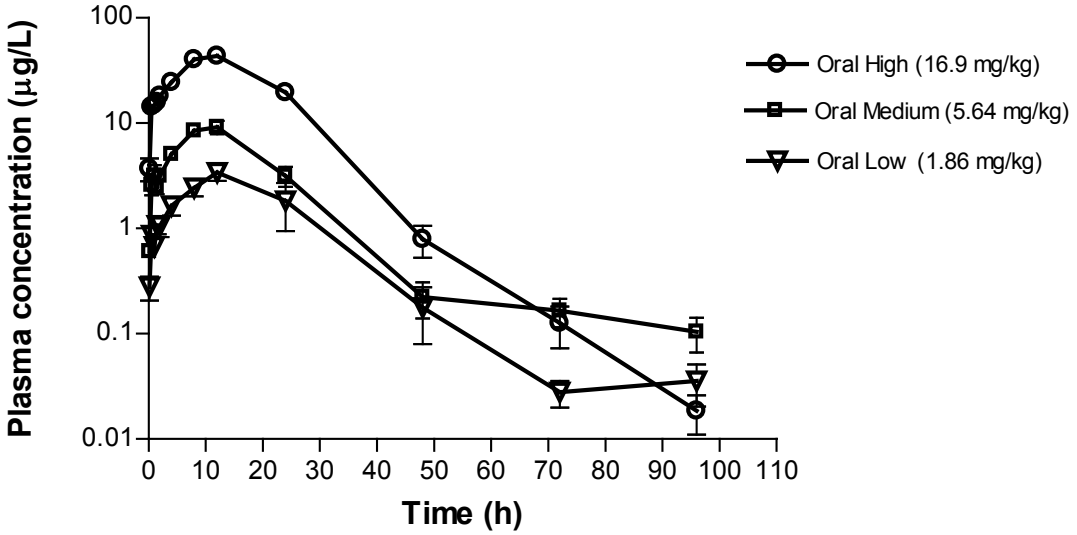

Figure 4-4. Semilogarithmic plot of mean plasma concentration–time data of isoxanthohumol obtained from Sprague Dawley rats (n = 12/dose) given a single oral low, med, or high dose (1.86, 5.64 or 16.9 mg / kg BW).

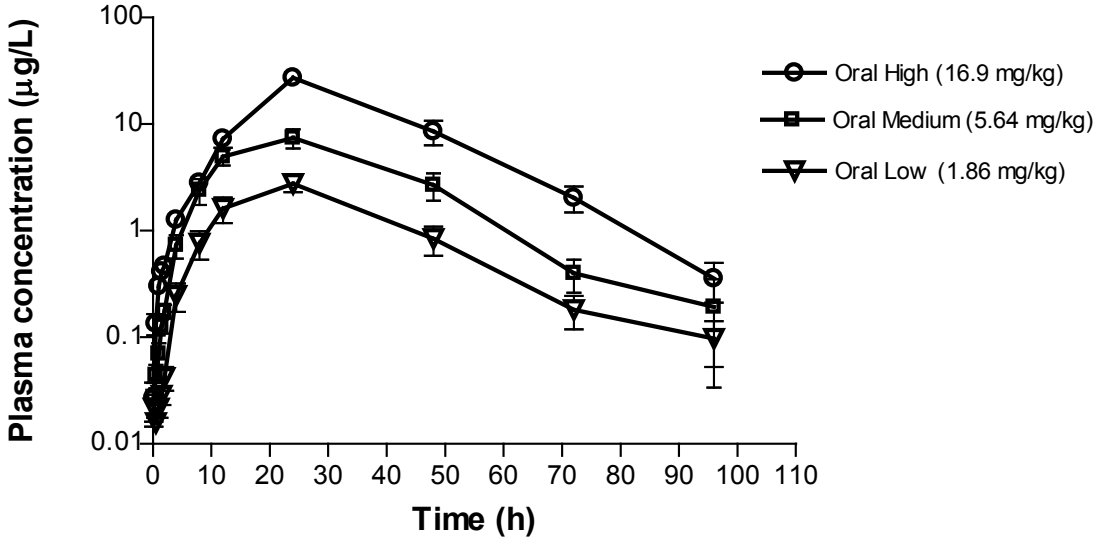

Figure 4-5. Semilogarithmic plot of mean plasma concentration–time data of 8-prenylnarigenin obtained from Sprague Dawley rats (n = 12/dose) given a single oral low, med, or high dose (1.86, 5.64 or 16.9 mg / kg BW).

REFERENCES

(2005) "Guidance for Industry: Estimating the Maximum Safe Starting Dose in Initial Clinical Trials for Therapeutics in Adult Healthy Volunteers."

Bolca, S., S. Possemiers, V. Maervoet, I. Huybrechts, A. Heyerick, S. Vervarcke, H. Depypere, D. De Keukeleire, M. Bracke, S. De Henauw, W. Verstraete and T. Van de Wiele (2007). "Microbial and dietary factors associated with the 8-prenylnaringenin producer phenotype: a dietary intervention trial with fifty healthy post-menopausal Caucasian women." Br J Nutr **98**(5): 950-959.

Bovee, T. F., R. J. Helsdingen, I. M. Rietjens, J. Keijer and R. L. Hoogenboom (2004). "Rapid yeast estrogen bioassays stably expressing human estrogen receptors alpha and beta, and green fluorescent protein: a comparison of different compounds with both receptor types." J Steroid Biochem Mol Biol **91**(3): 99-109.

Casaschi, A., G. K. Maiyoh, B. K. Rubio, R. W. Li, K. Adeli and A. G. Theriault (2004). "The chalcone xanthohumol inhibits triglyceride and apolipoprotein B secretion in HepG2 cells." J Nutr **134**(6): 1340-1346.

Chen, J., H. Lin and M. Hu (2003). "Metabolism of flavonoids via enteric recycling: role of intestinal disposition." J Pharmacol Exp Ther **304**(3): 1228-1235.

Coldham, N. G. and M. J. Sauer (2001). "Identification, quantitation and biological activity of phytoestrogens in a dietary supplement for breast enhancement." Food Chem Toxicol **39**(12): 1211-1224.

Colgate, E. C., C. L. Miranda, J. F. Stevens, T. M. Bray and E. Ho (2007). "Xanthohumol, a prenylflavonoid derived from hops induces apoptosis and inhibits NF-kappaB activation in prostate epithelial cells." Cancer Lett **246**(1-2): 201-209.

Dietz, B. M., Y. H. Kang, G. Liu, A. L. Eggler, P. Yao, L. R. Chadwick, G. F. Pauli, N. R. Farnsworth, A. D. Mesecar, R. B. van Breemen and J. L. Bolton (2005). "Xanthohumol isolated from Humulus lupulus Inhibits menadione-induced DNA damage through induction of quinone reductase." Chem Res Toxicol **18**(8): 1296-1305.

Dorn, C., B. Kraus, M. Motyl, T. S. Weiss, M. Gehrig, J. Scholmerich, J. Heilmann and C. Hellerbrand "Xanthohumol, a chalcon derived from hops, inhibits hepatic inflammation and fibrosis." Mol Nutr Food Res **54 Suppl 2**: S205-213.

FDA (2003) "Guidance for Industry: Bioavailability and Bioequivalence Studies for Orally Administered Drug Products — General Considerations."

Ferrari, C. K. (2004). "Functional foods, herbs and nutraceuticals: towards biochemical mechanisms of healthy aging." Biogerontology **5**(5): 275-289.

Ford, E. S., W. H. Giles and W. H. Dietz (2002). "Prevalence of the metabolic syndrome among US adults: findings from the third National Health and Nutrition Examination Survey." JAMA **287**(3): 356-359.

Gerhauser, C. (2005). "Beer constituents as potential cancer chemopreventive agents." Eur J Cancer **41**(13): 1941-1954.

Gerhauser, C. (2005). "Broad spectrum anti-infective potential of xanthohumol from hop (Humulus lupulus L.) in comparison with activities of other hop constituents and xanthohumol metabolites." Mol Nutr Food Res **49**(9): 827-831.

Gerhauser, C., A. Alt, E. Heiss, A. Gamal-Eldeen, K. Klimo, J. Knauft, I. Neumann, H. R. Scherf, N. Frank, H. Bartsch and H. Becker (2002). "Cancer chemopreventive activity of Xanthohumol, a natural product derived from hop." Mol Cancer Ther **1**(11): 959-969.

Guo, J., D. Nikolic, L. R. Chadwick, G. F. Pauli and R. B. van Breemen (2006). "Identification of human hepatic cytochrome P450 enzymes involved in the metabolism of 8-prenylnaringenin and isoxanthohumol from hops (Humulus lupulus L.)." Drug Metab Dispos **34**(7): 1152-1159.

Hanske, L., G. Loh, S. Sczesny, M. Blaut and A. Braune (2010). "Recovery and metabolism of xanthohumol in germ-free and human microbiota-associated rats." Mol Nutr Food Res **54**(10): 1405-1413.

Heber, D. (2004). "Vegetables, fruits and phytoestrogens in the prevention of diseases." J Postgrad Med **50**(2): 145-149.

Jeong, H. M., E. H. Han, Y. H. Jin, Y. H. Choi, K. Y. Lee and H. G. Jeong "Xanthohumol from the hop plant stimulates osteoblast differentiation by RUNX2 activation." Biochem Biophys Res Commun **409**(1): 82-89.

Jia, X., J. Chen, H. Lin and M. Hu (2004). "Disposition of flavonoids via enteric recycling: enzyme-transporter coupling affects metabolism of biochanin A and formononetin and excretion of their phase II conjugates." J Pharmacol Exp Ther **310**(3): 1103-1113.

Jirasko, R., M. Holcapek, E. Vrublova, J. Ulrichova and V. Simanek (2010). "Identification of new phase II metabolites of xanthohumol in rat in vivo biotransformation of hop extracts using high-performance liquid chromatography electrospray ionization tandem mass spectrometry." J Chromatogr A.

Kitaoka, M., H. Kadokawa, M. Sugano, K. Ichikawa, M. Taki, S. Takaishi, Y. Iijima, S. Tsutsumi, M. Boriboon and T. Akiyama (1998). "Prenylflavonoids: a new class of non-steroidal phytoestrogen (Part 1). Isolation of 8-

isopentenylnaringenin and an initial study on its structure-activity relationship." Planta Med **64**(6): 511-515.

Kris-Etherton, P. M., K. D. Hecker, A. Bonanome, S. M. Coval, A. E. Binkoski, K. F. Hilpert, A. E. Griel and T. D. Etherton (2002). "Bioactive compounds in foods: their role in the prevention of cardiovascular disease and cancer." Am J Med **113 Suppl 9B**: 71S-88S.

Ludden, T. M., S. L. Beal and L. B. Sheiner (1994). "Comparison of the Akaike Information Criterion, the Schwarz criterion and the F test as guides to model selection." J Pharmacokinet Biopharm **22**(5): 431-445.

Lupinacci, E., J. Meijerink, J. P. Vincken, B. Gabriele, H. Gruppen and R. F. Witkamp (2009). "Xanthohumol from hop (Humulus lupulus L.) is an efficient inhibitor of monocyte chemoattractant protein-1 and tumor necrosis factor-alpha release in LPS-stimulated RAW 264.7 mouse macrophages and U937 human monocytes." J Agric Food Chem **57**(16): 7274-7281.

Mendes, V., R. Monteiro, D. Pestana, D. Teixeira, C. Calhau and I. Azevedo (2008). "Xanthohumol influences preadipocyte differentiation: implication of antiproliferative and apoptotic effects." J Agric Food Chem **56**(24): 11631-11637.

Milligan, S., J. Kalita, V. Pocock, A. Heyerick, L. De Cooman, H. Rong and D. De Keukeleire (2002). "Oestrogenic activity of the hop phyto-oestrogen, 8-prenylnaringenin." Reproduction **123**(2): 235-242.

Milligan, S. R., J. C. Kalita, A. Heyerick, H. Rong, L. De Cooman and D. De Keukeleire (1999). "Identification of a potent phytoestrogen in hops (Humulus lupulus L.) and beer." J Clin Endocrinol Metab **84**(6): 2249-2252.

Milligan, S. R., J. C. Kalita, V. Pocock, V. Van De Kauter, J. F. Stevens, M. L. Deinzer, H. Rong and D. De Keukeleire (2000). "The endocrine activities of 8-prenylnaringenin and related hop (Humulus lupulus L.) flavonoids." J Clin Endocrinol Metab **85**(12): 4912-4915.

Milner, J. A. (2004). "Molecular targets for bioactive food components." J Nutr **134**(9): 2492S-2498S.

Miranda, C. L., G. L. Aponso, J. F. Stevens, M. L. Deinzer and D. R. Buhler (2000). "Prenylated chalcones and flavanones as inducers of quinone reductase in mouse Hepa 1c1c7 cells." Cancer Lett **149**(1-2): 21-29.

Miranda, C. L., J. F. Stevens, A. Helmrich, M. C. Henderson, R. J. Rodriguez, Y. H. Yang, M. L. Deinzer, D. W. Barnes and D. R. Buhler (1999). "Antiproliferative and cytotoxic effects of prenylated flavonoids from hops (Humulus lupulus) in human cancer cell lines." Food Chem Toxicol **37**(4): 271-285.

Miranda, C. L., J. F. Stevens, V. Ivanov, M. McCall, B. Frei, M. L. Deinzer and D. R. Buhler (2000). "Antioxidant and prooxidant actions of prenylated and nonprenylated chalcones and flavanones in vitro." J Agric Food Chem **48**(9): 3876-3884.

Miranda, C. L., Y. H. Yang, M. C. Henderson, J. F. Stevens, G. Santana-Rios, M. L. Deinzer and D. R. Buhler (2000). "Prenylflavonoids from hops inhibit the metabolic activation of the carcinogenic heterocyclic amine 2-amino-3-methylimidazo[4, 5-f]quinoline, mediated by cDNA-expressed human CYP1A2." Drug Metab Dispos **28**(11): 1297-1302.

Nikolic, D., Y. Li, L. R. Chadwick, S. Grubjesic, P. Schwab, P. Metz and R. B. van Breemen (2004). "Metabolism of 8-prenylnaringenin, a potent phytoestrogen from hops (Humulus lupulus), by human liver microsomes." Drug Metab Dispos **32**(2): 272-279.

Nookandeh, A., N. Frank, F. Steiner, R. Ellinger, B. Schneider, C. Gerhauser and H. Becker (2004). "Xanthohumol metabolites in faeces of rats." Phytochemistry **65**(5): 561-570.

Nozawa, H. (2005). "Xanthohumol, the chalcone from beer hops (Humulus lupulus L.), is the ligand for farnesoid X receptor and ameliorates lipid and glucose metabolism in KK-A(y) mice." Biochem Biophys Res Commun **336**(3): 754-761.

Overk, C. R., P. Yao, L. R. Chadwick, D. Nikolic, Y. Sun, M. A. Cuendet, Y. Deng, A. S. Hedayat, G. F. Pauli, N. R. Farnsworth, R. B. van Breemen and J. L. Bolton (2005). "Comparison of the in vitro estrogenic activities of compounds from hops (Humulus lupulus) and red clover (Trifolium pratense)." J Agric Food Chem **53**(16): 6246-6253.

Peluso, M. R., C. L. Miranda, D. J. Hobbs, R. R. Proteau and J. F. Stevens (2010). "Xanthohumol and related prenylated flavonoids inhibit inflammatory cytokine production in LPS-activated THP-1 monocytes: structure-activity relationships and in silico binding to myeloid differentiation protein-2 (MD-2)." Planta Med **76**(14): 1536-1543.

Plazar, J., M. Filipic and G. M. Groothuis (2008). "Antigenotoxic effect of Xanthohumol in rat liver slices." Toxicol In Vitro **22**(2): 318-327.

Possemiers, S., S. Bolca, C. Grootaert, A. Heyerick, K. Decroos, W. Dhooge, D. De Keukeleire, S. Rabot, W. Verstraete and T. Van de Wiele (2006). "The prenylflavonoid isoxanthohumol from hops (Humulus lupulus L.) is activated into the potent phytoestrogen 8-prenylnaringenin in vitro and in the human intestine." J Nutr **136**(7): 1862-1867.

Possemiers, S., A. Heyerick, V. Robbens, D. De Keukeleire and W. Verstraete (2005). "Activation of proestrogens from hops (Humulus lupulus L.) by

intestinal microbiota; conversion of isoxanthohumol into 8-prenylnaringenin." J Agric Food Chem **53**(16): 6281-6288.

Qiu, F., X. Y. Chen, B. Song, D. F. Zhong and C. X. Liu (2005). "Influence of dosage forms on pharmacokinetics of daidzein and its main metabolite daidzein-7-O-glucuronide in rats." Acta Pharmacol Sin **26**(9): 1145-1152.

Rayalam, S., J. Y. Yang, M. A. Della-Fera, H. J. Park, S. Ambati and C. A. Baile (2009). "Anti-obesity effects of xanthohumol plus guggulsterone in 3T3-L1 adipocytes." J Med Food **12**(4): 846-853.

Reeves, P. G., F. H. Nielsen and G. C. Fahey, Jr. (1993). "AIN-93 purified diets for laboratory rodents: final report of the American Institute of Nutrition ad hoc writing committee on the reformulation of the AIN-76A rodent diet." J Nutr **123**(11): 1939-1951.

Setchell, K. D., N. M. Brown, P. B. Desai, L. Zimmer-Nechimias, B. Wolfe, A. S. Jakate, V. Creutzinger and J. E. Heubi (2003). "Bioavailability, disposition, and dose-response effects of soy isoflavones when consumed by healthy women at physiologically typical dietary intakes." J Nutr **133**(4): 1027-1035.

Sfakianos, J., L. Coward, M. Kirk and S. Barnes (1997). "Intestinal uptake and biliary excretion of the isoflavone genistein in rats." J Nutr **127**(7): 1260-1268.

Stevens, J. F., M. Ivancic, V. Hsu and M. L. Deinzer (1997). "Prenylflavonoids from Humulus lupulus " Phytochemistry **44**: 1575-1585.

Stevens, J. F., C. L. Miranda, B. Frei and D. R. Buhler (2003). "Inhibition of peroxynitrite-mediated LDL oxidation by prenylated flavonoids: the alpha,beta-unsaturated keto functionality of 2'-hydroxychalcones as a novel antioxidant pharmacophore." Chem Res Toxicol **16**(10): 1277-1286.

Stevens, J. F. and J. E. Page (2004). "Xanthohumol and related prenylflavonoids from hops and beer: to your good health!" Phytochemistry **65**(10): 1317-1330.

Stevens, J. F., A. W. Taylor, J. E. Clawson and M. L. Deinzer (1999). "Fate of xanthohumol and related prenylflavonoids from hops to beer." J Agric Food Chem **47**(6): 2421-2428.

Stevens, J. F., A. W. Taylor and M. L. Deinzer (1999). "Quantitative analysis of xanthohumol and related prenylflavonoids in hops and beer by liquid chromatography-tandem mass spectrometry." J Chromatogr A **832**(1-2): 97-107.

Xuan, N. T., E. Shumilina, E. Gulbins, S. Gu, F. Gotz and F. Lang (2010). "Triggering of dendritic cell apoptosis by xanthohumol." Mol Nutr Food Res **54 Suppl 2**: S214-224.

Yang, J. Y., M. A. Della-Fera, S. Rayalam and C. A. Baile (2007). "Effect of xanthohumol and isoxanthohumol on 3T3-L1 cell apoptosis and adipogenesis." Apoptosis **12**(11): 1953-1963.

Yilmazer, M., J. F. Stevens and D. R. Buhler (2001). "In vitro glucuronidation of xanthohumol, a flavonoid in hop and beer, by rat and human liver microsomes." FEBS Lett **491**(3): 252-256.

Yilmazer, M., J. F. Stevens, M. L. Deinzer and D. R. Buhler (2001). "In vitro biotransformation of xanthohumol, a flavonoid from hops (Humulus lupulus), by rat liver microsomes." Drug Metab Dispos **29**(3): 223-231.